NOVEL TECHNOLOGY FOR RECOVERY OF WATER AND SOLID SALTS FROM HYPERSALINE BRINES: EUTECTIC FREEZE CRYSTALLIZATION

Report to the
Water Research Commission

by

A Lewis, J Nathoo, T Reddy, D Randall, L Zibi & R Jivanji

Crystallization and Precipitation Unit
Department of Chemical Engineering
University of Cape Town

WRC Report No. 1727/1/10
ISBN 978-1-4312-0006-1

August 2010

DISCLAIMER

This report has been reviewed by the Water Research Commission (WRC) and approved for publication. Approval does not signify that the contents necessarily reflect the views and policies of the WRC, nor does mention of trade names or commercial products constitute endorsement or recommendation for use.

EXECUTIVE SUMMARY

i. BACKGROUND

Two major problems currently facing South African water users are the declining availability of sufficient quantities of water and the deterioration of the quality of the available water. However, with the increasing use of water recycling, the result has been an increased generation of inorganic brines and concentrates.

Eutectic Freeze Crystallization (EFC) offers a novel, sustainable method for treating brines and concentrates that were previously regarded as difficult to treat due their complex nature and were consequently discharged to evaporation ponds. With EFC, pure water and pure individual salts can be recovered, thereby making a significant leap towards achieving zero effluent discharge. Furthermore, because the heat of fusion of ice (6.01 kJ/mol) is six times less than the heat of evaporation of water (40.65 kJ/mol), the energy required to separate the water as ice is significantly less than that required to separate it by evaporation, although obviously the energy for freezing will be more expensive than that for heating.

Although EFC has been shown to be effective in separating a single salt and water, it has yet to be applied to the complex hypersaline brines that are typical of reverse osmosis retentates in South Africa. Thus, the overall aim of this research was to investigate the applicability of EFC to the hypersaline brines and inorganic effluents produced by major South African industries. The research project aims were as follows:

1. Establish the eutectic freeze crystallization phase diagrams for the hypersaline brines and saline effluents under investigation.
2. Establish the effect of the complex aqueous chemistry and impurities on the applicability of eutectic freeze crystallization to these aqueous systems.
3. Establish the expected costs and economic benefits of applying eutectic freeze crystallization to these aqueous systems.

ii. PROGRESS

Aim 1: Establish the eutectic freeze crystallization phase diagrams for the hypersaline brines and saline effluents under investigation.

It has been established that binary phase diagrams are inadequate for the design of multicomponent EFC processes, since interactions between salts in hypersaline solutions cause multiple pseudo eutectic and eutectic temperatures.

Although it is extremely difficult to establish the complex phase diagrams for multicomponent brines, the eutectic conditions can still be determined. For a ternary system, there will be 2 pseudo eutectic lines where ice will coexist with each solid as well as the ternary eutectic point where ice will coexist with both solids. A sequential EFC process can theoretically be operated along the first eutectic line in order to recover the first salt and then along the second eutectic line to recover the second salt.

Since a phase diagram defines a state of thermodynamic equilibrium, for practical EFC applications, it is necessary to establish the kinetic considerations that will define design and operation. The most important of these is the metastable zone.

Aim 2: Establish the effect of the complex aqueous chemistry and impurities on the applicability of eutectic freeze crystallization to these aqueous systems.

Thermodynamic modelling of the effects of salts on eutectic temperatures was carried out using a Reverse Osmosis retentate as the stream of interest. It was found that, at these relatively low concentrations, the ice always crystallizes first, followed by the higher hydrated salts. No significant shifts in salt freezing points were observed due to the relatively low concentration of salts in the retentate.

Experimental studies were carried out on various types of synthetic brines to establish the eutectic temperatures and compositions. The metastable zone width, an important parameter for EFC process operation, was also established for a number of different cases.

Synthetic brines

- The eutectic temperature and composition of the binary Na_2SO_4 -water system correlated well with literature values.
- For synthetic brine containing 4 wt% Na_2SO_4, the presence of low concentrations of F^-, Cl^-, K^+, Li^+, Mg^{2+}, Ca^{2+}, NO_3^- and NH_4^+ impurities depressed the eutectic temperature of $Na_2SO_4 \cdot 10H_2O$ crystallization from -1.24°C to -2.22°C. Using EFC, pure ice crystals were obtained (<20 ppm impurities), ranging from 100 μm to 450 μm in size, after seven washing steps. Pure $Na_2SO_4 \cdot 10H_2O$ crystals (identified using thermal analysis), without any detectable impurities, were also produced. The salt crystal sizes ranged from 20-100 μm one residence time after reaching eutectic conditions and 50-350 μm after three residence times.
- For a concentrated synthetic brine containing 4 wt% Na_2SO_4 and 20 wt% NaCl the metastable point for $Na_2SO_4.10H_2O$ was reached at 6.68 wt% and 3.1°C. The freezing point for ice was depressed to -19°C. The eutectic point for the system was found to be -21.22°C. 90% recovery of $Na_2SO_4.10H_2O$ was achieved, with crystal sizes ranging from 50-400μm. The solubility limit of NaCl was not reached for this system and NaCl was not recovered as a salt.
- The ternary Na_2SO_4-NaCl-H_2O system reached its eutectic point at approximately -21.29°C and the $Na_2SO_4 \cdot 10H_2O$ nucleated at 10.45°C. There was no significant change in the nucleation temperature as compared with Experiment E3 results. The ice reached its solubility limit at -22.5°C and greater than 90% of the $Na_2SO_4 \cdot 10H_2O$ crystals were recovered from this system. The $Na_2SO_4 \cdot 10H_2O$ crystals were pure, prismatic and monoclinic in shape.

  For the 4 wt% Na_2SO_4 – 23.5 wt% NaCl – brine system, the $Na_2SO_4 \cdot 10H_2O$ nucleated at 9.08°C, whereas the ice nucleated at -21.85°C. The presence of impurities did not have a significant impact on the eutectic point of the system. The system reached the eutectic point at -21.27°C. At this low temperature, the production of ice was high, leading to the crystalliser contents forming a slush mixture of ice and salt. Therefore, the purity of ice could not be determined owing to the difficulty in separation of the ice and salt from the crystalliser. Hence, it is important to establish the critical solid mass content within the reactor.

Metastable zone width determination

- The average MSZ for the ice region of Na_2SO_4-H_2O system is 4.1°C at a cooling rate of 1.5°C/hour. The MSZ is also wider in the region of ice formation compared to the region where salt forms. The average MSW for the salt region is 2.9°C.
- A faster cooling rate increases the average MSZW for the region where ice forms. The average MSZ for the ice trendline is 4.5°C at a cooling rate if 4°C/hour, which is 0.4°C higher than the average MSZW obtained for a cooling rate of 1.5°C/hour. The average width of the MSZ for the ice line at a cooling rate of 6°C/hour is 5.5°C.

- The average MSZ at a cooling rate of 4°C/hour for the salt line is, however, 2.1°C which is 0.8°C smaller than the MSZW for a cooling rate of 1.5°C. The fastest cooling rate investigated, 6°C/hour, results in the greatest average MSZ for the salt line with a value of 3.4°C.
- The metastable eutectic composition decreases with the fastest cooling rate of 6°C/hour. The metastable eutectic composition is around 4.5 wt% for a cooling rate of 6°C/hour while for a cooling rate of 1.5°C/hour it is 4.79 wt%. However, this trend was not observed for a cooling rate of 4°C/hour.
- Seeding can be used to test the accuracy of the experimentally determined metastable boundary. Salt seeding promotes the formation of salt but only to the limit of the MSZ after which ice nucleation occurs.

Aim 3: Establish the expected costs and economic benefits of applying eutectic freeze crystallization to these aqueous systems.

The key objective of the preliminary economic evaluation was to provide an approximation of the expected operating and capital costs associated with using EFC. These were compared to triple-effect evaporative crystallization (EC). The costs of electricity to the compressor in the EFC refrigeration unit and the steam requirement for the evaporative crystallization process were identified as the major contributors to the operating costs for the two processes. Hence, these were used as the basis for calculating the operating costs.

Two brines broadly representative of typical South African industrial brines i.e. consisting of Na_2SO_4 and NaCl were investigated. The concentration factor difference between the two brines was approximately 10 with Brine 2 being more concentrated than Brine 1. A basis of 100 m^3/day of brine was used.

The operating cost calculated for using EFC to treat Brine 1, without heat integration, with a cooling requirement of 534kW was R28/m^3. In contrast, the operating cost for a triple-effect EC process to treat Brine 1 was R132/m^3.

The operating cost calculated for using EFC to treat Brine 2, without heat integration, with a cooling requirement of 556kW was R29/m^3. In contrast, the operating cost for a triple-effect EC process to treat Brine 2 was R126/m^3.

Hence, the operating cost savings of using EFC over EC are 79% and 76% for Brine 1 and Brine 2 respectively. The cost savings of using EFC could potentially be further enhanced by incorporating the income generated from the sale of the pure salts produced by the EFC process, as well as taking into consideration the additional mixed salt disposal costs for EC.

Three heat integration options were investigated to determine their effect on further reducing the EFC operating costs. The first option involved pre-cooling the incoming feed with the product ice stream. The second option investigated using the product ice to cool the condenser in a two-stage refrigeration system. The third option was a combination of Option 1 and 2 above. The most cost effective option was found to be Option 3. Using Option 3, the operating cost for Brine 1 was calculated to be R21/m^3 as compared to R28/m^3 without heat integration. Similarly, for Brine 2 using Option 3, the operating cost was calculated to be R21/m^3 as compared to R29/m^3 without heat integration. Thus, operating cost savings of 27% and 29% were achieved for Brines 1 and 2 respectively with heat integration according to Option 3.

The capital equipment cost for EFC for treating 100 m^3/day of Brine 1 and Brine 2 were calculated to be R6.6 million and R7.9 million respectively. In comparison, the capital costs for treating the

same volume of brine using EC were R5.2 million and R4.9 million for Brine 1 and Brine 2 respectively. As expected, the EFC capital costs were significantly higher than those for EC. However, it is important to note that the capital cost calculations for EC are based on a technology that is already well established, with only relatively marginal future equipment cost savings expected as a result of improvements in the existing technology. In contrast, EFC is a new technology with future improvements expected in the technology resulting in capital cost reductions in particular with regards to the EFC reactor.

iii. CONCLUSIONS

In summary, the results of the experimental work aimed at investigating the effect of complex aqueous chemistry and impurities on the EFC process showed that the eutectic temperature for a pure binary system of Na_2SO_4-H_2O was -1.24°C and -21.29°C for a pure ternary system of Na_2SO_4-NaCl-H_2O. The presence of impurities, even in small concentrations, had a significant depressing impact on the eutectic temperature of the binary system. Maintaining a critical solid mass content i.e. the amount of ice and salt crystals in the reactor was found to be of significant importance as it directly affected the purity and yield of the crystalline products.

The study showed that the MSZ for ice was generally wider than that for salt, regardless of the cooling rate used. For the sodium sulphate system, a faster cooling rate resulted in a wider MSZ. The difference in the nucleation temperatures for repeat experiments was attributed to the stochastic nature of nucleation. The findings from the experimental work have emphasised the importance of identifying the appropriate EFC operating conditions (operating temperatures and the operating region within the phase diagram) in order to promote good product characteristics and maximise yields.

The results of the economic study showed that the operating cost savings achieved by using EFC over EC significantly outweighed the initial higher capital cost investment required for EFC. This continued to be the case despite the projected increases in the electricity price tariffs as stipulated by ESKOM up to 2011.

In conclusion, EFC offers an innovative solution for the treatment of hypersaline brines. It is a technology that can be used either in isolation or in conjunction with other water treatment processes such as reverse osmosis, towards achieving zero effluent discharge sustainably. Future studies in EFC will need to focus on further refining the understanding of the scientific fundamentals together with investigating key operating parameters that will enable the process to be tested at pilot scale before full-scale implementation.

iv. OUTPUTS

Specific outputs from the project included:

- 2 international peer reviewed journal publication (accepted);
- 6 international conference presentations;
- 8 local conference presentations as shown below:

1. Lewis, A.E., Nathoo, J., Thomsen, K., Kramer, H.J., Witkamp, G.J., Reddy, S., and Randall, D., 2010. Design of a Eutectic Freeze Crystallization process for multicomponent waste water stream, Chemical Engineering Research and Design (2010), doi:10.1016/j.cherd.2010.01.023
2. Reddy, S.T., Lewis, A.E., Witkamp, G.J., and Van Spronsen, J., 2010. Recovery of $Na_2SO_4 \cdot 10H_2O$ from a reverse osmosis retentate by eutectic freeze crystallisation technology, Chemical Engineering Research and Design (2010), doi:10.1016/j.cherd.2010.01.010
3. Lewis, A.E., Randall, D.G., Reddy, S.T., Jivanji, R., and Nathoo, J., 2009. Worth its Salt – How Eutectic Freeze Crystallization can be used to recover salt from hypersaline mine waters, Water in Mining, AusIMM, 15-17 September, Perth Australia, pp 5-11
4. Randall, D.G., Nathoo, J., Lewis, A.E., 2009, Seeding for selective salt recovery during Eutectic Freeze Crystallization. International Mine Water Conference, 19-22 October, Pretoria, South Africa, pp 639-646
5. Nathoo, J., Jivanji, R., and Lewis, A.E., 2009. Freezing your brines off: Eutectic Freeze Crystallization for brine treatment, International Mine Water Conference, 19-22 October, Pretoria, South Africa, pp 431-437
6. Reddy, S.T., Kramer, H.J.M., Lewis, A.E., and Nathoo, J., 2009. Investigating factors that affect separation in a eutectic freeze crystallisation process, International Mine Water Conference, Pretoria, 19-23 October, pp 649-655
7. Zibi, L., Nathoo J., and Lewis A.E., 2009. Modelling and characterisation of industrial brine, SAIMM Conference, Cape Town, 6-7 August 2009
8. Reddy, S.T., Kramer, H.J.M., Nathoo, J., and Lewis, A.E., 2009. Investigating factors that affect separation in a eutectic freeze crystallisation process, SAIMM Conference, Cape Town, 6-7 August 2009.
9. Jivanji, R., Nathoo, J., Lewis, A.E., 2009. Application of Eutectic Freeze Crystallization on industrial brines, SAIMM Conference, Cape Town, 6-7 August 2009
10. Randall, D.G., Lewis, A.E., Nathoo, J., 2008. Kinetic aspects of multi-component systems operated under eutectic freeze crystallization conditions, SAIMM Conference, Cape Town, 6-8 August 2008
11. Reddy, S.T., Lewis, A.E., Nathoo, J., 2008. Treatment of reverse osmosis retentate using eutectic freeze crystallization, SAIMM Conference, Cape Town, 6-8 August 2008
12. Lewis, A.E., 2008. A novel approach to the treatment of water containing high dissolved salts, SAIMM Conference, Cape Town, 6-8 August 2008
13. Reddy, S.T., Lewis, A.E., Witkamp, G.J., Van Spronsen, J., Kramer, H. and Van Rosmalen, G.M., Investigating the applicability of Eutectic Freeze Crystallization for the treatment and disposal of reverse osmosis retentates. In Janssens, P., (ed), 17th International Symposium on Industrial Crystallization, Maastricht, The Netherlands, 14-17 September, 2008
14. Randall, D.G., and Lewis, A.E., Investigating characteristics of ice crystals formed in eutectic freeze crystallization, SAIMM Conference, Cape Town, 2-3 August 2007.
15. Reddy, S.T., and Lewis, A.E., 2006. Water and Salt Recovery from Brine Solutions, 13th International Workshop on Industrial Crystallization (BIWIC), 13 -15 September 2006, Delft, the Netherlands
16. Reddy, S.T. and Lewis, A.E., 2006, Innovative approaches to brine treatment, Mineral Processing 2006, Cape Town, 3-4 August 2006.

ACKNOWLEDGEMENTS

The authors wish to express their gratitude:

- To the staff of the Crystallization and Precipitation Unit and the Mechanical Workshop, in the Chemical Engineering Department at the University of Cape Town for their contribution to the research reported here;
- To the Water Research Commission (WRC) for the funding support
- To Coaltech and Mr Johan Beukes for their support and input to the project
- To the members of the Steering Committee for their contributions and guidance of the project. Special acknowledgement to the following members of the steering committee for peer-reviewing this report prior to final publication.
    - Dr JE Burgess, Water Research Commission
    - Dr L Petrik, University of the Western Cape
    - Mr A Wurster, Golder Associates (Africa) Pty Ltd
    - Dr NE Ristow, Phathamanzi Water Treatment Pty Ltd
    - Mr IW van der Merwe, Proxa Ltd
    - Mr PJ du Toit Roux, SASOL Technology
    - Ms S Mudau, Chamber of Mines
    - Mr HM du Plessis, Water Research Commission
    - Mr R Munnik, Golder Associates (Africa) Pty Ltd
    - Dr AS Parsons, Anglo Gold
    - Mr P Gunther, Anglo Coal
    - Mr TM Morokane, Department of Water Affairs
    - Mr DJ Hanekom, Eskom
    - Ms R Muhlbauer, BHP Billiton
    - Mr J Beukes, Coaltech
- To the Process and Energy Laboratory at the Technische Universiteit Delft, specifically the Process Equipment department, for hosting Traci Reddy, Dyllon Randall and Jeeten Nathoo.

TABLE OF CONTENTS

LIST OF FIGURES

LIST OF TABLES

1 INTRODUCTION

The two major problems currently facing South African water users are firstly: the declining availability of sufficient quantities of water, and secondly: the deterioration of the quality of the available water (Buckley, 2005). However, with the increasing use of water recycling technology such as desalination, ion exchange regeneration, inorganic precipitation, biological processes and membrane treatments, the result has been an increased generation of inorganic brines and concentrates.

Handling aqueous salt–bearing streams, either for the recovery of the salt, or for the reduction of waste streams via a concentration process, is energy intensive and thus costly. For mixtures with high solute concentrations, crystallization-based separation processes can be applied. In evaporative crystallization, however, the extremely large energy requirements to evaporate the water can be prohibitive and cooling crystallization is limited by the temperature dependence of the solubility. Anti solvent crystallization combines extraction with crystallization, but requires an additional step to recover the anti-solvent after the crystallization. Membrane crystallization has many advantages, but is often limited by scale formation on the membrane surface. (Himawan, 2005).

Eutectic freeze crystallization (EFC) is an alternative technology for the separation of highly concentrated aqueous streams. Eutectic Freeze Crystallization is a technique that is capable of separating aqueous solutions into pure water and pure, solidified solutes (Van der Ham, 2002) and that is highly energy efficient, without the introduction of any solvents. In addition, the simultaneous production of pure ice and pure salt(s) is a major advantage. Because the heat of fusion of ice (6.01 kJ/mol) is six times less than the heat of evaporation of water (40.65 kJ/mol), the energy required to separate the water as ice is significantly less than that required to separate it by evaporation, although obviously the energy for freezing will be more expensive than that for heating.

The principle of the process is as follows: when a solution containing dissolved contaminants is slowly frozen, water ice crystals form on the surface, and the contaminants are concentrated in the remaining solution (the mother liquor) (Gertner et al., 2005). The ice crystals can be separated from the mother liquor, washed and melted to yield a nearly pure water stream. The mother liquor will contain a pure salt, which crystallizes at the eutectic temperature. Theoretically, a 100% yield can be obtained in a binary system, which is one of the advantages of EFC technology. The level of accumulation of impurities can be controlled by means of purge streams (Vaessen, 2003). The reduction in energy consumption for a Eutectic Freeze Crystallization process was compared to a three-stage evaporative crystallization and was found to be 65% for a copper sulphate system and 30% for a sodium nitrate system (Van der Ham et al., 1998).

2 OBJECTIVES

The main aim of the research is to investigate the applicability of EFC to the hypersaline brines and inorganic effluents produced by major South African industries.

1. Establish the eutectic freeze crystallization phase diagrams for the hypersaline brines and saline effluents under investigation.
2. Establish the effect of the complex aqueous chemistry and impurities on the applicability of eutectic freeze crystallization to these aqueous systems.
3. Establish the expected costs and economic benefits of applying eutectic freeze crystallization to these aqueous systems.

3 LITERATURE REVIEW

3.1 Advantages and disadvantages of the EFC process

Freeze crystallization can be used to separate water from organic chemicals as well as a wide range of materials such as water from seawater, brines or organic waste (Conlon, 1992).

Eutectic Freeze Crystallization is an extension of freeze crystallization where the solution is cooled to the specific EFC conditions. Ice and salt continue to form at the eutectic temperature and below until no solid liquid phase is left (Vaessen et al., 2003). Eutectic Freeze Crystallization can be applied to solutions of any concentration (Van der Ham et al., 2004) but it is best to operate with concentrations near the eutectic point. In a simple experiment conducted by Conlon (1992), it was demonstrated that the separation of food colouring from distilled water was possible with freeze crystallization. Ice cubes were formed while the crystals grew from the outside to the inside while vividly concentrating the food colouring in the centre of the cube (Conlon, 1992).

Pure water and salt can be simultaneously recovered from aqueous solutions by EFC at low energy costs and very high yields (Genceli et al., 2005). This, however, has never led to an industrial application for EFC because the process is currently uneconomical (Vaessen et al., 2003).

The energy reductions under EFC operation were found to be 30% for sodium nitrate and 65% for copper sulphate when compared to conventional multi-step evaporation (Van der Ham, 1999). EFC can also in principle achieve a 100 percent separation of the solution into ice and salt, provided no purge stream is needed (Van der Ham et al., 1998). Corrosion of construction materials is also subsequently reduced because of the low operating temperatures (Vaessen et al., 2003). The technology can also treat a wide variety of feed solutions without the addition or need of adding further solvents or chemicals (Genceli, 2008).

The most significant disadvantages of EFC concerning investment costs and scale limitations can be overcome with time (Van der Ham et al., 1998). When brine disposal has to be considered, the economic focus changes since the cost of disposal may be as much as the cost of fresh water produced thus making technologies such as EFC more attractive as a separation method (Barduhn and Manudhane, 1979).

In the early 1950s Nelson and Thompson (as cited in Vaessen, 2003) investigated the crystallization of salts from sea water by freezing. However, it was not until the 1970s that EFC was considered as a viable separation technology by Stepakoff et al. (1974).

In the 1980s Swenne, (as cited in Vaeseen, 2003), investigated the eutectic freezing of sodium chloride. The investigations were focused on direct cooling and the growth behaviour of both the salt and ice crystals. It was concluded that the use of EFC for producing sodium chloride could be economically feasible.

Van der Ham started EFC research in 1998 with the goal of developing an EFC process using indirect cooling. The cooled disk column crystallizer was proposed for EFC. It focused on a suspension crystallizer in which both crystallization and solid/solid separation are achieved in one apparatus (Vaessen, 2003). EFC technology has low energy requirements and theoretically the feed can be completely converted to water and solidified solutes. The most prominent disadvantages of EFC are investment costs and scale limitations but the current view is that these can be overcome (Van der Ham et al., 1998).

The current goal is to develop eutectic freezing equipment for industrial scale. The ice and salt crystals need to have a high purity, should be easily separable and should be economically viable to compete with conventional separation techniques (Vaessen, 2003).

3.2 The EFC process

Stepakoff and co-workers (1974) suggest that a continuous process is required to establish economic validity, facilitate control and to avoid subcooling. The EFC process has four principal unit operations: crystallization of ice and salts, separation of this ice and salts, counter-current washing and crystal filtering. Figure 1 is a simplified schematic representation of the EFC process.

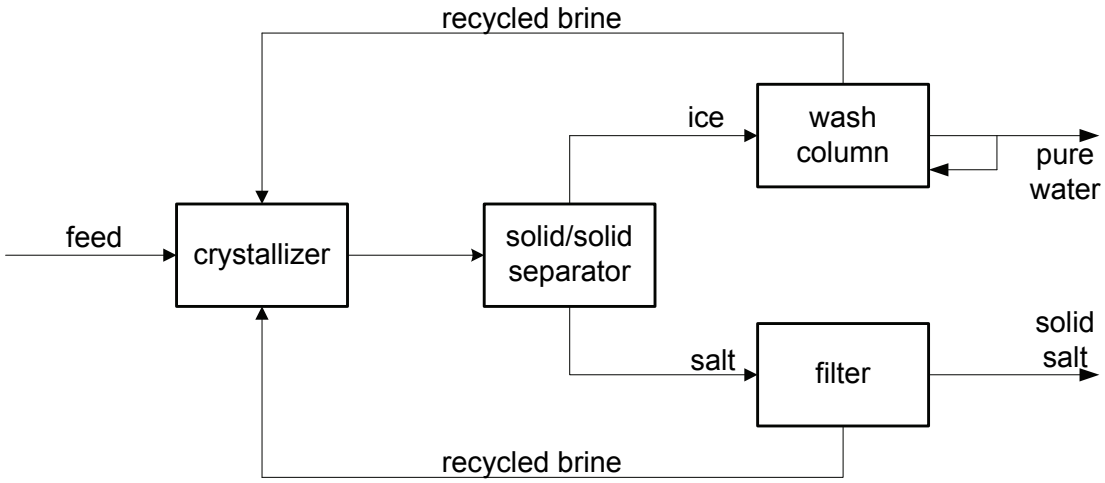

Figure 1: Schematic representation of the EFC process for the production of pure water and salt from waste or process streams (Van der Ham et al., 1998)

The possibility of using staged EFC was also suggested. A two stage EFC process will provide savings in power costs when the feed stream contains 7% TDS or less. A two-stage process does not require washing to potable quality in the eutectic stage and potential problems such as channelling and freezing are avoided.

3.3 Seeding

Seeding can be used to stabilize a process of batch crystallization. However, no accurate prediction can be made about how much and what size of seeds are needed to stabilize crystallization during seeding (Kubota et al., 2001). Seeding can also increase the productivity of each batch and lead to a better final product (Nagy et al., 2008).

It is well known that seeding suppresses secondary nucleation (Kubota et al., 2001). If the seed size is small, nucleation suppression is determined by the number of seed particles (Itoh et al., 2002). Large crystal seeds should not be used because attrition induces a limit in crystal size. Also, large crystals result in a slow growth rate (Loi Mi Lung-Somarriba et al., 2004).

In a seeding operation, the seed is added shortly after the solubility curve is crossed. Operation should then continue in the region where spontaneous nucleation does not occur. In unseeded operations, the seeds are generated in the bulk once the system first reaches the metastable limit. The supersaturation needs to be kept below the limit where spontaneous nucleation will occur. This is known as the metastable limit (Nagy et al., 2008). Figure 2 shows this graphically.

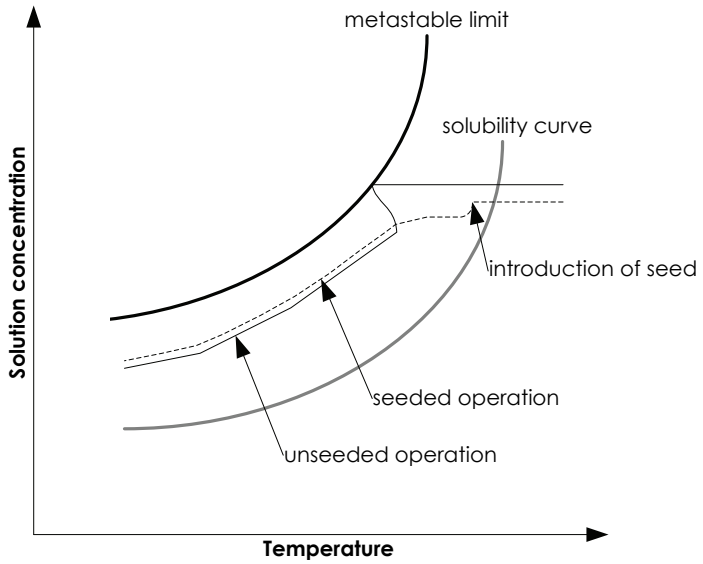

Figure 2: Solubility diagram showing seeded and unseeded batch cooling crystallization operation (Nagy et al., 2008)

Also, ice can be formed without any salt formation by manipulating the system with the addition of ice seed crystals in the MSZ. Ice seeding promotes the formation of ice. Similarly, salt is formed by seeding with salt crystals. Seeding with both salt and ice crystals results in two distinct solid phases (Van der Ham et al., 1999).

3.4 Review of previous experimental work

3.4.1 Case study: $MgSO_4$ solution

Himawan and co-workers (2006) investigated the use of EFC for the treatment of a magnesium sulphate stream. They determined that there was a narrow window of operation for batch crystallization during the crystallization of $MgSO_4.12H_2O$ (between -4°C to 0°C and 17.4 wt% to 20 wt%) (Himawan and Witkamp, 2006). The $MgSO_4.12H_2O$ crystals were unstable above 0°C since they spontaneously transformed to $MgSO_4.7H_2O$. This made the measurement of the crystal product difficult (Himawan and Witkamp, 2006). The metastable zone width of $MgSO_4.12H_2O$ was also wide since ice crystallized almost always above the thermodynamic eutectic composition (Himawan et al., 2006).

The EFC experimental procedure for a $MgSO_4$-H_2O system was as follows:

A 20 wt% magnesium sulphate solution, with a solubility temperature of 3.09°C, was cooled down to -1.5°C and at this point seed crystals were added. The crystallizer temperature increased immediately to about -0.9°C because of the heat of crystallization. The temperature was then kept constant at this temperature for about 10 to 15 minutes. A linear or natural cooling policy was then adopted (Himawan and Witkamp, 2006).

Genceli and co-workers ran similar experiments using a magnesium sulphate solution. The coolant temperature was set to vary between -7.6°C to -11.7°C with a residence time of 1.1-3.0 hours in the crystallizer (Genceli et al., 2005).

In other experiments conducted by Himawan et al. (2006) also on the magnesium sulphate system, a 2 ℓ cylindrical jacketed glass vessel equipped with a three bladed scraper was used. The refrigerant used was ethylene glycol-water circulated using a Lauda RK 8 KP thermostatic unit. All experiments were performed batchwise. The solution was left to stabilize at 0°C for 2 hours. A cooling rate of 2 to 4°C/hour was adopted until the first temperature jump occurred. Ice seeds were in some cases introduced. The suspension was then cooled further with a cooling rate of 1°C/hour until the second jump occurred. After this second jump the cooling rate was kept constant. The experiments were stopped once an overload indication was signalled by the motor as a result of excessive scaling of the reactor contents which made stirring more difficult. This usually occurred two hours after the first temperature jump. Ultra pure water and a saturated magnesium sulphate solution were used to wash ice and salt crystals when measuring the purity of the products. The actual purity was obtained by chemical analysis (Himawan et al., 2006).

The most stable hydrate at subzero temperatures was magnesium sulphate dodecahyrate ($MgSO_4.12H_2O$) (Himawan et al., 2006). Marion and co-workers (1999) reported that the hydrates of $MgSO_4$ can persist in metastable equilibrium over a wide temperature range (Himawan et al., 2006).

The salt that forms near the eutectic conditions in a magnesium sulphate system is $MgSO_4.11H_2O$ (Meridianiite) crystals and not the commonly reported $MgSO_4.12H_2O$. It has been accepted by the IMA as a mineral (Genceli et al., 2008).

3.4.2 Case study: $CuSO_4$ solution

Van der Ham and co-workers (1999) ran EFC experiments using a copper sulphate solution. Experiments were performed in a 250 mℓ jacketed glass vessel. Indirect cooling, with ethylene glycol as the coolant, was used in the experiments. A Lauda RK 8 KP thermostatic unit was used to cool the ethylene glycol. Agitation was provided by a magnetic stirrer. The crystallizer temperature was measured using a PT-100 sensor connected to the RK 8 KP.

In batch experiments the solution was supercooled to 1.0°C below the eutectic temperature of the system. The temperature was kept constant and ice seeds were added. After one hour a solid ice phase formed. The reactor was then heated until all the solids vanished. The liquid was again supercooled and the experiment was repeated, but this time with salt seeds (Van der Ham et al., 1999).

The eutectic temperature of the copper sulphate system from the experiments was found to be -1.55°C (Van der Ham et al., 1999).

3.4.3 Case study: K_2SO_4 solution

Drummond and co-workers (2002) used EFC technology on an industrial solution containing potassium sulphate and organic impurities and successfully demonstrated EFC as a separation technique for this stream (Drummond et al., 2002).

The experimental equipment of Drummond and co-workers (2002) consisted of a 2 ℓ batch suspension crystallizer with a three legged scraper set at a speed of 80 rpm. A thermostatic unit provided the cooling. Experiments were conducted in a climate chamber kept at 10°C. All experiments were unseeded. A linear cooling rate of 0.1°C/min was applied before the eutectic condition was reached. After the eutectic temperature was reached, the cooling rate was set at 0.03°C/min. During the experiments, samples were taken using a 5 mℓ pipette. Ice crystals were

washed with sub-cooled demineralised water. Both solid and liquid samples were analysed by inductive coupled spectrometry. The purity of the ice increased from about 85 to 99 wt% (Drummond et al., 2002).

3.4.4 Case study: KNO_3 solution

In experiments conducted by Vaessen and co-workers (2003), a ternary system of KNO_3-HNO_3-H_2O was investigated. The aqueous solution of KNO_3 and HNO_3 stems from an industrial waste stream producing starch. Washed salt contained less than 5ppm of ionic impurities.

The experimental equipment consisted of a crystallizer with a conical shape at the top and bottom for collection of solids. The conical sections of the crystallizer were not cooled. Scrapers were used to prevent scaling on the walls of the crystallizer. The rotation rate of the scraper was 7-43 rpm. Ice samples were taken directly from the crystallizer and filtered on a glass filter. Washing was performed with sub-cooled demineralised water on a glass filter. All samples were quickly transported to a climate chamber kept at -2°C. Samples of both ice and salt were analysed for cationic impurities by ICP-AES spectrometry. Anionic impurities in the KNO_3 samples were determined by ion chromatography (Vaessen et al., 2003).

4 THEORY

4.1 Introduction to crystallization theory

Crystallization can be defined as a phase change where a crystalline solid is obtained from the solution (Myerson, 2002). The solid phase will crystallize from the solvent if the chemical potential of the solid is less than that of the corresponding component in solution (Nyvlt, 1971).

4.2 Defining supersaturation

A solution that has a concentration of the solute exceeding the equilibrium solute concentration is known as a supersaturated solution (Myerson, 2002). Supersaturation is the thermodynamic driving force for crystallization, hence the rate of nucleation and growth of crystals is driven by the existing supersaturation in the solution (Loffelmann and Mersmann, 2002).

Supersaturation is usually expressed as a concentration difference (Myerson, 2002):

$$\Delta C = c - c^* \tag{1}$$

and as a ratio of concentrations

$$S = c/c^* \tag{2}$$

Where c – concentration, kg/m^3
c^* – equilibrium concentration, kg/m^3

4.3 The Kinetics of crystallization

4.3.1 Nucleation and crystal growth

Crystals can only develop if there is some number of nuclei or seeds in the system. The nucleation process may occur spontaneously or the system can be forced to nucleate. The process of artificially

inducing nucleation with crystal seeds is known as secondary nucleation while the process of nucleation in systems with no crystalline matter is termed primary nucleation. The primary nucleation process can be further subdivided into homogenous and heterogeneous nucleation. Homogenous nucleation is spontaneous formation of crystals in the bulk solution while heterogeneous nucleation occurs on a solid surface typically because of impurities in the system (Mullin, 2001).

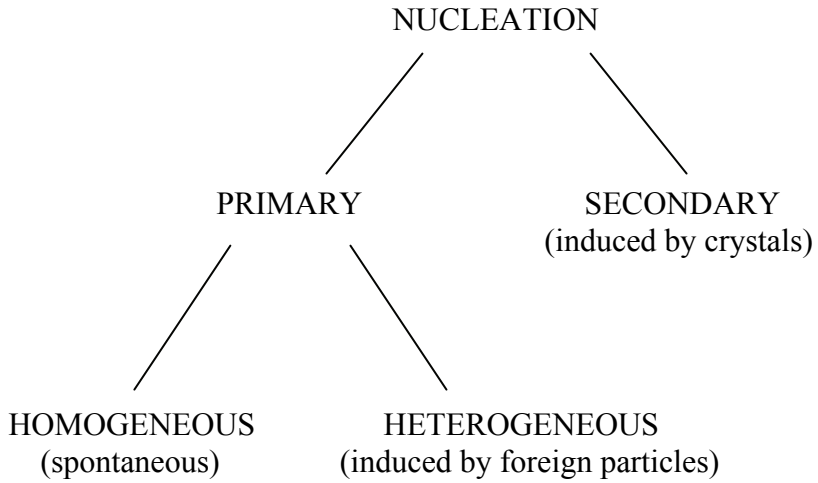

Figure 3: Nucleation scheme (Mullin, 2001)

4.3.2 Nucleation

Nucleation involves the birth of a new crystal and this describes the crystallization process (Myerson, 2002). There are currently two techniques that can be used to detect the formation of the first nuclei. The first technique detects changes related to the amount of grown nuclei while the second technique detects changes in solution concentration. Solution concentration changes can be measured using electrical conductivity (Kubota, 2008). Nucleation can also be observed as a sudden increase in crystallizer temperature (Vaessen, 2003).

A zone of nucleation temperatures instead of a single point is more likely to be recorded for the nucleation event. The reason for the zone of values is because nucleation measurements are strongly dependent on the statistical distribution of nucleation incidents (Myerson, 2002).

4.4 Freezing Point Depression

When a small amount of solute is added to a liquid solvent, and the overall temperature of the mixture is lowered to T_f where the pure solvent begins to separate out of the mixture as a solid, this temperature will be lower than the freezing temperature (melting temperature) of the pure solvent, T_m. The difference in these two temperatures due to the addition of a solute gives rise to the freezing point depression:

$$\Delta T = T_m - T_f \tag{3}$$

In this case, the solvent is pure water and the solid that freezes from the mixture will be pure ice. Using a simplified equation for the freezing point depression from Sandler (1999):

$$\Delta T = -\frac{RT_m^{\ 2}}{\Delta H^{fus}(T_m)} \ln(\gamma_1 x_1) \quad (4)$$

the relationship between solute concentration and freezing point can be plotted. R is the universal gas constant, ΔH_{fus} for water is 6025 J/mol, γ_1 represents the activity coefficient for water and x_1 represents the mole fraction of water in the solution.

4.5 Eutectic Phase Diagram

This freezing point depression at changing solute concentrations is reflected in a phase diagram, which indicates the phases present at thermodynamic equilibrium for a given temperature and composition. A phase diagram enables the determination of a number of parameters, such as the operating temperature and theoretical yields of ice and salt. Since these are critical parameters, phase diagrams for brine solutions are essential if EFC technology is to be used for brine treatment. Kinetic considerations are not reflected on phase diagrams. These need to be determined experimentally.

4.5.1 Binary Phase Diagrams – $CuSO_4.5H_2O$

The diagram presented in Figure 4 represents the eutectic phase diagram for a $CuSO_4 \cdot 5H_2O$- water system. This is a simplified diagram and only considers the "pentahydrate" form of copper sulphate whose eutectic conditions are 11.9 wt% and -1.5°C (Pronk, 2006).

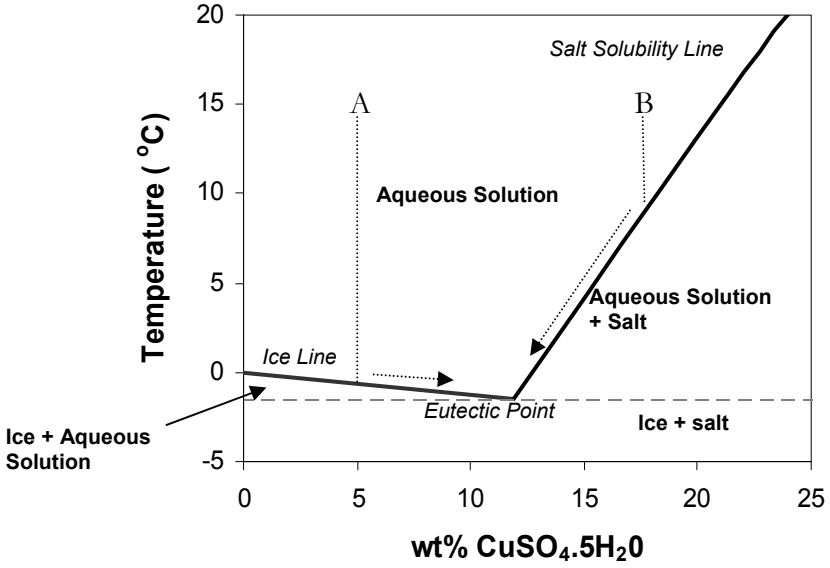

Figure 4: Eutectic Diagram for the binary $CuSO_4 \cdot 5H_2O$ – water system

Starting on the left side of the eutectic point at point A, at a temperature of 15°C and concentration of 5 wt%, the solution is cooled until it reaches the ice line. At this point, the first crystals of ice are seen. On further cooling, the path will follow the ice line, with the concentration of the solution increasing due to ice formation, until the eutectic point is reached, where both ice and salt crystallize simultaneously.

The inverse phenomenon is observed on the right of the eutectic point. When a solution is cooled from point B, at a concentration of 18 wt%, the salt solubility line is reached where the first crystal

of salt forms. Upon further cooling, more salt crystals form, decreasing the concentration of the solution until the eutectic point is reached where simultaneous crystallization of ice and salt occurs.

4.5.2 Binary Phase Diagrams – $MgSO_4$

The diagram presented in Figure 5 represents the eutectic phase diagram for a $MgSO_4$-H_2O system. Binary eutectic phase diagrams are freely available for a range of systems (Thomsen, 2007).

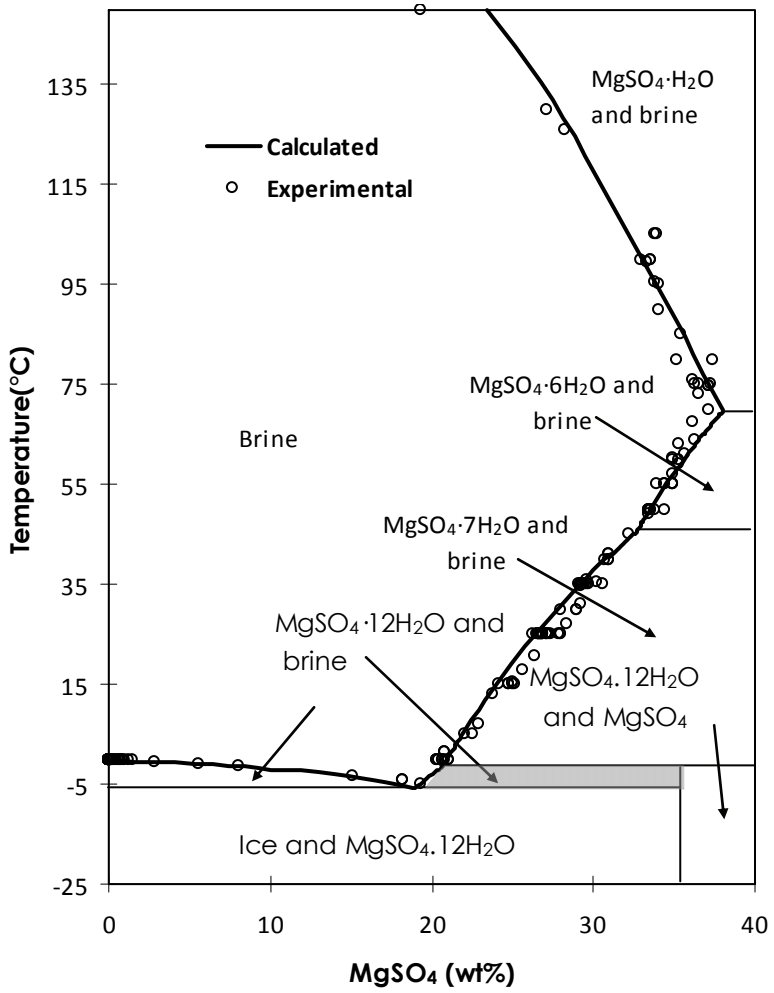

Figure 5: Eutectic Diagram for the binary $MgSO_4$- water system (Thomsen, 2007)

Figure 6 represents the phase diagram for the Na_2SO_4-$MgSO_4$-H_2O ternary system. As can be seen by comparing Figure 5 with Figure 6, in a ternary system the eutectic temperature is shifted due to the interactions between the components. Figure 5 indicates that a magnesium sulphate binary system has a eutectic temperature of ~ -4°C while Figure 6 for the Na_2SO_4-$MgSO_4$-H_2O ternary system has a eutectic temperature of -7°C. It is therefore not sufficient to model multicomponent or ternary systems using binary phase diagrams, as the critical parameter of the eutectic temperature will be incorrectly predicted.

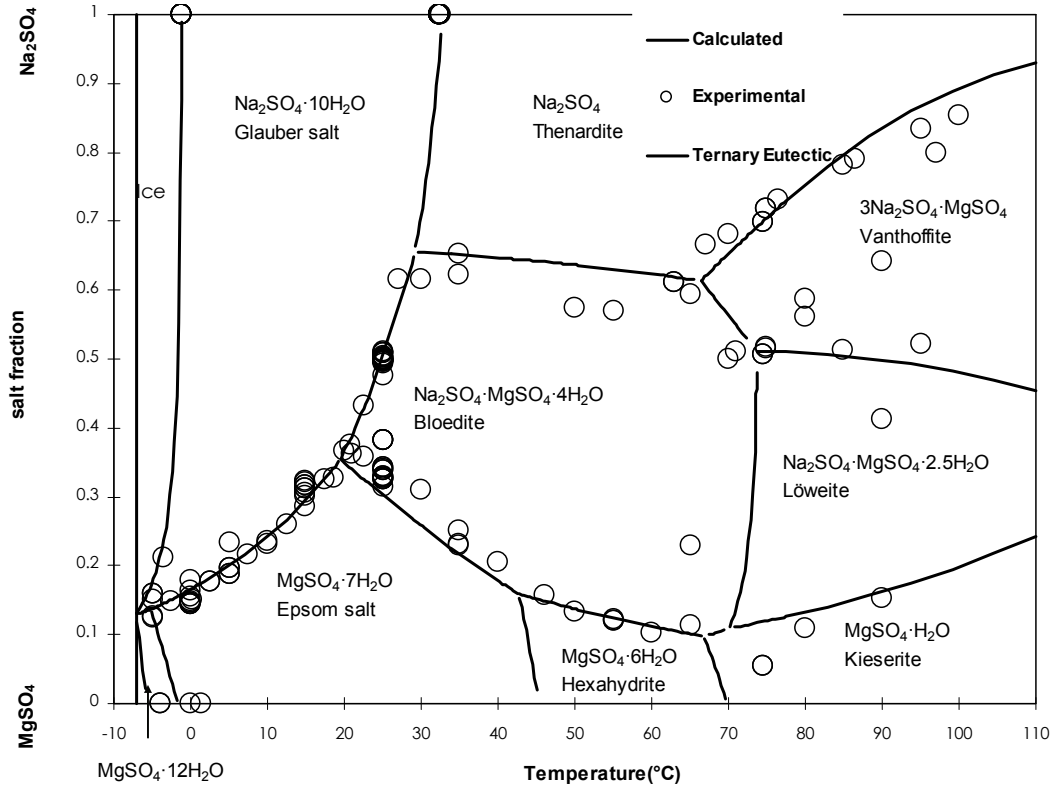

Figure 6: Phase diagram for the Na_2SO_4-$MgSO_4$-H_2O system from -10 to 110°C, showing the eutectic temperature at -7°C (Thomsen, 2007)

4.6 Metastable zone

The phase diagrams presented so far have all been based on principles of thermodynamic equilibrium. Thermodynamically, solutions in the supersaturated state are highly unstable. However, kinetically, the solution may appear to be stable in that no property changes can be observed for some time. This is referred to as a "metastable state". The formal definition of the metastable zone width is that value of undercooling below which the old phase can remain metastable longer than a previously chosen induction time.

The metastable zone width can be expressed either by the maximum obtainable undercooling or by the supersaturation, as they are equivalent. For this application, the metastable zone will be defined in terms of the maximum obtainable undercooling temperature. In Figure 7, the starting point is shown as A′ at solute concentration c_{eq}. Cooling of this solution to T2 will bring the solution to point A, which is the thermodynamic solubility limit. Further cooling would cause the solution to move along line AB into the metastable region until the metastable limit is reached at point B. In the metastable zone, between points A and B, crystallization will only occur in the presence of seeds. When the metastable limit is exceeded, the solution becomes labile and spontaneous formation of the solid phase immediately occurs. The supersaturation corresponding to the metastable limit is defined as the critical supersaturation (Söhnel and Garside, 1992).

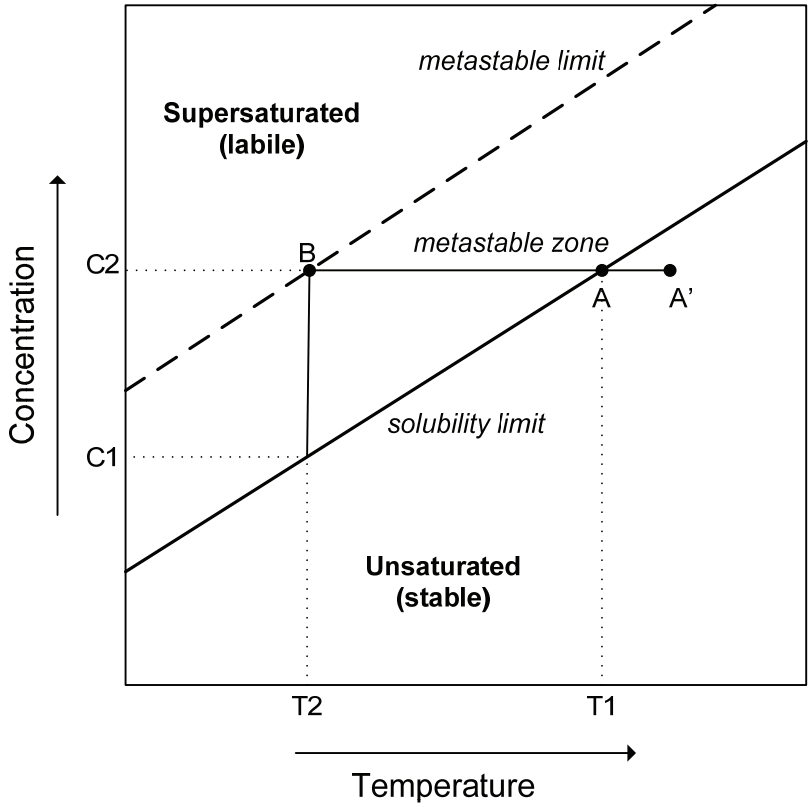

Figure 7: Phase diagram of a binary solid-liquid system showing metastable region

Information about the metastable zone width is an essential parameter in the process of growing crystals from a solution as it is a direct measurement of the stability of the solution in its supersaturated region. (Srinivasen et al. (2000) and Zaitseva et al. (1995)). The metastable zone is also the only region where it is possible to carry out seeded crystallization. EFC processes must be operated in the metastable zone and thus the establishment of the width of the zone for both ice and salt is critical.

4.7 Least squares method for metastable limit determination

The operating region for an EFC process is obtained by measuring the nucleation temperature at different concentrations of the solute. These data points are plotted together with the thermodynamic ice solubility line and salt solubility line. The operating line can then be defined as the best fit trend line with the same gradient as the ice line or the salt line. This technique is an extension of the least squares method of linear regression. Provided the slope of the thermodynamic line is known, and by an iterative procedure the $\Sigma\left(\left(T_{trend}-T_{nuc}\right)^2\right)$, where T_{trend} is the operating trendline and T_{nuc} is the experimentally determined nucleation temperature, term is minimized resulting in a best fit line through the scatter of the nucleation temperatures is achieved (see Figure 8).

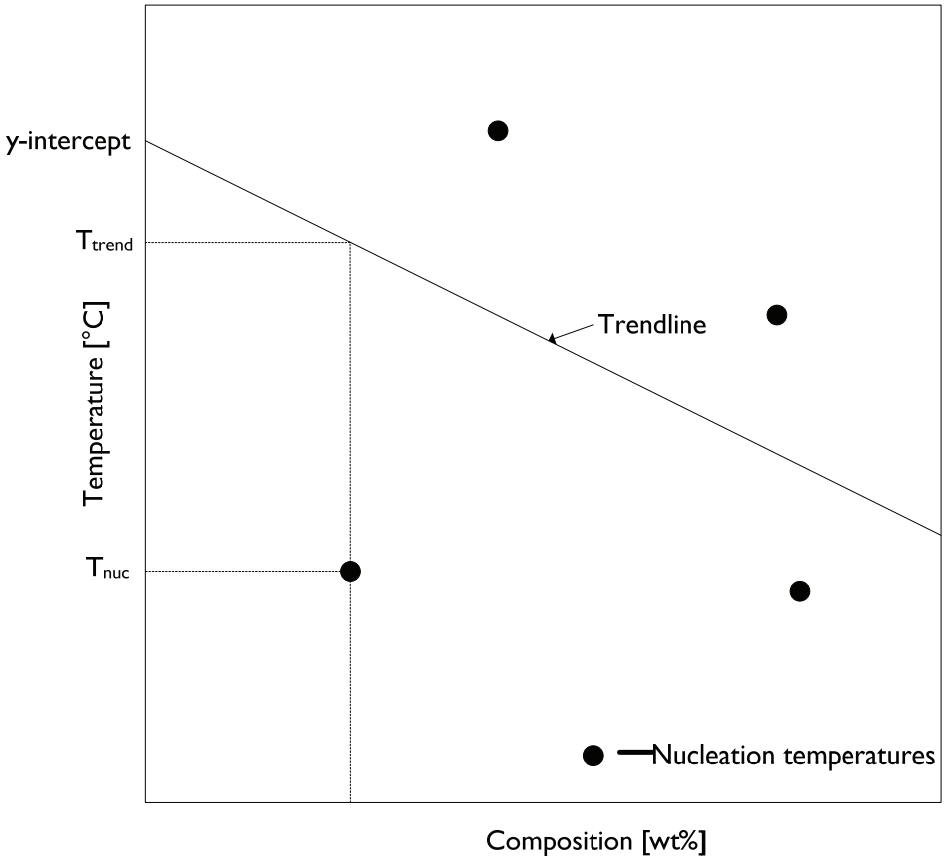

Figure 8: Determination of the y-intercept for a best fit line through a scatter of nucleation temperatures

5 THERMODYNAMIC MODELLING OF THE EFFECT OF SALTS ON EUTECTIC TEMPERATURES

Due to the limited availability of experimental solubility data for complex brines at low temperatures, aqueous thermodynamic modelling provides a valuable tool for determining the thermodynamically predicted solubilities, as well as other relevant stream parameters for complex, multi-component systems. For example, the eutectic temperatures of the individual salts, the expected yields and the chemical identity of the most stable form of the salts formed can be determined.

The initial focus of this study was finding on the most appropriate thermodynamic modelling software that accurately predicted the behaviour of multi-component brine streams at these subzero temperatures. Two thermodynamic software packages, namely MINTEQ and OLI Stream Analyzer, were compared for this purpose and the results are presented in following sections.

5.1 Thermodynamic modelling software

5.1.1 MINTEQ

MINTEQ (Gustafsson, 2007) is an equilibrium speciation model that can be used to calculate the equilibrium composition of dilute aqueous solutions in the laboratory or in natural aqueous systems. The model employs a pre-defined set of components that includes free ions such as Na^+ and neutral and charged complexes (e.g., H_4SiO_4, $Cr(OH)_2^+$). The database of reactions is written in terms of these components as reactants. Errors that have been identified with the software include

deficiencies in data for metal-organic complexes, but do not pose a problem for the calculations carried out in this work as they only consist of inorganic complexes thus far (Serkiz et al., 1996).

MINTEQ uses the Davies equation to calculate activity coefficients:

$$\log \gamma_i = -0.51 z_i^2 \left[\frac{\sqrt{\mu}}{1+\sqrt{\mu}} \right] - 0.3\mu \tag{5}$$

where the subscript *i* refers to each of the components in the reaction, z_i is the ionic charge of the species and μ_i is the ionic strength. The activity coefficients are used to correct the equilibrium constant to $\mu=0$:

$$K_{\mu=0} = K_{\mu} \frac{\Pi_i \gamma_i^{\nu}{}_{,products}}{\Pi_i \gamma_i^{\nu}{}_{,reac\tan ts}} \tag{6}$$

where ν represents the stoichiometric coefficient. MINTEQ also incorporates the Van't Hoff equation to adjust the equilibrium constants during speciation for those reactions having non-zero enthalpies for temperature other than ambient. However, this software cannot model streams that are below 0°C.

5.1.2 OLI Stream Analyzer

The OLI software uses a speciation-based thermodynamic model to calculate speciation and chemical equilibria as well as phase equilibria for multi-component aqueous systems. This software has inbuilt aqueous models which it applies to water based solvent electrolyte systems. The Helgeson-Kirkham-Flowers Equation of state is incorporated to predict the equilibrium constants. The built in model also integrates the Bromley-Meissner, Pitzer, Helgeson and Bromley-Zematis equations for calculations of the activity calculations (Berthold, 2001). The OLI software also incorporates a Mixed Solvent Electrolyte (MSE) database, which uses the Helgeson direct method and has the capability of successfully modelling temperatures as low as -200°C.

The limitations of using the OLI software program are:

- A separate activity coefficient model is lacking, i.e., it does not incorporate NRTL, Unifac or Uniquac models;
- The non aqueous and vapour fugacity coefficients are defined from the Enhanced Soave-Redlich-Kwong Equation of State;
- Vapour critical parameters are correlated to find a fugacity coefficient.

Currently, these limitations do not affect the results obtained for the systems under investigation. This can be re-evaluated at a later time.

5.2 Thermodynamic modelling results

Table 1 shows the composition of three typical reverse osmosis concentrate streams. As can be seen, the three streams are quite similar in composition in terms of the dominant ions present i.e. Na^+, Cl^- and SO_4^{2-}. Hence, for the purposes of this study, the TRO-Secunda brine was selected as a case study, with the understanding that the results presented would be largely applicable to the two other brines in terms of the observed trends.

Table 1: Composition of streams to be studied

		RO Retentate (Tutuka)	FAM (Eastern Steam Plant – Secunda)	TRO – Secunda
Species	**Units**	**Concentration**	**Concentration**	**Concentration**
Na^+	mg/ℓ	5400	1400	2300
K^+	mg/ℓ	300	100	220
Mg^{2+}	mg/ℓ	41	<0.04	2
Ca^{2+}	mg/ℓ	390	770	790
Li^+	mg/ℓ	0	0	4.8
NH_4^+	mg/ℓ	0.5	80	19
Br^-	mg/ℓ	<0.1	<0.01	
Cl^-	mg/ℓ	4010	1000	2260
F^-	mg/ℓ	13.86	16.53	8.31
NO_3^-	mg/ℓ	29.6	22.3	24.5
SO_4^{2-}	mg/ℓ	8690	2780	7440
pH		7.26	11.47	5.23
EC	mS/cm	>20	10.72	11.52
TDS	ppt	>10	5.6	5.99

5.3 Using thermodynamic modelling as a tool for the preparation of a synthetic stream

In order to prepare a synthetic solution, it is necessary to obtain a comprehensive water analysis which accounts for all the anions and cations. Thus, the first step involves calculating the total cumulative positive and negative charges as a result of the cations and anions respectively and consequently determining the extent of the charge imbalance. Once established, the charge imbalance is rectified by using the dominant ion addition method of charge balancing. Furthermore, based on the measured pH of the water sample, any necessary pH adjustments to match the modelled pH with the actual measured pH is carried out by adding the appropriate amount of acid (HCl) or base (NaCl) to the modelled input stream.

Table 2 shows the extent of the charge imbalance obtained for the TRO-Secunda stream based on the analysis carried out.

Table 2: Table showing the charge balance for the TRO-Secunda stream (pH 6.47)

	Charge [eq/ℓ]
Cation	0.147003
Anion	-0.219476
Imbalance	-0.072473

From Table 2 above, it is apparent that the stream has an excess negative charge and thus 1666.16 mg/ℓ Na^+ is required to balance the charge.

In order to calculate the speciation of the stream, Visual MINTEQ Version 2.52 (Gustafsson, 2007) was used. This speciation was used to determine the salt make-up for synthesising the stream in the lab. MINTEQ was chosen in preference to OLI Stream Analyzer for the purpose of the speciation calculations since the salts generated by the MINTEQ database were more appropriate for the composition of the synthetic brine stream than those generated by the OLI software.

Table 3: Results of speciation of Na^+ as predicted by MINTEQ

Component	% of total component concentration	Species name
Na^{+1}	90.654	Na^{+1}
	0.019	NaF (aq)
	1.423	NaCl (aq)
	7.899	$NaSO_4^-$

It can clearly be seen that the salts generated by the Na^+ ions in solution will be NaF and NaCl. From the knowledge of the most likely salts to be generated by the stream, it is thus possible to create a salt make-up for a synthetic stream by carrying out a mole balance on the ions in solution. The list of salts that are required to synthesise the TRO-Secunda stream for experimental purposes is shown in Table 4 below.

Table 4: Salt make-up for TRO-Secunda stream

Salt species	milliMolal [mmol/kg]
NaCl	57.8
KCl	5.23
$CaSO_4$	19.7
$MgSO_4$	0.08
$(NH_4)_2SO_4$	0.53
LiCl	0.69
NaF	0.44
Na_2SO_4	57.1
KNO_3	0.40

The following protocol was thus followed for all streams:

1. Perform dominant charge balance in OLI Stream Analyzer 2.0.52
2. Input stream into MINTEQ for speciation
3. Construct list of salts from this speciation
4. Construct the synthetic brine stream according to this list of salts.

5.4 Prediction of salt crystallization at reduced temperatures

Prediction of salt crystallization was carried out using OLI Stream Analyser due to its ability to accurately simulate aqueous chemistry at high ionic strengths. Figure 9 below shows the predictions of the successive crystallization of the various salts as the temperature is lowered from ambient (from right to left on the x axis). Even at ambient temperatures, the TRO-Secunda stream was supersaturated with $CaSO_4$, and this is reflected by the crystallization of $CaSO_4 \cdot 2H_2O$ across the entire temperature range. This would need to be taken into account in designing an appropriate EFC process.

Once the temperature reaches -1°C, ice crystallizes out, followed by $Na_2SO_4 \cdot 10H_2O$ at -2°C and $NaCl \cdot 2H_2O$ at -23°C. Thermodynamically, the higher hydrates crystallize out first, since less energy is required to form a crystal that incorporates water, where water is the solvent. Trace quantities of CaF_2 and KNO_3 also crystallize out of the brine – these are species that will accumulate with increased brine volumes. Shifts in freezing points of salts are not apparent due to the relatively low concentration of the retentate.

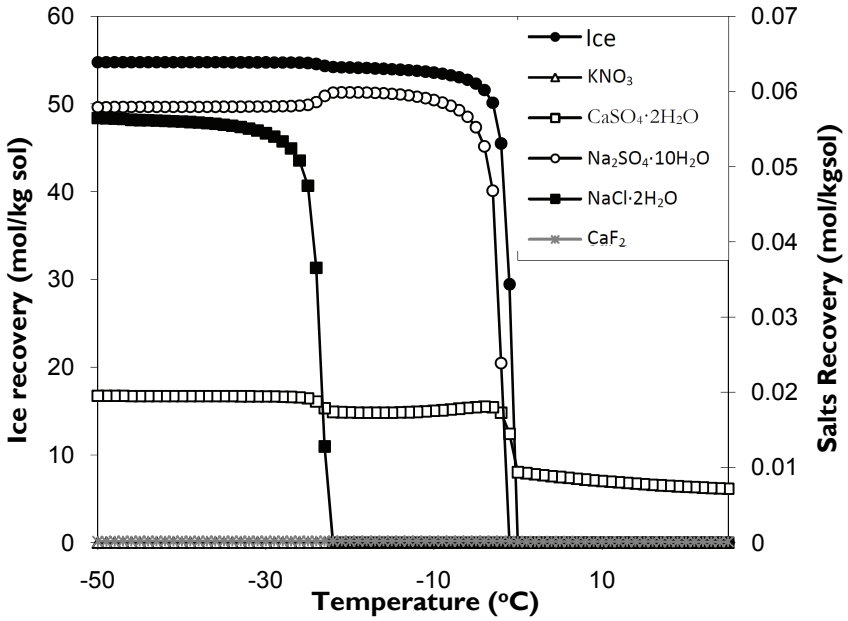

Figure 9: Salt and ice crystallization as a result of cooling for the TRO-Secunda brine

Table 5 presents the predicted eutectic compositions and temperatures for the binary salt-water species found in the various streams obtained from the OLI Stream Analyzer. These are in good agreement with results from literature.

Table 5: Predicted eutectic compositions and temperatures from OLI Stream Analyzer 2.0.52 compared to those obtained from Pronk (2006).

Salt	Predicted Eutectic Composition (wt%)	Literature Eutectic Composition (wt%)	Predicted Eutectic Temperature (°C)	Literature Eutectic Temperature (°C)
CaF_2	0.001		-0.01	
$CaSO_4$ ($2H_2O$)	0.17		-0.05	
Na_2SO_4 ($10H_2O$)	3.97	3.8	-1.14	-1.2
$CuSO_4$ ($5H_2O$)	11.9	11.9	-1.59	-1.5
NaF	3.33		-2.67	
KNO_3	9.79	10.4	-2.80	-2.9
$MgSO_4$ ($12H_2O$)	16.93	18	-3.94	-3.9
KCl ($1H_2O$)	19.5	19.7	-10.61	-10.6
NaCl ($2H_2O$)	23.27	23.3	-21.02	-21.2

This table provides vital information for the evaluation of sequential EFC applications to selectively crystallise out different salts.

5.5 Multi-component Systems

It is extremely difficult to determine the complex phase diagrams for multicomponent brines, although the eutectic conditions can still be determined (Stepakoff et al., 1974). If the solution has a number of different ions present, then the eutectic temperature of the multicomponent system will be significantly altered. Van der Ham (1997) explains that in a ternary system [S1, S2, water], there will be regions where ice coexists with solid S1 (pseudo eutectic 1), ice with solid S2 (pseudo eutectic 2) and ice with both solid S1 and S2 (ternary eutectic point). This is analogous for systems

with more components. EFC processes can operate at either the eutectic point or one of the pseudo eutectic points.

Barduhn and Manudhane (1979) investigated the eutectic temperatures of a synthetic aqueous mixture consisting of seven ions (Na^+, K^+, Ca^{2+}, Mg^{2+}, Cl^-, SO_4^{2-} and HCO_3^-) and found that the EFC process will operate and be economically viable if the eutectic temperatures are no lower than -25°C. EFC systems with eutectic temperatures of approximately -20°C generally require less energy than evaporative systems. A reasonable indication of the practical and economical feasibility of EFC is provided by the eutectic temperature (Vaessen, 2003).

5.5.1 Generating ternary phase diagrams by thermodynamic modelling

The Extended UNIQUAC model is a thermodynamic model that can be used to create binary, ternary and quaternary phase diagrams. This model is used by The Centre for Phase Equilibria and Separation Processes (IVC – SEP), which is an online databank of phase equilibria that can be retrieved for numerous systems. (IVC – SEP, 2007). Figure 6, page 10, is an example of a binary phase diagram for a ternary system (Na_2SO_4-$MgSO_4$-H_2O) showing the eutectic temperature at -7°C. A ternary phase diagram would need three axes and is normally represented by an equilateral triangle with each component represented on the side of the triangle. Figure 10 is a ternary phase diagram for the Na_2SO_4-$MgSO_4$-H_2O system at a single temperature of 85°C. A number of these isotherms can be constructed to create a three dimensional figure of the system.

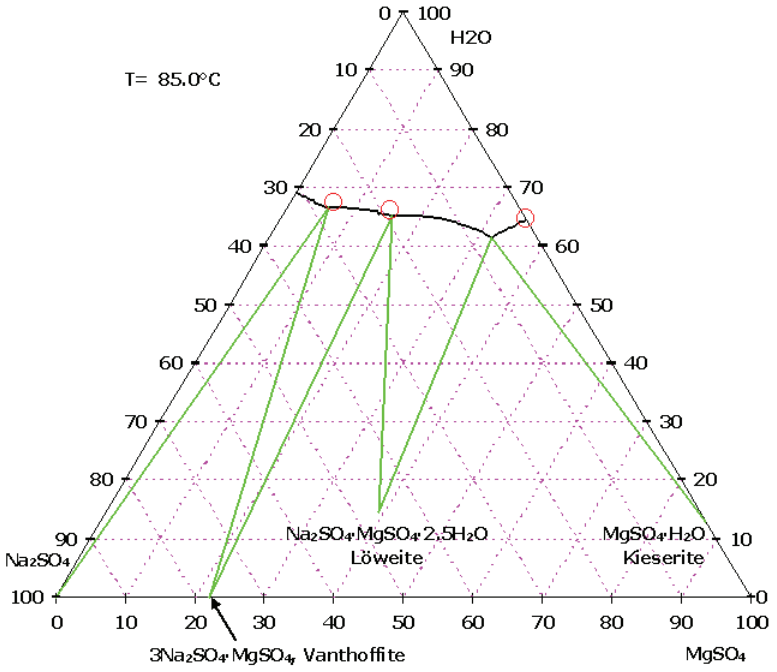

Figure 10: 85°C isotherm for the Na_2SO_4-$MgSO_4$-H_2O system (Thomsen, 2007)

Figure 11 shows the concentration ranges for the (Na^+,K^+) - (Cl^-,SO_4^{2-})-H_2O system and the water mass percent at each grid intersection. Each corner of Figure 11 represents a component of the ternary system. The lower left corner represents a KCl solution, the lower right corner a K_2SO_4 solution, the upper left corner a NaCl solution and the upper right corner a Na_2SO_4 solution. A contour chart of the same system is shown in Figure 12 (Thomsen, 2007). The major components of a brine can be used to construct phase diagrams much like those in these figures. More phase diagrams for various systems can be found in Appendix A.

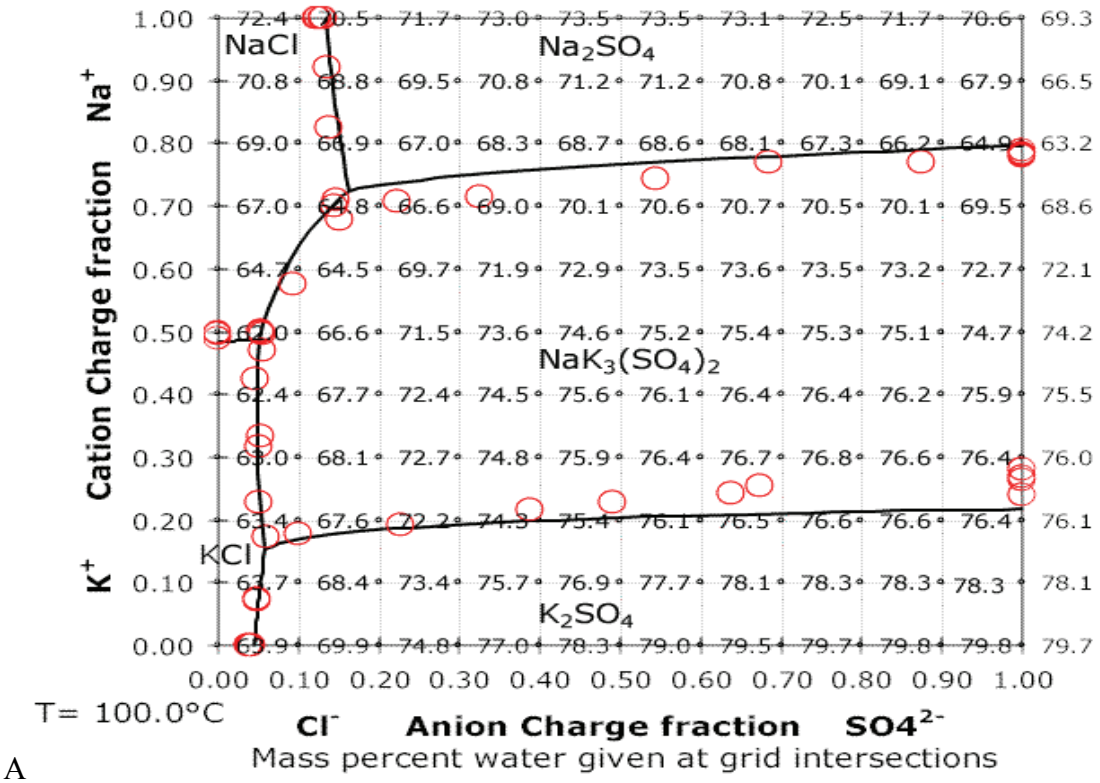

Appendix A

Figure 11: The (Na^+, K^+) - (Cl^-, SO_4^{2-})-H_2O system at 100°C (Aqueous Electrolytes, 2007)

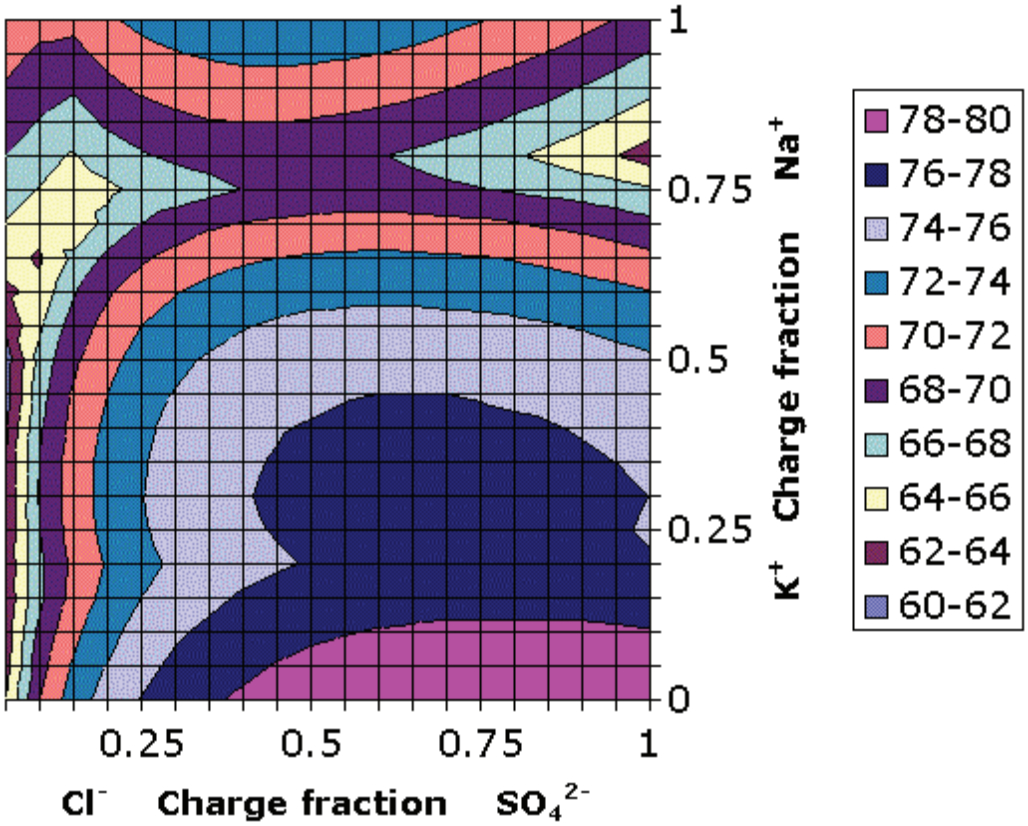

Figure 12: The (Na^+,K^+) - (Cl^-,SO_4^{2-})-H_2O system at 100°C, shown as a contour plot, the contours mark the water content in mass percent (Thomsen, 2007)

6 EXPERIMENTAL STUDIES – KINETIC CONSIDERATIONS

6.1 Kinetic considerations

6.1.1 Na_2SO_4 binary and synthetic brine systems

The main focus of these experiments was on establishing the recovery and purity of sodium sulphate. Table 6 gives the species used to prepare the synthetic brine.

Table 6: Composition of Brine

Species
Na_2SO_4
NaCl
KCl
KF
KNO_3
$Li_2SO_4 \cdot 1H2O$
$CaSO_4 \cdot 2H2O$
$MgSO_4 \cdot 7H2O$
$(NH_4)Cl$

Table 7 summarises the matrix of experiments that were carried out by outlining the aim and conditions at which each experiment was run.

The experiments carried out encompass a range of brine compositions from the simple, pure, synthetic, binary Na_2SO_4-H_2O system (E1) through to the complex, synthetic, multi-component system (E2). Experiment E3 investigated a pure, ternary, Na_2SO_4-NaCl-H_2O brine as well as the effect of an increase in the NaCl concentration in experiments E4 and E5.

Table 8 (page 21) gives the compositions of the experimental streams.

6.1.2 Experimental set-up and operation

A 12 ℓ scraped cooled wall crystalliser (SCWC) was used for conducting batch crystallization experiments in which the scraper speed was set to 20 rpm, sufficient for good mixing. Cooling was achieved using a Lauda Kryomat RUK90S cooling unit. Built-in Labview™ software allowed for the recording and capturing of temperature readings every 10 seconds using the ASL F250 precision thermometer connected to a PT-100 temperature sensor with an accuracy of ±0.01°C. The sensors were placed at various points in the reactor to record, the change in temperature of the reactant solution and temperatures of the inlet and outlet streams of the coolant. The flowrate of the coolant, Kryo 85™, was kept constant at 1500 kg/hr and a recycle stream, which also served as a sampling outlet, was maintained at 1.2 kg/min. Each experiment was repeated three times and the results presented are the means.

6.1.3 Solution Preparation

Weighed quantities of analytical grade (> 99 wt%) salts were dissolved in 10 ℓ of ultra pure water (18 mΩ) using an overhead stirrer for 30 minutes to obtain a homogeneous solution. The synthetic solutions were subsequently transferred to the crystallizer. For these experiments, the minor ions (F^-, Cl^-, K^+, Li^+, Mg^{2+}, Ca^{2+}, NO_3^- and NH_4^+) in solution were treated as impurities in the system.

Table 7: Matrix of experimental work for $Na_2SO_4 \cdot 10H_2O$ system

Experiment number	Aim	Concentration (wt% $Na_2SO_4 \cdot 10H_2O$)	Conditions
E1: Binary Na_2SO_4- water	Determine the eutectic composition and temperature of a synthetic, binary Na_2SO_4-water system for comparison with data obtained from literature	5 wt% Na_2SO_4	• Batch operated • Cooling maintained at -5°C throughout the experiment • No seeds added
E2: Na_2SO_4-brine system	Investigate the eutectic conditions of Na_2SO_4 from the concentrated RO retentate stream. Determine the shape, size and purity of the salt and ice crystals produced	4 wt% Na_2SO_4	• Batch operated • Cooling maintained at -5°C throughout the experiment • No seeds added
E3: Na_2SO_4 – NaCl system	Determine the recovery of $Na_2SO_4.10H_2O$ from a concentrated NaCl stream Determine the size, shape and purity of the salt crystals formed from this stream	4 wt% Na_2SO_4 20 wt% NaCl	• Batch operated • Reactant solution was cooled at a rate of 5°C/hr for 6 hours, thereafter the coolant liquid temperature was maintained at a constant temperature of -25°C until the system reached eutectic conditions. • Seeded with 5 g/ℓ ice seeds at various temperatures: -10°C, -15°C and -19°C.
E4: Na_2SO_4 – NaCl system	Determine the recovery of $Na_2SO_4 \cdot 10H_2O$ from a concentrated NaCl stream Determine the eutectic temperature for the pure binary system Determine the size and purity of the salt crystals formed from this stream	4 wt% Na_2SO_4 23.5 wt% NaCl	• Reactant solution was cooled at a rate of 5°C/hr for 6 hours; thereafter the coolant liquid temperature was maintained at a constant temperature of -25°C until the system reached eutectic. • This system was seeded with 5 g/ℓ seeds at -19°C.
E5: Na_2SO_4 – NaCl brine system	Investigate the eutectic conditions of the Na_2SO_4 from the concentrated RO retentate stream Determine the shape and purity of the salt and ice crystals produced	4 wt% Na_2SO_4 23.5 wt% NaCl	• Reactant solution was cooled at a rate of 5°C/hr for 6 hours; thereafter the coolant liquid temperature was maintained at a constant temperature of -25°C until the system reached eutectic. • This system was seeded with 5 g/ℓ of ice seeds at -19°C.

Table 8: Compositions of the synthetic experimental streams investigated

Experiment Species	E1 Na_2SO_4-H_2O mol/kg	E2 Na_2SO_4- Brine mol/kg	E3 Na_2SO_4- NaCl- H_2O mol/kg	E4 Na_2SO_4- NaCl-H_2O mol/kg	E5 Na_2SO_4- NaCl-Brine mol/kg
Na_2SO_4	0.352	0.287	0.296	0.38842	0.0287
NaCl		0.0594	2.05	5.54	0.3478
NH_4^+		0.0014			0.0079
Li^+		0.0007			0.0013
K^+		0.0004			0.0329
Mg^{2+}		0.0001			0.0005
Ca^{2+}		0.0116			0.0012
F^-		0.0004			0.0026
NO_3^-		0.0004			0.0023
Remaining Cl^-		0.0062			0.0360
Remaining SO_4^{2-}		0.0120			0.0043

6.1.4 Sampling and Analysis

Twenty millilitre filtered samples were taken at 30 minute intervals and analysed using ion chromatography (± 2.5% error) to measure the cations and anions in the mother liquor and the impurity content of the salt crystals produced. Micrographs of the ice and salt crystals were taken using the Nikon Optiphot 200 microscope and the size was determined visually using image analysis software, Image Pro Plus 5. The moisture content of the salt crystals was determined via thermal analysis using the Denver Instrument Company: Mark 2 Moisture Analyser to establish the hydrate number of the salt crystals produced.

Before reporting on the results of the experimental studies for the binary Na_2SO_4-water system, it must be noted that the original RO retentate streams to be studied contained <3 wt% salt content and were therefore very dilute. Thus, using this original system produced a substantial ice slurry without any salt recovery being achieved due to the solubilities of the various salts never being exceeded. Therefore, the streams presented in Table 1 have been concentrated to ensure that the solubility of Na_2SO_4 was exceeded during the experimental studies.

6.1.5 Results and discussion

i Experiment E1: The binary Na_2SO_4-water system

Figure 13 (Thomsen, 2007) shows the binary phase diagram for the Na_2SO_4 – water system. The diagram shows the regions of stability for various hydrates of sodium sulphate as a function of concentration and temperature. Sodium sulphate exists in three hydrated forms: anhydrous Na_2SO_4, $Na_2SO_4 \cdot 7H_2O$ and $Na_2SO_4 \cdot 10H_2O$ (Lide, 2006). The transition point, where the stable crystalline form of sodium sulphate changes from Na_2SO_4 to $Na_2SO_4.10H_2O$, is at a concentration of approximately 33.13 wt% and 32.27°C. Thus, for this research, the focus is on the lower temperature region where $Na_2SO_4.10H_2O$ is the dominant crystalline form of the sodium sulphate.

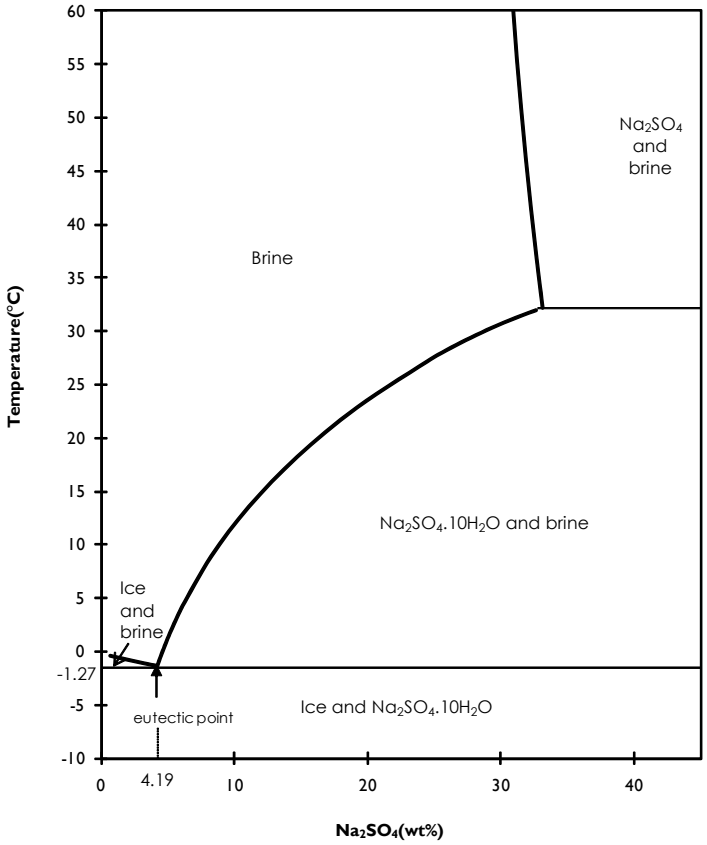

Figure 13: Binary phase diagram for Na_2SO_4 – water showing regions of stable phases (Thomsen, 2007)

Figure 14 presents the temperature of the 5 wt% Na_2SO_4 reactant solution as a function of time. The reported eutectic temperature and composition for a binary $Na_2SO_4.10H_2O$ system is -1.2°C and 3.8 wt% (Pronk, 2007; Vaessen, 2003). The system reached supersaturation at a temperature of -0.96°C (point A) where the first salt crystals were visible. Upon further cooling, there was an increase in salt crystallization, resulting in the reactant solution decreasing in concentration until point B was reached where ice began to crystallise out simultaneously with the salt product at a temperature of -2.27°C. The release of the crystallization enthalpy at the nucleation point resulted in the sudden rise of the reactant temperature to -1.27°C. After a short period of time the temperature of the system gradually began to rise to -1.24°C where it reached a plateau and the concentration at the eutectic temperature was measured to be approximately 4 wt%. This is in good agreement with values reported above.

Conclusions:

- The eutectic temperature and concentration of the binary Na_2SO_4-water system studied was determined experimentally to be -1.24°C and approximately 4 wt%, which is in good agreement with literature.

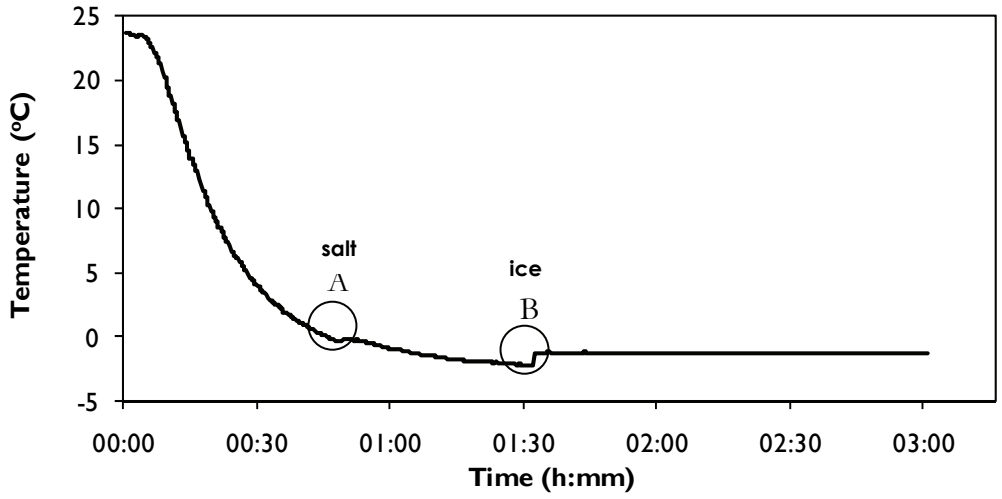

Figure 14: Graph showing the temperature profile for a 5 wt% Na_2SO_4 – H_2O system cooled from ambient to eutectic

ii Experiment E2: The Na_2SO_4-brine system

A synthetic reverse osmosis retentate with a 4 wt% Na_2SO_4 concentration containing the following impurities (F^-, Cl^-, K^+, Li^+, Mg^{2+}, Ca^{2+}, NO_3^- and NH_4^+) was investigated to determine the effect on the eutectic point of the system as well as to monitor crystal size and purity. The coolant temperature was maintained at -5°C. Figure 15 gives the temperature profile for the reactant solution for the above system. Point C is the point where the first $Na_2SO_4 \cdot 10H_2O$ crystals were produced at 0.38°C. This is significantly higher than the temperature of the pure binary system. The presence of 0.06 m NaCl in the brine decreased the solubility of the $Na_2SO_4 \cdot 10H_2O$ ion by the common ion effect, resulting in the higher $Na_2SO_4 \cdot 10H_2O$ nucleation temperature. The ice nucleation (point D) occurred at a temperature of -2.75°C. As the ice crystallized, releasing the heat of fusion, the energy release caused the temperature of the overall system to increase until equilibrium was reached at the eutectic point of -2.22°C, which is also significantly lower than the pure binary system. This shows that the presence of impurities (F, Cl, K, Li, Mg, Ca, NO_3 and NH_4), even in low concentrations, have a clear effect on the eutectic temperature by depressing the freezing point of ice and, subsequently, the eutectic point.

Figure 16 shows the concentration of the different components measured as a function of time. Between 60 and 150 minutes, a decrease in the concentration of the Na^+ and SO_4^{2-} ions was noted, corresponding to the crystallization phase between the temperature jump at point C and D where only $Na_2SO_4.10H_2O$ is crystallised. After 150 minutes, where both ice and salt crystals are produced, the concentration of the Na^+ and SO_4^{2-} ions remained more or less constant, close to the composition of the eutectic point, while the concentration of the remaining ions started to increase due to the removal of water from solution in the form of ice.

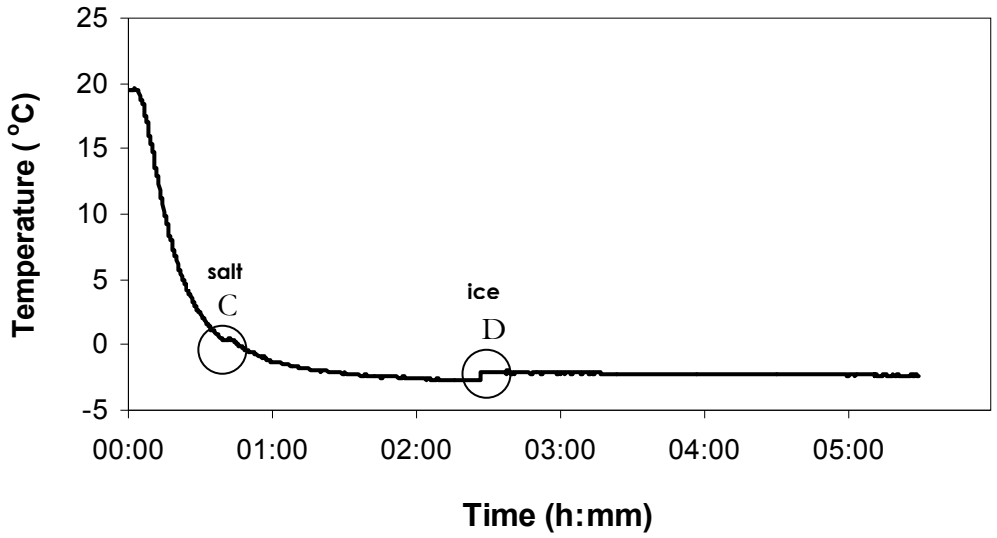

Figure 15: Temperature profile for a 4 wt% Na2SO4 –brine system cooled down from ambient to eutectic

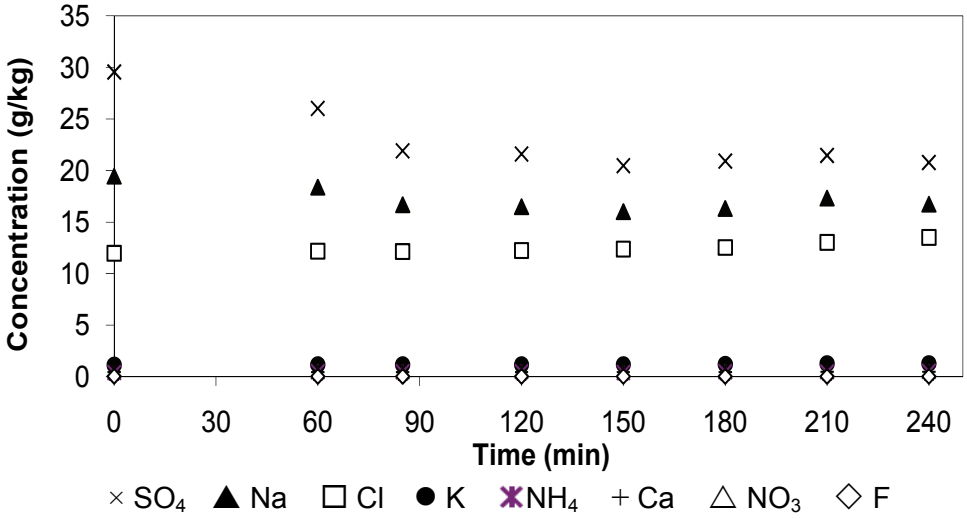

Figure 16: Change in concentration of the different ions in solution for a 4 wt% Na_2SO_4 – brine system cooled down from ambient to eutectic (No error bars presented as study was only carried out once)

The $Na_2SO_4 \cdot 10H_2O$ crystals presented in Figure 17 do not show any imperfections that could result in impurities being incorporated into the crystal structure. The well faceted crystals are prismatic and monoclinic in shape. The size range was approximately 20-100 μm at one residence time after reaching the eutectic point. (τ = 30min). After three residence times the crystal sizes were 50-350 μm. The ice crystals produced ranged from 100-450 μm and contained an impurity content of <20 ppm after seven washing stages with super-cooled water.

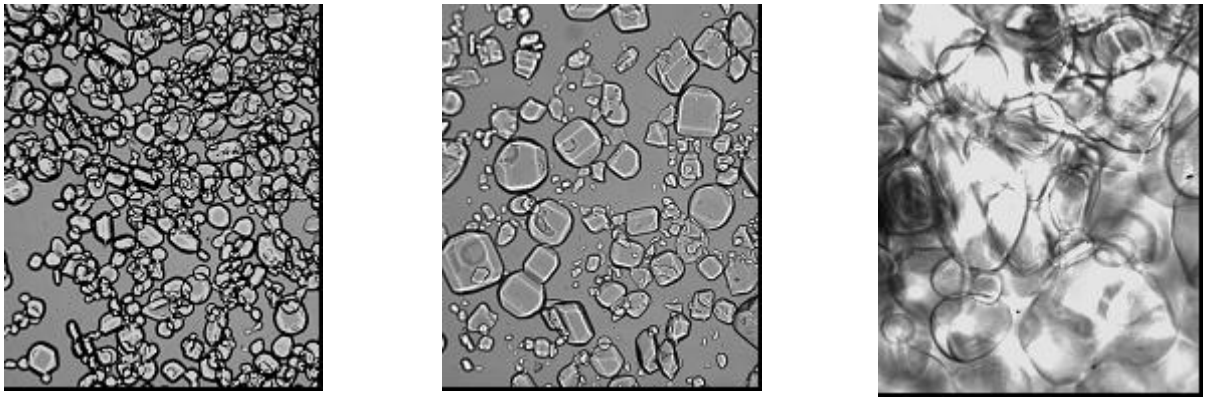

(a) (b) (c)

Figure 17: Micrographs of $Na_2SO_4 \cdot 10H_2O$ crystals after 1τ(a) and after 3τ(b) {Scale bar = 300 µm}. Micrograph (c) represents the ice crystal product after 3τ {Scale bar = 400 µm}

The $Na_2SO_4 \cdot 10H_2O$ crystals were washed initially with a saturated solution of sodium sulphate and then with ethanol to remove any impurities. The crystals were analysed to determine if there were any traces of impurities within the crystal structure. The analysis showed that 100% pure crystals were produced from the synthetic reverse osmosis retentate stream. A thermal analysis was carried out on a small amount of washed salt product (1.5g) to determine the hydrate number of the crystals. $Na_2SO_4 \cdot 10H_2O$ is unstable and, with a melting point of 32.1°C (Lide, 2006), it loses the waters of crystallization quickly. The analysis showed a loss of mass of approximately 56% which corresponds to a ten water hydrate.

Conclusions:

- The presence of low concentrations of F^-, Cl^-, K^+, Li^+, Mg^{2+}, Ca^{2+}, NO_3^- and NH_4^+ impurities in a Na_2SO_4 – water system depresses the eutectic point of $Na_2SO_4.10H_2O$ crystallization from -1.24°C to -2.22°C.
- Using EFC, pure water crystals were obtained (<20 ppm impurities) from a synthetic retentate stream after seven washing steps.
- Very pure $Na_2SO_4 \cdot 10H_2O$ crystals, without any detectable impurities, were produced from a synthetic retentate stream using a batch eutectic freeze process.
- Salt crystal sizes ranged from 20-100 µm after 1τ to 50-350 µm after three residence times.
- Ice crystals produced were 100-450µm in size
- Thermal analysis revealed that the crystals produced were $Na_2SO_4 \cdot 10H_2O$.

iii Experiment E3: The 4 wt% Na_2SO_4 – 20 wt% NaCl system

Due to the high concentration of NaCl, the common ion effect reduced the solubility of $Na_2SO_4.10H_2O$ and the system reached the meta-stable point with regards to $Na_2SO_4.10H_2O$ crystallization (visual observation) at approximately 11.64 wt% and 10.45°C. However, the temperature "jump" only occurred when the reactant solution reached 6.68 wt% and 3.1°C respectively. At the moment, there is no clear explanation for this "jump", as there is no other hydrate of Na_2SO_4 that exists at that temperature and no other salt crystallized during the experiment. The system was seeded with 5g/ℓ ice seeds at various temperatures: -10°C, -15°C and -19°C. Only at -19°C was the system sufficiently supersaturated for the ice seeds to create nucleation.

This is an extremely significant drop in the freezing point of the water in the system. Upon further cooling, the system reached a plateau at -21.22°C, which is in good agreement with the temperature reported by Marion and Farren (1999) as the eutectic temperature for a H_2O- Na_2SO_4-NaCl system, which was -21.34°C (calculated). The concentration of NaCl in this study is much lower than that reported by Marion and Farren, and therefore explains the lack of recovery of halite from the system.

Figure 18 shows the theoretical recovery of $Na_2SO_4 \cdot 10H_2O$ as a function of time. The recovery was calculated from the chemical analysis of the ions remaining in solution, as filtering the entire 10 ℓ of solution was not feasible. It was assumed that the depletion of sulphate ions from the solution was entirely due to the formation of $Na_2SO_4 \cdot 10H_2O$. 270 minutes after nucleation, a 90% recovery of $Na_2SO_4 \cdot 10H_2O$ is seen at a temperature of -15°C. This has significant implications for sequentially removing salts from the brine.

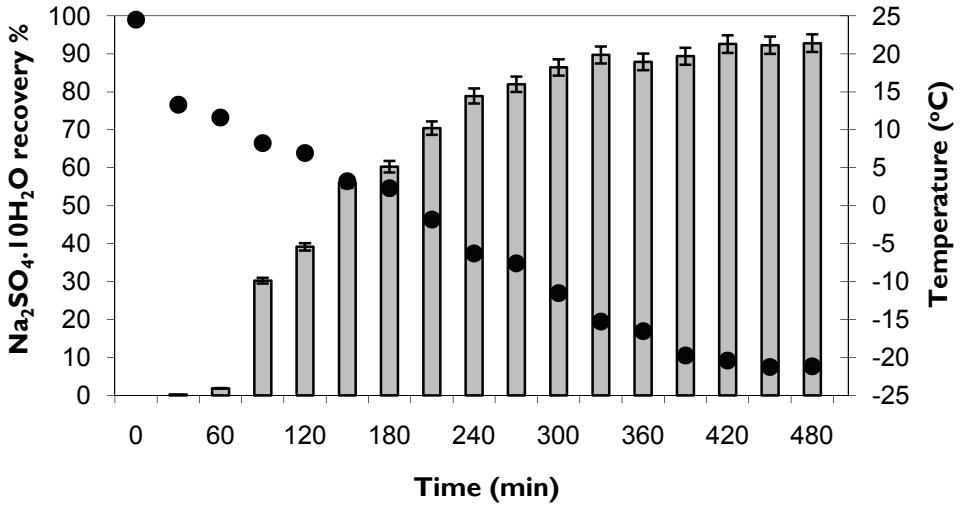

Figure 18: Theoretical recovery of $Na_2SO_4 \cdot 10H_2O$ (bars) from a concentrated NaCl solution at with decreasing temperature (dots) over time. Errors bars denote error in measurement of $Na_2SO_4 \cdot 10H_2O$.

Figure 19 shows the trend in the concentrations of the different ions as the system is cooled to the eutectic point. The decrease in the concentration of SO_4^{2-} ions reflects the recovery of the $Na_2SO_4 \cdot 10H_2O$ already shown in Figure 19. The increase in concentration of Cl^- ions indicates that the system became concentrated with respect to $NaCl \cdot 2H_2O$, due to the crystallization of ice and $Na_2SO_4 \cdot 10H_2O$, however, the solubility limit for NaCl was never reached and no $NaCl \cdot 2H_2O$ crystals were produced. This was further confirmed by a chemical analysis of the salt crystals. The study revealed a recovery of >90% of sodium sulphate with $Na_2SO_4 \cdot 10H_2O$ crystal sizes ranging from 50-400 μm.

Conclusions

- For a 4 wt% Na_2SO_4 – 20 wt% NaCl system, the solubility of Na_2SO_4 was lowered due to the common ion effect. The metastable point with respect to $Na_2SO_4 \cdot 10H_2O$ crystals was reached at 6.6 wt% and 3.1°C. At the same time, there was a strong depression of the freezing point of water to -19°C.
- The eutectic point for the 4 wt% Na_2SO_4 – 20 wt% NaCl system was found to be -21.22°C.
- Mirabilite crystals without any traces of impurities were produced from this system.

- Salt crystal sizes ranged from 50-400 μm
- A recovery of >90% pure $Na_2SO_4 \cdot 10H_2O$ crystals with sizes ranging from 50 to 400 μm was obtained from a concentrated NaCl stream prior to any sodium chloride crystals being produced. This has significant implications for possible sequential removal of salts from a brine.

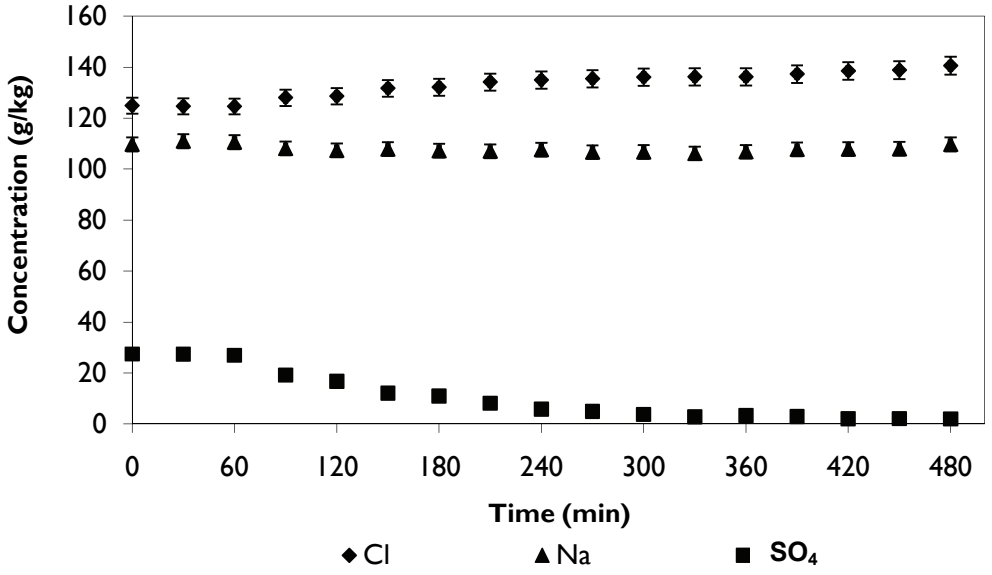

Figure 19: Graph showing the concentration profile of the ions in solution as a function of times

iv Experiment E4: The 4 wt% Na_2SO_4 - 23.5 wt% NaCl system

Conditions

- Reactant solution was cooled at a rate of 5°C/hr for 6 hours; thereafter the coolant liquid temperature was maintained at a constant temperature of -25°C until the system reached eutectic conditions.
- This system was seeded with 50 g/ℓ ice seeds at -19°C.

Discussion

This was a repeat of experiment E3 with an increased concentration of NaCl from 20 wt% to 23.5 wt%. This increase was necessary to ensure the crystallization of the $NaCl \cdot 2H_2O$. In this system, the meta-stable point for $Na_2SO_4 \cdot 10H_2O$ crystallization occurred at 10.45°C, which was similar to Experiment E3 where there was a 20 wt% concentration of NaCl. It was expected that the nucleation temperature would occur at a higher temperature due to the increased presence of Na^+ ions in the system. In the presence of ice seeds, the system did not reach its solubility limit with respect to ice until -22.5°C. The system reached the eutectic at approximately -21.29°C.

Presented in Figure 20 is the concentration profile showing the change in concentration of the Na^+, SO_4^{2-} and Cl^- ions. There is a definite decrease in the mass of sulphate ions from approximately 30 g/kg to approximately 2 g/kg indicating a greater than 90% recovery of $Na_2SO_4 \cdot 10H_2O$. An increase in the Cl^- ions is expected as the system becomes more concentrated in the NaCl due to the removal of the $Na_2SO_4 \cdot 10H_2O$. The majority of the Na^+ ions exist as a result of the NaCl concentration, and hence very little change is seen in the concentration of the Na^+ ions over time, even though the SO_4^{2-} concentration is almost depleted. In addition, concentration trends are given in terms of mass and not moles, hence the change seems minimal.

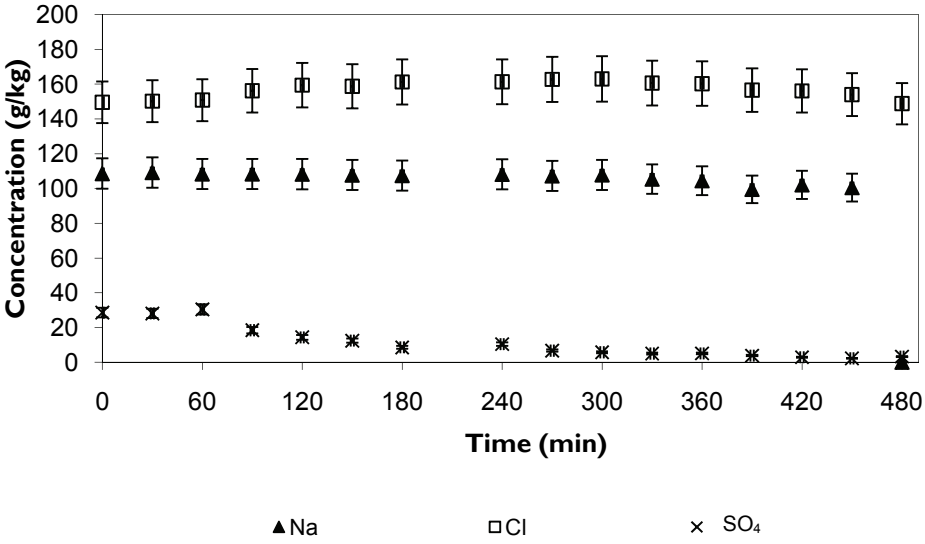

Figure 20: Graph showing the change in concentration of the different ions in solution for a 4 wt% Na_2SO_4 – 23.5 wt% NaCl system cooled down from ambient to eutectic conditions

The recovery of $Na_2SO_4 \cdot 10H_2O$ as a function of temperature is presented in Figure 21. It can be seen that a greater than 90% recovery was achieved, which occurred at approximately -21.29°C. This is evidence that pure $Na_2SO_4 \cdot 10H_2O$ crystals can be recovered prior to the crystallization of $NaCl \cdot 2H_2O$. The $Na_2SO_4 \cdot 10H_2O$ did not show any imperfections. The well faceted crystals were prismatic and monoclinic in shape.

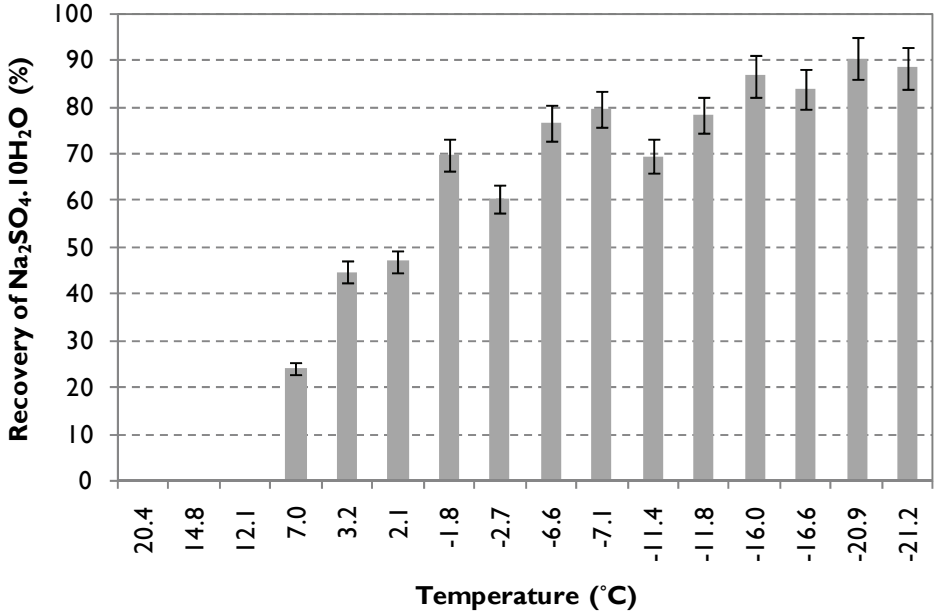

Figure 21: Graph showing the theoretical recovery of $Na_2SO_4.10H_2O$ from a concentrated NaCl solution at with decreasing temperature

Conclusions

- The ternary Na_2SO_4-NaCl-H_2O system reached its eutectic point at approximately -21.29°C.
- The $Na_2SO_4 \cdot 10H_2O$ nucleated at 10.45°C. There was no significant change in the nucleation temperature as compared with Experiment E3 results.
- The ice reached its solubility limit at -22.5°C.
- Greater than 90% of the $Na_2SO_4 \cdot 10H_2O$ crystals were recovered from this system

- The $Na_2SO_4 \cdot 10H_2O$ crystals were pure and prismatic and monoclinic in shape.
- No $NaCl \cdot 2H_2O$ was found to crystallise in this system.

v Experiment E5: The 4 wt% Na_2SO_4 - 23.5 wt% NaCl – Brine system

Conditions

- Reactant solution was cooled at a rate of 5°C/hr for 6 hours; thereafter the coolant liquid temperature was maintained at a constant temperature of -25°C until the system reached eutectic.
- This system was seeded with 5 g/ℓ ice seeds at -19°C.

Discussion

Figure 22 gives the change in concentration of the cations and anions for the above system. A decrease in the concentration of the SO_4^{2-} ions is seen. In this system, $Na_2SO_4 \cdot 10H_2O$ crystallized at 9.08°C. The ice nucleated at -21.85°C. The system reached the ternary eutectic point at -21.27°C at which all three crystal phases were present.

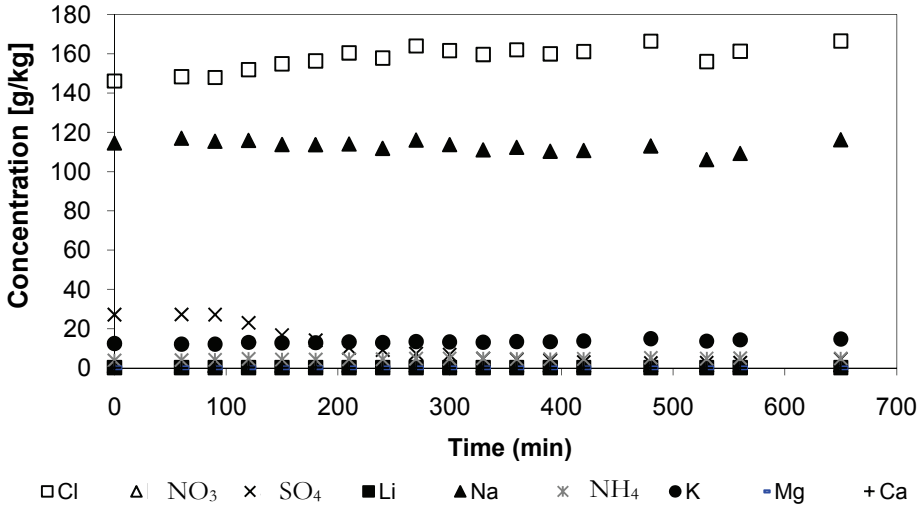

Figure 22: Graph showing the change in concentration of the different ions in solution for a 4 wt% Na_2SO_4 – 23.5 wt% NaCl – brine system cooled down from ambient to eutectic (No error bars presented as study was only carried out once)

The $NaCl \cdot 2H_2O$ crystals were highly unstable and dissolved readily (Figure 23(b)) once removed from the reactor. The crystals are hexagonal in shape, which can be seen clearly in Figure 23(c). The figures below show the various crystals present in the reactor. At the lower temperatures, due to the high solid content in the reactor, separation of ice and salt crystals proved difficult.

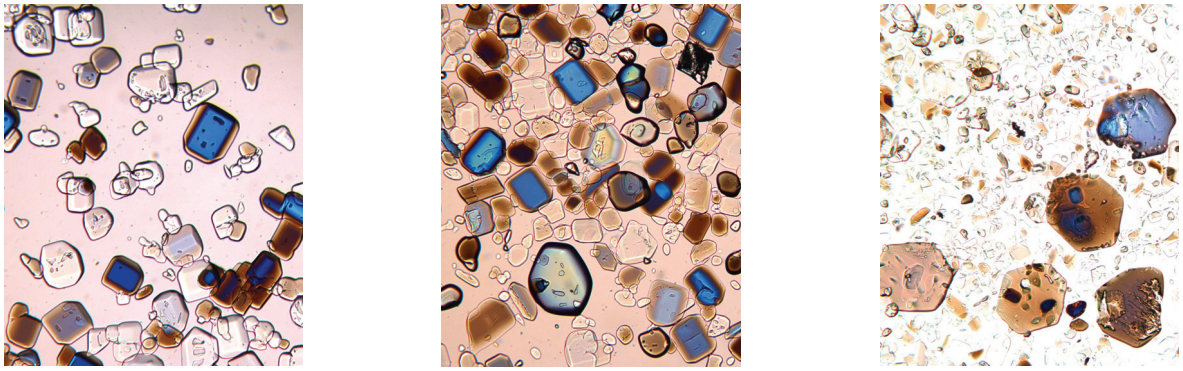

(a) (b) (c)

Figure 23: (a) $Na_2SO_4 \cdot 10H_2O$ crystals present in the reactor at 0°C, (b) $Na_2SO_4 \cdot 10H_2O$ and $NaCl \cdot 2H_2O$ crystal present at -21.27°C, (c) $NaCl \cdot 2H_2O$ crystals present in the ice filter cake

Figure 24 shows the presence of impurities, Mg^{2+}, K^+ and Ca^{2+}, with the crystallization of the salt products. The thermodynamic modelling results of the stream for Experiment E5 do not show the crystallization of the impurities since they will not be incorporated into the crystal lattice, but entrained with the mother liquor. Experimentally, from a chemical analysis of the salt crystals, traces of impurities were found.

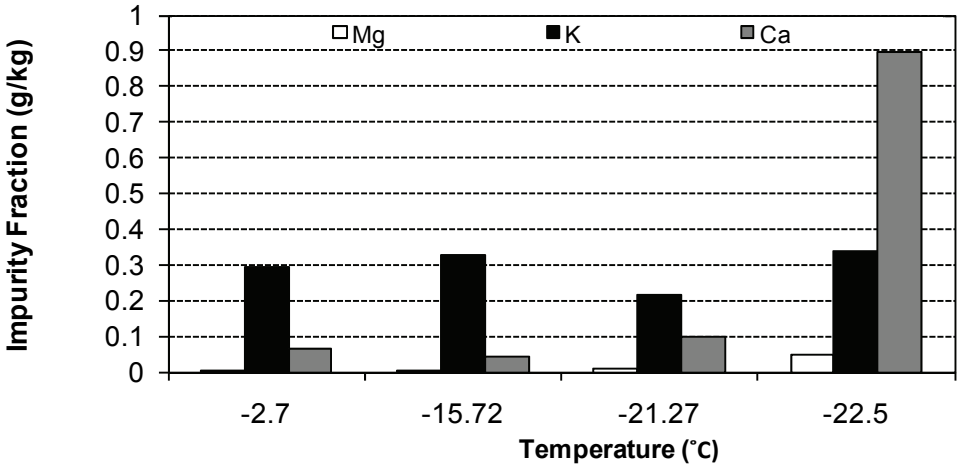

Figure 24: Graph showing the impurity concentration in the $Na_2SO_4 \cdot 10H_2O$ and $NaCl \cdot 2H_2O$ crystals produced from the 4 wt% Na_2SO_4 – 23.5 wt% NaCl - brine system cooled down from ambient to eutectic at various points during the crystallization process

Conclusions

- The $Na_2SO_4 \cdot 10H_2O$ nucleated at 9.08°C, whereas the ice nucleated at -21.85°C.
- The presence of impurities did not have a significant impact on the eutectic point of the system. The system reached the eutectic point at -21.27°C.
- At this low eutectic temperature, the production of ice was high, leading to the crystalliser contents forming a slush mixture of ice and salt. Therefore, the purity of ice could not be determined owing to the difficulty in separation of the ice and salt from the crystalliser. Hence, it is important to establish the critical solid mass content within the reactor.

6.2 Metastable zone width for the binary sodium sulphate system

6.2.1 Materials and methods

i Solution preparation

Sodium sulphate solutions were prepared from 99 wt% Na_2SO_4 (Merck) and de-ionized water of 18.2 mΩ. Table 9, Table 10 and Table 11 indicate the concentrations for the experiments at a cooling rate of 1.5°C/hour, 4°C/hour and 6°C/hour respectively. Experiments E_e, L_e and Q_e were concentration ranges around the eutectic point for ice while F_e, M_e and R_e were for concentration ranges around the eutectic point for salt.

Table 9: Experiments used to determine the MSZW at a cooling rate of 1.5°C/hour

	wt% Na_2SO_4 (anhydrous)					Solid phase
Exp #	**1**	**2**	**3**	**4**	**5**	**formed**
Exp A	1.04	1.05	1.05			ice
Exp B	2.00	2.02	2.02			ice
Exp C	2.87	2.89				ice
Exp D	3.44	3.47	3.55	3.64		ice
Exp $E_{eutectic}$	4.32	4.46	4.64	4.72	4.79	ice
Exp $F_{eutectic}$	4.76	4.79	4.84	5.12	5.12	salt
Exp G	5.95	5.97				salt
Exp H	6.81	6.81				salt
Exp I	8.18	8.18	8.20			salt

Table 10: Experiments used to determine the MSZW at a cooling rate of 4°C/hour

	wt% Na_2SO_4 (anhydrous)		Solid phase
Exp #	**1**	**2**	**formed**
Exp J	3.36	3.36	ice
Exp K	3.46	3.46	ice
Exp L_e	3.85		ice
Exp M_e	4.25		salt
Exp N	4.51	4.51	salt
Exp O	4.96	4.96	ice

Table 11: Experiments used to determine the MSZW at a cooling rate of 6°C/hour

	wt% Na_2SO_4 (anhydrous)			Solid phase
Exp #	**1**	**2**	**3**	**formed**
Exp P	3.47	3.47		ice
Exp $Q_{eutectic}$	4.5	4.76	4.8	ice
Exp $R_{eutectic}$	4.5	4.5	4.76	salt
Exp S	5.27	5.27		salt

ii Experimental setup

Experiments were performed in a 250 mℓ jacketed glass reactor. The reactor had a four blade baffle installed and a Heidolph overhead stirrer to provide adequate mixing. The stirrer was a 6 blade rushton turbine. The rotation of the stirrer was 300 rpm for all experiments. Cooling was achieved by circulating methanol through the reactor jacket with a Lauda RE207, thermostatic unit. A 712 Metrohm conductometer was used to measure the conductivity of the solution. A Testo 175-177 temperature logging device was used to measure the solution temperature of the reactor, the chiller temperature and the outlet temperature of the coolant from the reactor.

iii Experimental procedure

All experiments were performed batchwise. An experiment was initiated by maintaining the solution temperature at approximately 1.5°C or a chiller temperature set point of 0°C for approximately 30 minutes or until the temperature of the system had stabilized. The specific cooling rate was then applied until the first sudden temperature increase, indicating nucleation had occurred. The formation of ice or salt could be easily recognized from visual observation and confirmed by a sudden change in the conductivity reading. The nucleation temperatures together with their corresponding concentrations were used to determine the MSZW.

During seeded experiments ice and salt seeds were added and the temperature of the solution was cooled at the same cooling rate. For some seeded experiments the temperature was kept constant after the addition of the seed. All experiments were stopped once excessive ice scaling occurred.

6.2.2 Results and discussions

At the thermodynamic eutectic temperature (-1.27°C) the solubility is 4.4 g/100g H_2O, while at the transition temperature (32°C) from the hydrous form to the anhydrous form, the solubility is 48 g/100g H_2O. Thermodynamically, only ice and salt ($Na_2SO_4.10H_2O$) will form below the eutectic temperature.

i Nucleation temperature for unseeded experiments

The nucleation temperature is defined as the temperature at which a crystal begins to nucleate. The observed sudden increase in temperature is as a result of the release of crystallization heat (Vaessen et al., 2003). Figure 25 shows the change in temperature and conductivity for a dilute sodium sulphate system. The initial temperature drop is due to the cooling of the solution to the initial solution starting temperature of 1.5°C. The system was left at this temperature for approximately 15 minutes, after which the linear cooling rate of 1.5°C/hour was applied. The solution temperature increases dramatically when ice crystals form. The heat of crystallization of ice is 325 kJ/kg implying that for every kilogram of ice that is formed, 325 kJ of energy is released. The temperature of the solution reaches a constant value of approximately 0°C. This is the temperature at which ice reaches a new equilibrium with the aqueous solution. The solution temperature will increase only if the energy that is released is greater than the energy removed from the system by the thermostatic unit. The increase in temperature could be due to the nucleation of a significant number of crystals or the inadequate heat removal by the chiller.

The conductivity measurement is used to distinguish between ice and salt formation. The point on the phase diagram denoting a dilute system will be to the left of the binary eutectic point of the sodium sulphate phase diagram. A dilute system will always form ice first. This is confirmed by a measured conductivity increase.

The sudden conductivity drop visible in Figure 25 is as a result of the sudden temperature change when ice nucleation occurs and is not an indication of salt nucleation.

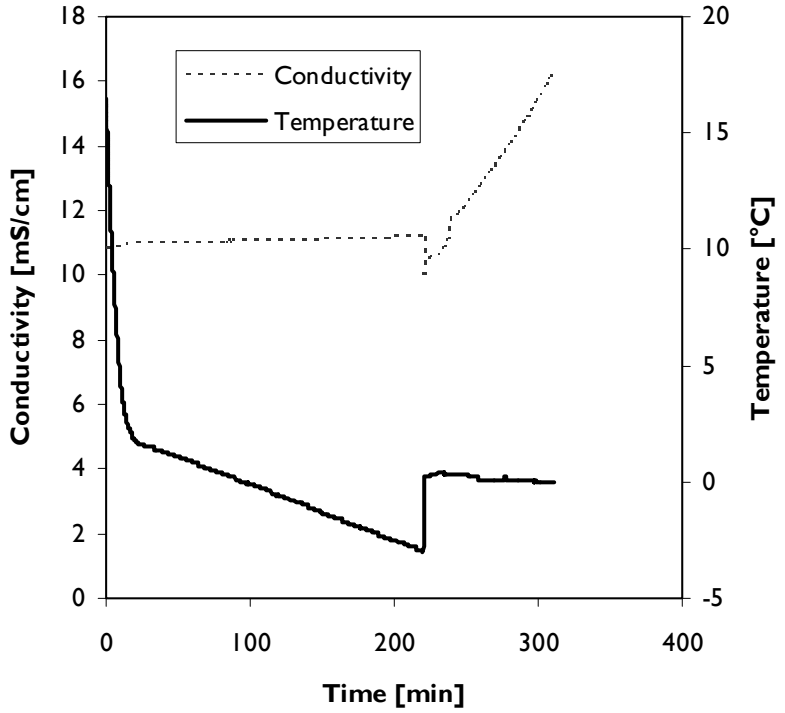

Figure 25: Change in temperature and conductivity during the nucleation process for a dilute Na_2SO_4-H_2O system

ii The operating region for the Na_2SO_4-H_2O system at a cooling rate of 1.5°C/hour

Table 12 shows the calculations using the least squares method of linear regression for the determination of the average metastable boundary ice line for a sodium sulphate solution at a cooling rate of 1.5°C/hour. The $\sum(\Delta T^2)$ corresponds to a y-intercept value of -4.315 for the trendline and minimized residual.

Figure 26 (page 35) shows the trendline through the experimental data, T_{nuc}, for sodium sulphate at a cooling rate of 1.5°C/hour using the data from Table 12. The average MSZW is given by the difference between the y-intercepts of the ice line and the trendline, which gives a value of 4.1°C. Generally, the MSZ is wider in the region of ice line for the sodium sulphate system. The data points are scattered and follow the same trend as the thermodynamic ice line until beyond the thermodynamic eutectic composition (4.2 wt%) at which point the number of data points increases and become more clustered. This could be attributed to the fact that the ice line is generally for dilute systems. A dilute system will have fewer solute molecules dissolved in the solvent and hence the probability that these molecules will collide with each other is lower compared to a more concentrated system. The reason for the large scatter is that the nucleation event is dependent on the probability that two molecules will meet, combine and form crystal nuclei.

Figure 27 (page 35) indicates that the MSZ for the ice line, with a supercooled temperature of -4.1°C, is on average 1.2°C wider that of the salt line, with a supercooled temperature of -2.9°C. The metastable salt line follows the same trend as the thermodynamic salt line. However, salt does not form to the right of the thermodynamic eutectic composition. This is different to the trend of the metastable ice line. Also, the salt data points are generally closer to the thermodynamic salt line compared to the ice data points in the ice region of the phase diagram. There is a small region to the right of the thermodynamic eutectic composition where either ice or salt could form first. If the salt forms first in this region it will generally form at a higher temperature. For a certain cooling rate,

ice nucleation will exceed the thermodynamic eutectic point to a certain limit. The composition at which this limit occurs is termed the kinetic eutectic composition. The kinetic eutectic composition for a sodium sulphate system cooled at a rate of 1.5°C/hour is 4.79 wt%.

Table 12: Trendline determination for the average metastable boundary ice line of a sodium sulphate system at a cooling rate of 1.5°C/hour

Na_2SO_4								
wt%	**T_{trend}**	**T_{nuc}**	**Abs T_{trend}**	**Abs T_{nuc}**	**T_{max}**	**T_{min}**	**ΔT**	**ΔT^2**
1.04	-4.6	-1.82	4.6	1.82	4.6	1.82	2.78	7.71
1.05	-4.6	-4.4	4.6	4.4	4.6	4.4	0.2	0.04
1.05	-4.6	-5.78	4.6	5.78	5.78	4.6	1.18	1.4
2	-4.86	-5.1	4.86	5.1	5.1	4.86	0.24	0.06
2.02	-4.86	-6.2	4.86	6.2	6.2	4.86	1.34	1.8
2.02	-4.86	-5.92	4.86	5.92	5.92	4.86	1.06	1.12
2.87	-5.09	-7.46	5.09	7.46	7.46	5.09	2.37	5.61
2.89	-5.1	-6.08	5.1	6.08	6.08	5.1	0.98	0.97
3.44	-5.24	-4.48	5.24	4.48	5.24	4.48	0.76	0.58
3.47	-5.25	-5.34	5.25	5.34	5.34	5.25	0.09	0.01
3.55	-5.27	-5.84	5.27	5.84	5.84	5.27	0.57	0.32
3.64	-5.3	-7.28	5.3	7.28	7.28	5.3	1.98	3.93
4.32	-5.48	-4.1	5.48	4.1	5.48	4.1	1.38	1.91
4.46	-5.52	-3.64	5.52	3.64	5.52	3.64	1.88	3.54
4.64	-5.57	-3.66	5.57	3.66	5.57	3.66	1.91	3.64
4.72	-5.59	-6.76	5.59	6.76	6.76	5.59	1.17	1.37
4.79	-5.61	-3.54	5.61	3.54	5.61	3.54	2.07	4.29
							$\sum(\Delta T^2)$	38.28

Where:
T_{trend} – temperature at the trendline corresponding to a fixed composition,
T_{nuc} – nucleation temperature obtained from experimental runs,
Abs – absolute value,
T_{max} – maximum temperature,
T_{min} – minimum temperature,
ΔT – difference between maximum temperature and minimum temperature.

The trendlines in Figure 27 can be viewed as the average MSZ line. They are useful only for determining nucleation parameters for a specific system and provide little practical significance alone since there is still the chance that spontaneous nucleation will occur above the trendline. The MSZW must therefore be defined as the region where spontaneous nucleation cannot occur. Another method is therefore to define the operating region as that region above the highest nucleation temperature at a specific concentration. This will then give the region where spontaneous nucleation will not occur.

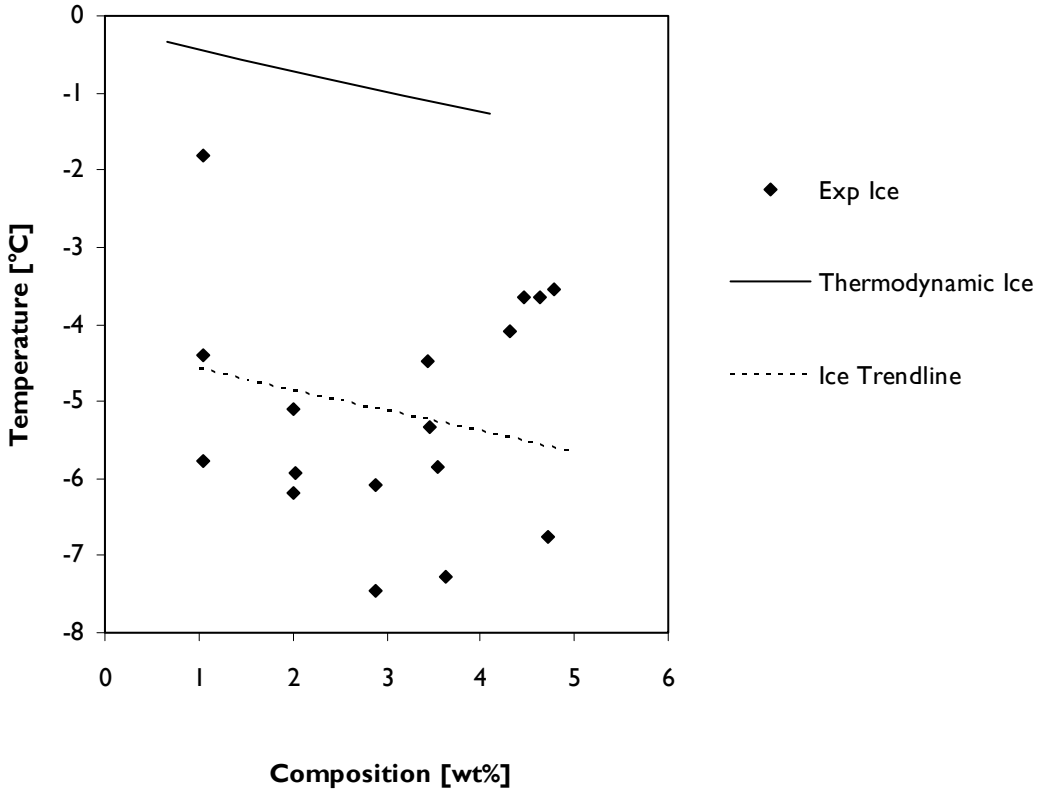

Figure 26: The average metastable boundary ice line for a Na_2SO_4-H_2O system solution at 1.5°C/hour

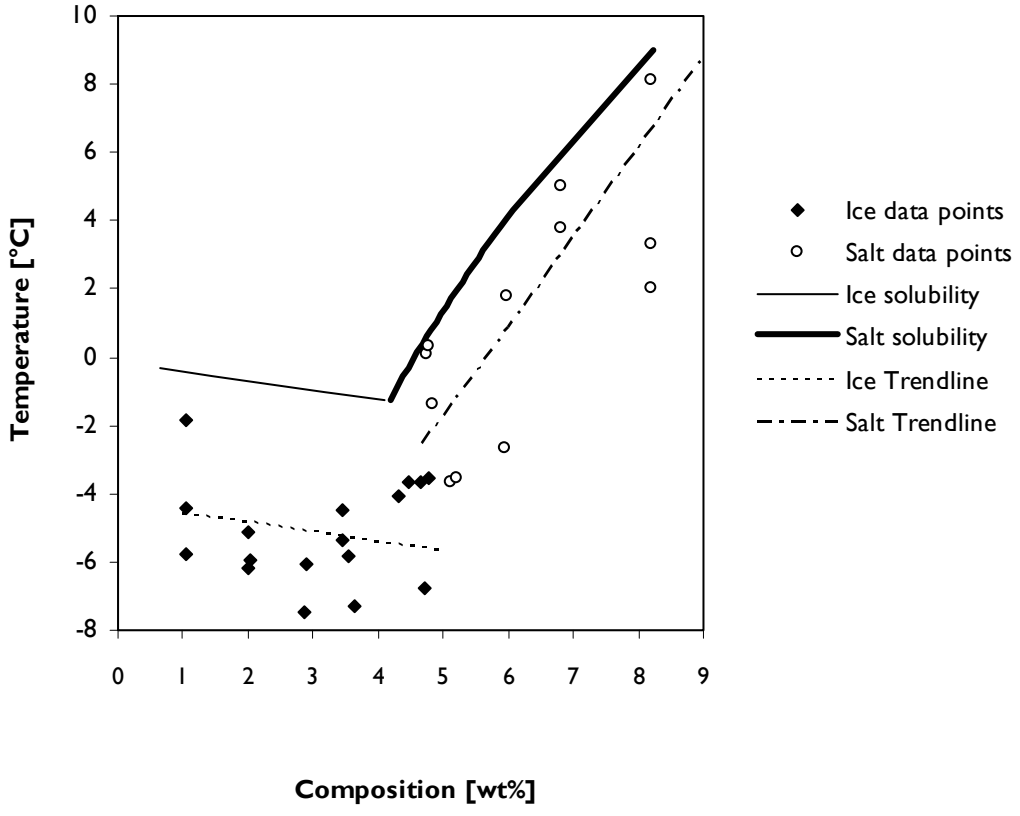

Figure 27: MSZ boundary for sodium sulphate at a cooling rate of 1.5°C/hour

iii The operating region for Na_2SO_4 at a cooling rate of 4°C/hour

A faster cooling rate should result in a wider MSZW. The thermodynamic line can be thought of as a line that is obtained from an infinitely slow cooling rate since this line is at equilibrium. A faster cooling rate should therefore result in a line that is further from this equilibrium line. Figure 28 shows the salt trendline and ice trendline for a sodium sulphate system at a cooling rate of 4°C/hour. The ice data are once again further from the thermodynamic ice line compared to the salt data which are closer to the thermodynamic salt line. The average MSZW for the ice trendline is 4.5°C, which is 0.4°C higher than the average MSZW obtained for a cooling rate of 1.5°C. This increase in the MSZW is expected. The average MSZW for the salt line is, however, 2.1°C which is 0.8°C smaller than the MSZW for a cooling rate of 1.5°C/hour. This could be attributed to the few data points on which this average MSZW is based. Since the nucleation event is highly dependent on the probability that two molecules will combine to form a nuclei or cluster it seems plausible then that the data points do not give an accurate assessment of the actual MSZW.

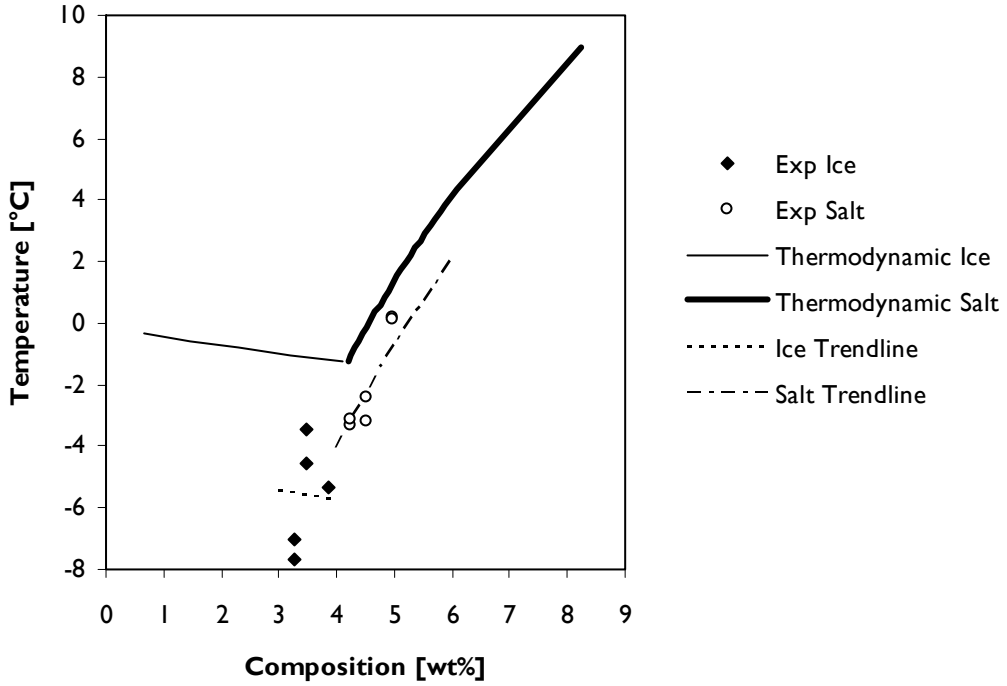

Figure 28: Ice trendline and salt trendline for a sodium sulphate solution at a cooling rate of 4°C/hour

iv The operating region for Na_2SO_4 at a cooling rate of 6°C/hour

The width of the MSZW for the ice line at a cooling rate of 6°C/hour is 5.5°C, while the width of the MSZW for the salt line is 3.4°C (Figure 29).

The kinetic eutectic composition is around 4.5 wt%. Once again ice nucleation occurs after the thermodynamic eutectic point. This is slightly lower than the kinetic eutectic composition obtained at a cooling rate of 1.5°C/hour. It would seem then that the range from the thermodynamic eutectic point becomes narrower with a faster cooling rate. This trend was not observed for a cooling rate of 4°C/hour.

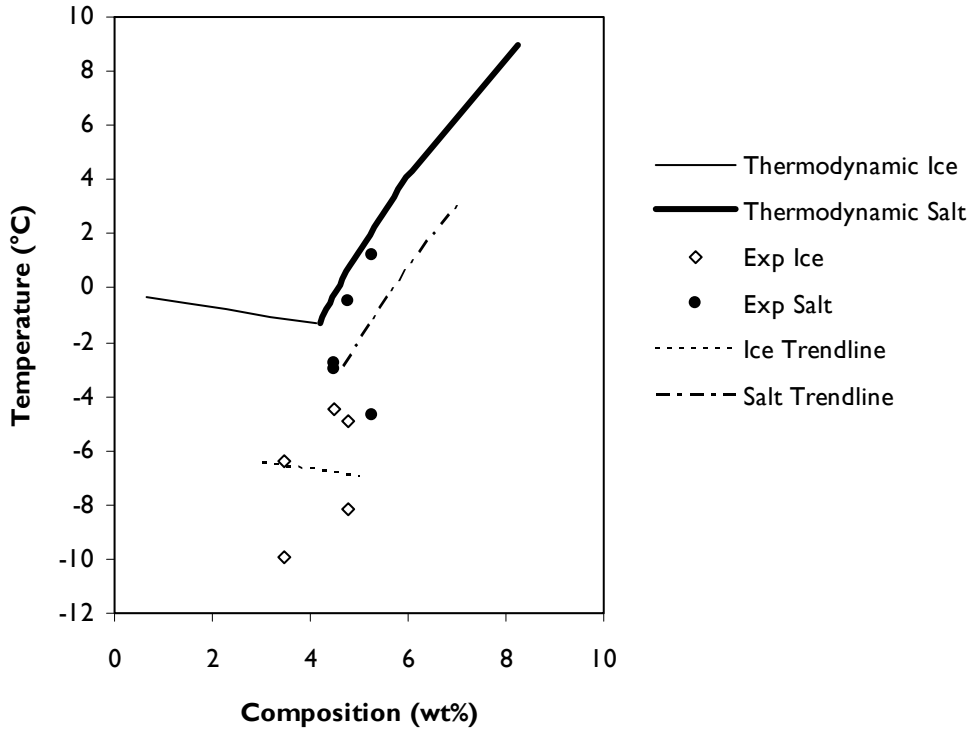

Figure 29: Ice trendline and salt trendline for a sodium sulphate solution at a cooling rate of 6°C/hour

Figure 30 is a comparison of three cooling rates, namely 1.5°C/hour, 4°C/hour and 6°C/hour. There is a large difference for the ice line compared to the salt line. Table 13 shows this comparison. The maximum undercooling increases as the cooling rate is increased for the ice line but this trend is not followed for the salt line. This could be attributed to the fact that too few data points were used to obtain the maximum undercooling and since the nucleation temperature is a probability event, this could have resulted in this unexpected trend.

Table 13: Maximum undercooling for sodium sulphate at different cooling rates.

Cooling Rate (°C/hour)	Maximum undercooling (°C)	
	Ice line	Salt line
1.5	4.2	2.9
4	4.5	2.1
6	5.5	3.4

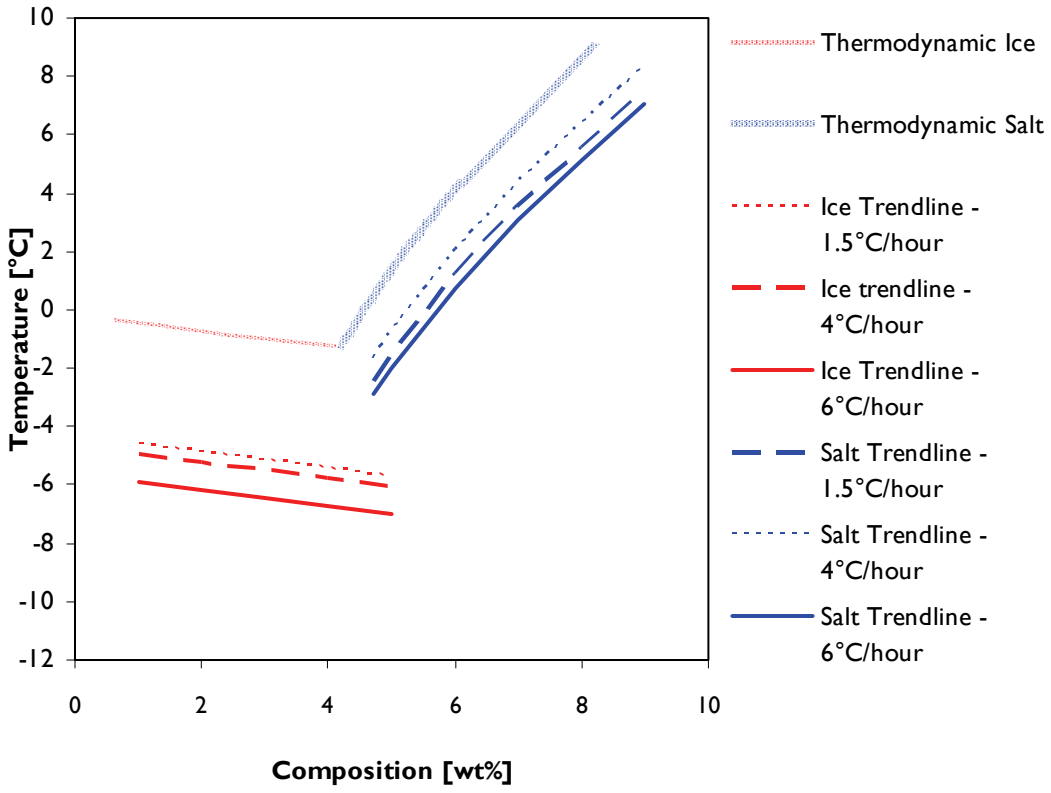

Figure 30: Comparison of the MSZW for sodium sulphate at a cooling rate of 1.5°C/hour, 4°C/hour and 6°C/hour

v Using seeding to validate the MSZW of Na_2SO_4

The width of the metastable region can be validated with seeding. Figure 31 shows a run for a seeded experiment. Sodium sulphate seed crystals were added at around 160min resulting in an increase in the solution temperature and a decrease in the conductivity thus confirming the formation of salt crystals. There is a gradual temperature increase due to the heat of crystallization of salt that is released. The heat of crystallization for sodium sulphate (243kJ/kg) is lower than that of ice resulting in a smaller temperature rise. This could also be attributed to fewer salt crystals forming in the same time period as ice crystal formation resulting in a lower energy release. It is also interesting to note that the conductivity decreases sharply for the duration that the temperature rises for salt formation and that when the original cooling rate is resumed, the conductivity gradually decreases until ice nucleation occurs. The temperature change during ice formation is much larger than the salt temperature change indicating more ice crystals are formed in a given time.

Figure 32 shows a region around the eutectic point of sodium sulphate where salt seeds were added. The Na_2SO_4 seeds were added within the MSZW so that ice nucleation could be suppressed. The seeds were added at a random solution temperature of -2.2°C but still within the MZSW. The solution was cooled to below -3.62°C to test the accuracy of the experimentally determined MSZW since this is the approximate temperature of the MSZ for a composition near the eutectic. Salt seeding will only suppress ice formation within the MSZW. Once the limits of the MSZ have been reached, ice nucleation will occur. The seeded solution formed ice at a temperature of -3.54°C. According to Figure 31, ice should have formed around -3.62°C. This is a small difference of 0.08°C thus confirming the accuracy of the MSZW for sodium sulphate.

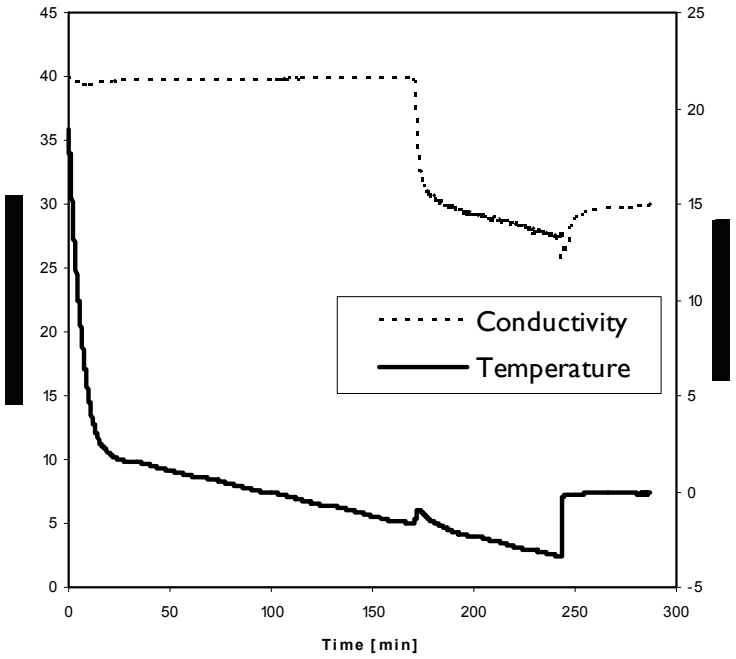

Figure 31: Seeding experimental run to validate the MSZW of sodium sulphate

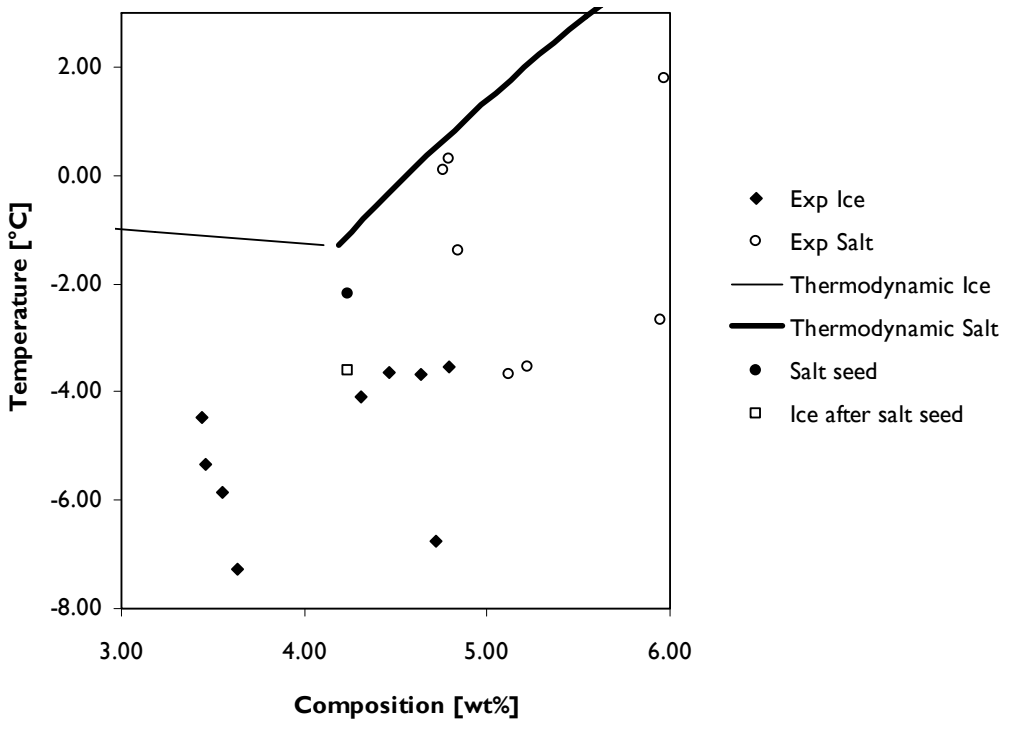

Figure 32: Seeding experiment to validate the MSZW of sodium sulphate at a cooling rate of 1.5°C/hour

6.3 The metastable zone width for the binary magnesium sulphate system

6.3.1 Materials and methods

i. Solution preparation

Magnesium sulphate solutions were prepared from 99 wt% $MgSO_4.7H_2O$ (Merck) and de-ionized water of 18.2 mΩ. Table 14 indicates the concentrations for various experiments at a cooling rate of 1.5°C/hour. A total volume of 250 mℓ of solution was used in all experiments.

Table 14: Experiments used to determine the MSZW at a cooling rate of 1.5°C/hour

	wt% $MgSO_4$ (anhydrous)				
Exp #	1	2	3	4	5
Exp A	1.91	1.91	1.93	1.93	1.93
Exp B	6.03	6.04	6.05		
Exp C	9.21	10.63			
Exp D	12.20	12.20	12.23	12.24	
Exp E	13.75	14.44	14.56		
Exp F	15.24	15.94	15.94		
Exp G	16.11	16.68	16.95	17.47	
Exp $H_{eutectic}$	18.55	18.62	18.68	18.82	
Exp $I_{eutectic}$	19.25	19.37	19.53		
Exp J	20.13	20.28			

ii. Experimental setup and procedure

The same setup used for the sodium sulphate experiments was used for magnesium sulphate experiments.

6.3.2 Results and discussions

i. The operating region for $MgSO_4$ at a cooling rate of 1.5°C/hour

Table 15 shows the calculations using the least squares method of linear regression for the determination of the ice line for a magnesium sulphate solution at a cooling rate of 1.5°C/hour.

These data are then used to plot the trendline through the experimentally determined nucleation temperatures, T_{nuc}. The plot is shown in Figure 33. It is interesting to note that once again, irrespective of the system, the more dilute a system is, the wider the MSZ.

Figure 34 shows both the ice trendline and the salt trendline. The salt nucleation begins close to the thermodynamic eutectic composition. The nucleation temperatures for salt are also generally at a higher temperature and closer to the salt thermodynamic line with one data point appearing on the actual line. The metastable eutectic composition (18.82 wt%) for a magnesium sulphate system at a cooling rate of 1.5°C/hour is very close to the thermodynamic eutectic composition of 18.83 wt%. The range from this point (18.82 wt%) to the first salt nucleation (19.25 wt%) is 0.42 wt%. The ice trendline has an average undercooling of 3.1°C while the salt line has an average undercooling of 2.0°C.

Table 15: Trendline determination for the ice line of a magnesium sulphate system at a cooling rate of 1.5°C/hour

wt%	T_{trend}	T_{nuc}	Abs T_{trend}	Abs T_{nuc}	Max T	Min T	ΔT	ΔT^2
1.91	-3.36	-3.08	3.36	3.08	3.36	3.08	0.28	0.08
1.91	-3.36	-3.08	3.36	3.08	3.36	3.08	0.28	0.08
1.93	-3.36	-5.00	3.36	5.00	5.00	3.36	1.64	2.68
1.93	-3.36	-4.90	3.36	4.90	4.90	3.36	1.54	2.36
1.93	-3.36	-3.90	3.36	3.90	3.90	3.36	0.54	0.29
6.03	-3.98	-5.60	3.98	5.60	5.60	3.98	1.62	2.63
6.04	-3.98	-5.40	3.98	5.40	5.40	3.98	1.42	2.02
6.05	-3.98	-5.00	3.98	5.00	5.00	3.98	1.02	1.04
9.21	-4.60	-5.18	4.60	5.18	5.18	4.60	0.58	0.34
10.63	-4.95	-5.52	4.95	5.52	5.52	4.95	0.57	0.33
12.20	-5.42	-6.40	5.42	6.40	6.40	5.42	0.98	0.97
12.20	-5.42	-6.60	5.42	6.60	6.60	5.42	1.18	1.39
12.23	-5.43	-5.10	5.43	5.10	5.43	5.10	0.33	0.11
12.24	-5.43	-5.94	5.43	5.94	5.94	5.43	0.51	0.26
13.75	-5.98	-4.62	5.98	4.62	5.98	4.62	1.36	1.84
14.44	-6.26	-5.14	6.26	5.14	6.26	5.14	1.12	1.25
14.56	-6.31	-6.18	6.31	6.18	6.31	6.18	0.13	0.02
15.24	-6.62	-6.60	6.62	6.60	6.62	6.60	0.02	0.00
15.94	-6.96	-6.82	6.96	6.82	6.96	6.82	0.14	0.02
15.94	-6.96	-5.20	6.96	5.20	6.96	5.20	1.76	3.09
16.11	-7.04	-6.98	7.04	6.98	7.04	6.98	0.06	0.00
16.68	-7.34	-5.10	7.34	5.10	7.34	5.10	2.24	5.03
16.95	-7.49	-6.32	7.49	6.32	7.49	6.32	1.17	1.38
17.47	-7.79	-6.30	7.79	6.30	7.79	6.30	1.49	2.22
18.55	-8.47	-9.00	8.47	9.00	9.00	8.47	0.53	0.28
18.62	-8.52	-9.00	8.52	9.00	9.00	8.52	0.48	0.23
18.68	-8.56	-8.10	8.56	8.10	8.56	8.10	0.46	0.21
18.82	-8.65	-6.86	8.65	6.86	8.65	6.86	1.79	3.20

$\sum(\Delta T^2)$	33.35

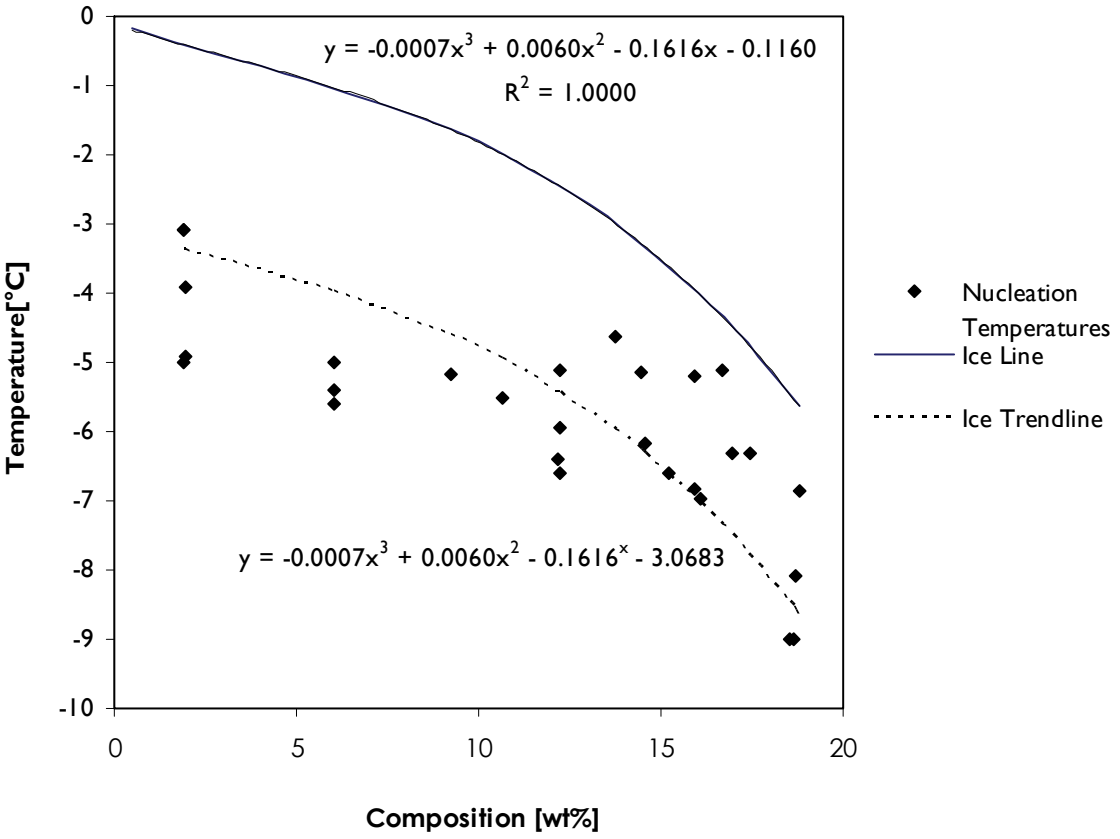

Figure 33: Ice trendline for a $MgSO_4$-H_2O system at a cooling rate of 1.5°C/hour

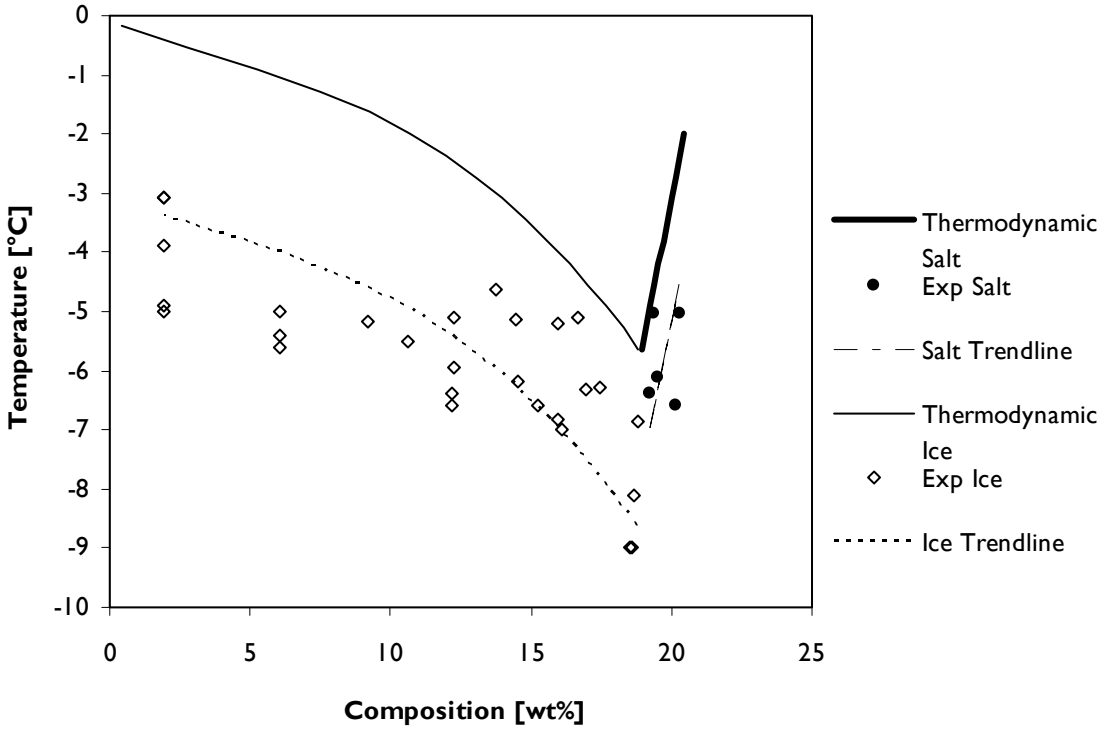

Figure 34: Ice trendline and salt trendline for a magnesium sulphate solution at a cooling rate of 1.5°C/hour

6.4 Conclusions from experimental studies

In summary, the results of the experimental work aimed at investigating the effect of complex aqueous chemistry and impurities on the EFC process showed that the eutectic temperature for a pure binary system of Na_2SO_4-H_2O is -1.24°C and for a pure ternary system of Na_2SO_4-NaCl-H_2O is -21.29°C. The presence of impurities, even in small concentrations, had a significant impact on the eutectic temperature of the binary system and depressed the eutectic temperature to -2.22°C. The results also showed that pure ice and pure salt crystals could be recovered from a dilute brine stream. The solid mass content, i.e. the amount of ice and salt crystals, in the reactor was identified to be of significant importance as it directly affected the purity and yield of the crystalline product. Hence, the salt to ice ratio needs to be controlled by ice removal rate.

The study showed that the MSZ for ice was generally wider than that for salt, regardless of the cooling rate used. For the sodium sulphate system, a faster cooling rate resulted in a wider MSZ. The difference in the nucleation temperatures for repeat experiments was attributed to the stochastic nature of nucleation.

The findings from the experimental work have emphasised the importance of identifying the appropriate EFC operating conditions (operating temperatures and the operating region within the phase diagram) in order to promote good product characteristics and maximise yields.

7 PRELIMINARY COSTS AND ECONOMIC BENEFITS OF APPLYING EFC

The key objective of the preliminary economic evaluation study of EFC was to provide an approximation of the expected operating and capital expenditure costs associated with using this novel technology for the treatment of a model brine that is broadly representative of a South African industrial brine i.e. brines typically consisting of Na_2SO_4 and NaCl such as the TRO Secunda described in Table 16.

Owing to the fact that, by and large, the largest operating cost for an EFC process is the electricity requirement for the compressor in the refrigeration unit that is used to cool down the brine stream, this was used as the principal basis for evaluating the operating cost for EFC. The inclusion of other less substantial peripheral operating costs such as the cooling water make up requirements fall outside the scope of this particular study and would need to be taken into account for a more detailed economic evaluation.

An economic evaluation using evaporative crystallization as an alternative treatment method to EFC is presented for comparison purposes. Whilst both EFC and evaporative crystallization significantly reduce the volume of the brines that would otherwise need to be stored in evaporation ponds, it is important to note that for a mixture of salts, EFC has the potential to separate the salts into pure products that can be sold and the income generated from the sale of these salts used to offset the operating costs. In contrast, evaporative crystallization typically produces a mixed salt, which subsequently needs to be disposed of – further adding to the operating cost. Furthermore, the revenue obtained by the sale of the pure salts produced by EFC is not included in this study.

7.1 Development of the brine-specific EFC operating temperature and process flow sheet

A brine of a similar composition to that of the TRO Secunda brine described in Table 1 excluding the minor elements (Brine 1) and a brine with a higher NaCl and Na_2SO_4 salt concentration (Brine 2) were used as a basis for this preliminary economic evaluation of EFC. Table 16 shows the composition of the two brines.

Table 16: Composition of Brine 1 and Brine 2

Brine 1		Brine 2	
Ions	Concentration [mg/ℓ]	Ions	Concentration [mg/ℓ]
Cl^-	2260	Cl^-	80800
SO_4^{2-}	7440	SO_4^{2-}	37400
Na^+	5027	Na^+	70300

7.1.1 Thermodynamic predictions of salt and ice crystallization temperatures

The prediction of salt and ice crystallization was carried out using OLI Stream Analyser due to its ability to accurately simulate aqueous chemistry at high ionic strengths.

Figure 35 shows the prediction of the successive crystallization of the various salts for 1 litre of Brine 1 with a reduction in the solution temperature from right to left on the x-axis. The results show that once the temperature reaches 0°C ice crystallizes out, followed by $Na_2SO_4.10H_2O$ at -1°C and $NaCl.2H_2O$ at -23°C.

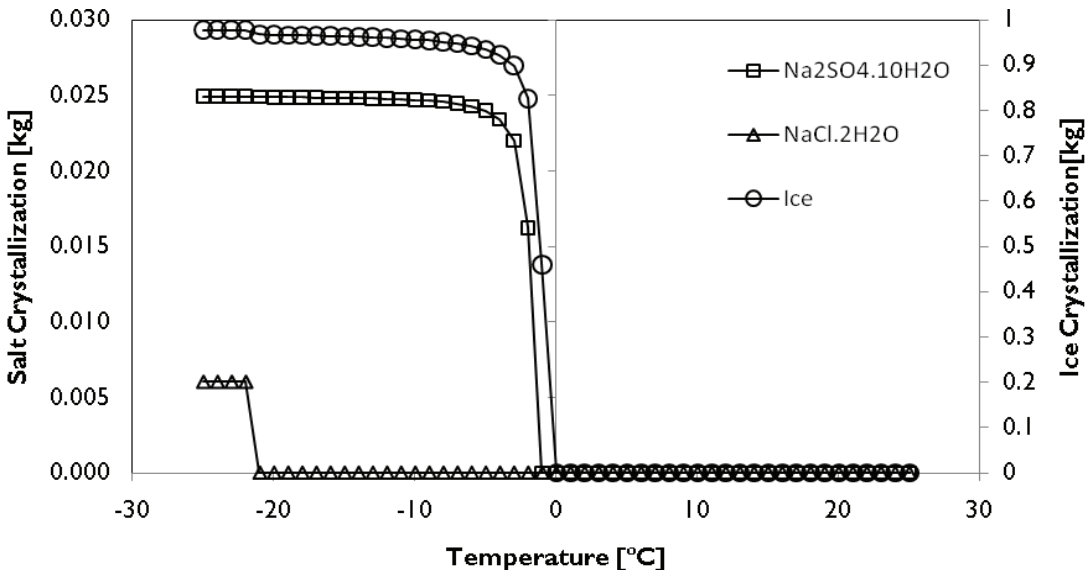

Figure 35: Thermodynamically predicted salt and ice crystallization temperatures for Brine 1 (Basis = 1 litre of brine)

Figure 36 shows the prediction of the successive crystallization of the various salts for Brine 2 with a reduction in the solution temperature from right to left on the x-axis. The results show that once the temperature reaches 14°C $Na_2SO_4.10H_2O$ crystallizes out, followed by ice at -9°C and $NaCl.2H_2O$ at -21°C.

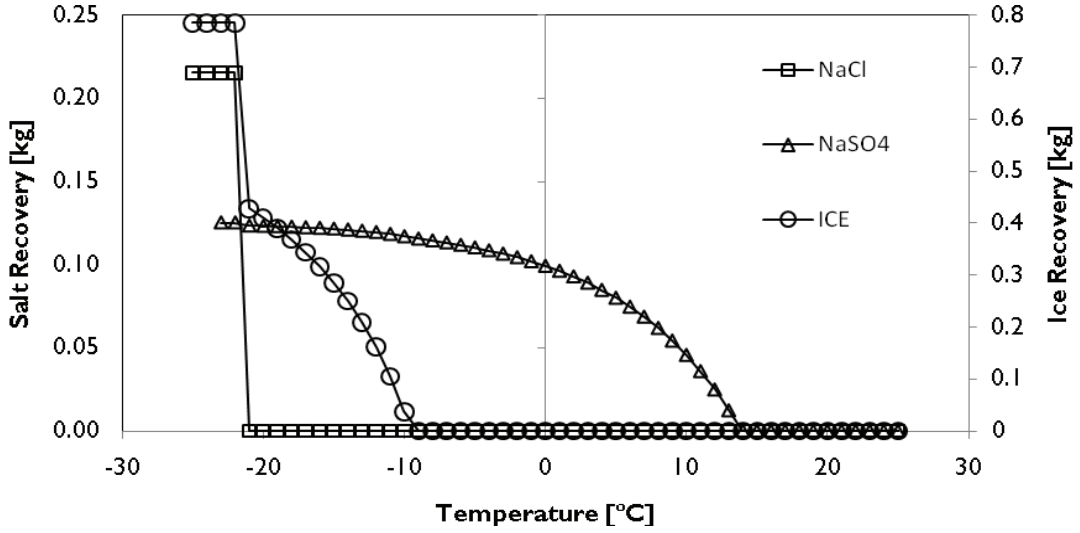

Figure 36: Thermodynamically predicted salt and ice crystallization temperatures for Brine 2 (Basis = 1 litre of brine)

7.1.2 Selecting the operating temperatures for the EFC process

Based on the thermodynamic modelling results shown in Figure 35 and Figure 36 there are two distinct operating regimes for both brines where, sequentially, the ice and $Na_2SO_4.10H_2O$ can be crystallized out in the first crystallizer operating at a higher temperature followed by ice and $NaCl.2H_2O$ in the second crystallizer operating at a lower temperature.

For Brine 1 the operating temperature for the first freeze crystallizer was selected to be -10°C in order to maximise the $Na_2SO_4.10H_2O$ recovery and to ensure sufficient undercooling for kinetic reasons. The operating temperature for the second, lower temperature crystallizer was set at -23°C.

For Brine 2 the operating temperature for the first freeze crystallizer was selected to be -16°C in order to maximise the $Na_2SO_4.10H_2O$ recovery and to ensure sufficient under cooling for kinetic reasons. The operating temperature for the second, lower temperature crystallizer was set at -23°C.

7.1.3 EFC process flow sheet

Based on the selected operating temperatures for the EFC process the following basic sequential EFC process flow sheet was used:

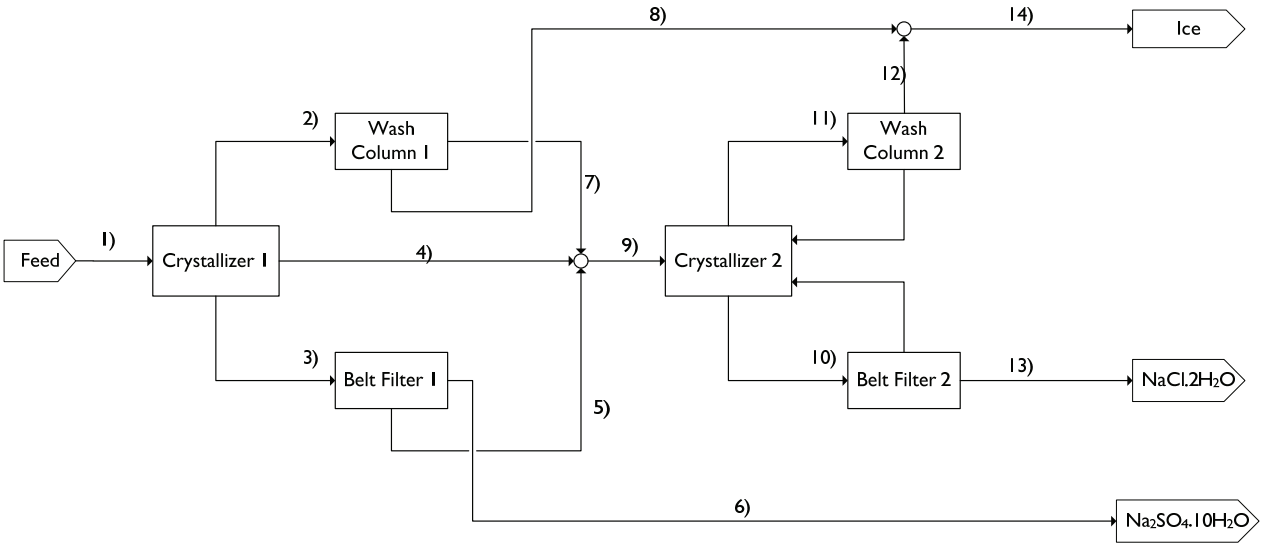

Figure 37: Basic sequential EFC process flow sheet for Brines 1 and 2

7.2 EFC operating cost approximation based on the refrigeration compressor duty

For this study a single stage refrigeration system was set up in Aspen Plus® as shown in Figure 38.

The selection of the refrigerant was based on the lowest temperature to which the brine would need to be cooled. Hence, for both Brines 1 and 2, ammonia was used as the refrigerant. The isentropic efficiency of the compressor was set to 75% based on state of compressor technology currently.

7.2.1 Operating cost for Brine 1 using EFC

The cumulative cooling requirement profile for a 100 m^3/day Brine 1 stream when cooling it down from 25°C to -23°C is shown in Figure 39.

The results show that the cooling requirements increase significantly once the operating temperature drops below 0°C, from 120 kW at 0°C to 500 kW at -4°C. As the operating temperature drops below -4°C the rate of increase of the cooling requirement is more gradual, with a second steep

increase in cooling requirement beginning at -22°C. The temperatures at which the cooling requirement curve steeply increases correspond to the crystallization temperatures of the salts – ice and $Na_2SO_4.10H_2O$ at -1°C and $NaCl.2H_2O$ at -23°C.

For a 100 m^3/day Brine 1 stream, with the first and second freeze crystallizers operating at -10°C and -23°C respectively, a summary of the respective cooling duties for the individual crystallizers and the rate of production of ice and salts are shown in Table 17.

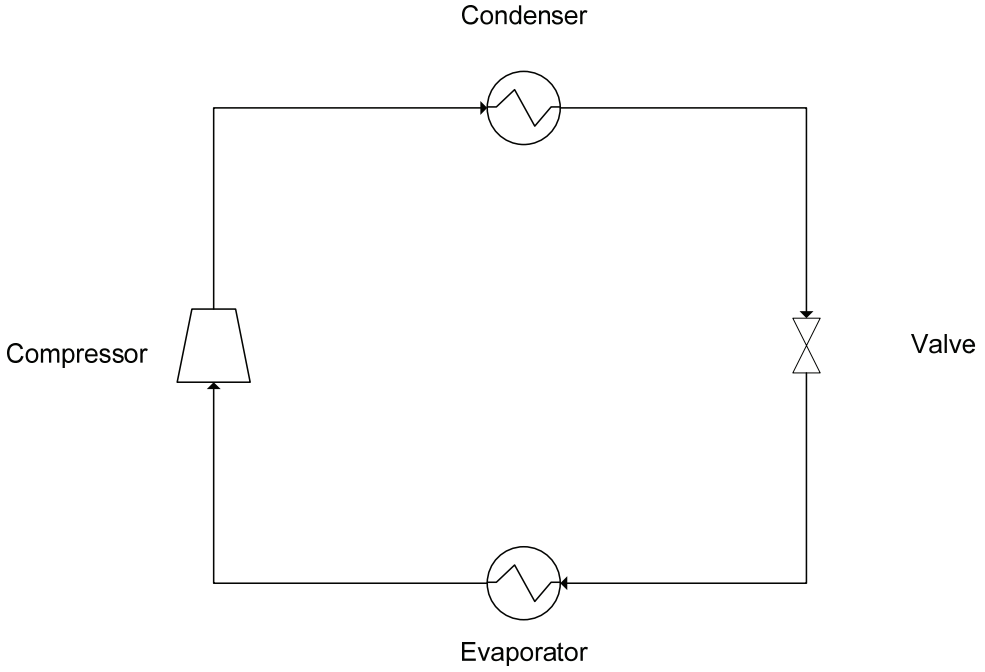

Figure 38: Flow sheet of refrigeration cycle set up in Aspen Plus®

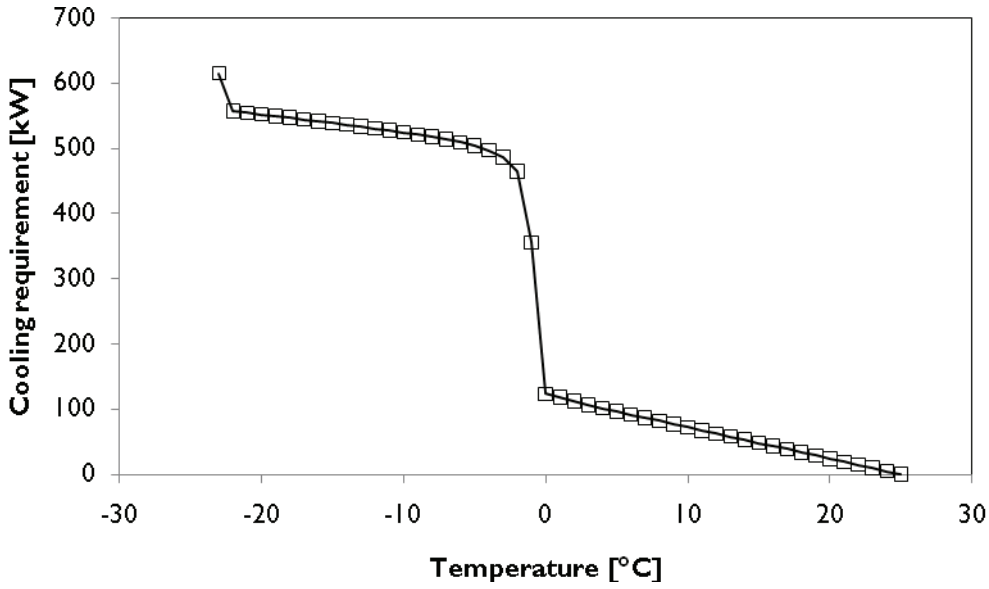

Figure 39: Cumulative cooling requirement for cooling 100 m^3/day of Brine 1 from 25°C to -23°C

Table 17: Summary of the respective cooling duties and the rate of production of ice and salts for 100 m^3/day of Brine 1

Crystallizer 1 (operating at -10°C)		
Cooling Duty [kW]	$Na_2SO_4.10H_2O$ produced [kg/hr]	Ice produced [kg/hr]
525	104	4000
Crystallizer 2 (operating at -23°C)		
Cooling Duty [kW]	$NaCl.2H_2O$ produced [kg/hr]	Ice produced [kg/hr]
10	25	88

The electricity requirements and the associated costs for Crystallizers 1 and 2 for 100 m^3/day of Brine 1 based on an electricity costing of R0.46/kWh are given in Table 18

Table 18: Compressor electricity requirements and associated costs for treating 100 m^3/day of Brine 1

Crystallizer 1 (operating at -10°C)			
Cooling Duty [kW]	Compressor Duty	Cost/day [R/day]	Cost/m^3 of brine[R/m^3]
525	250	R 2750	R 27.50
Crystallizer 2 (operating at -23°C)			
Cooling Duty [kW]	Compressor Duty	Cost/day [R/day]	Cost/m^3 of brine [R/m^3]
10	4.60	R 50.30	R 0.50
Total operating cost for 100 m^3 Brine 1		R 2800/day	R 28.00/m^3

7.2.2 Operating costs for Brine 2 using EFC

The cumulative cooling requirement profile for a 100 m^3/day Brine 2 stream when cooling it down from 25°C to -23°C is shown in Figure 40.

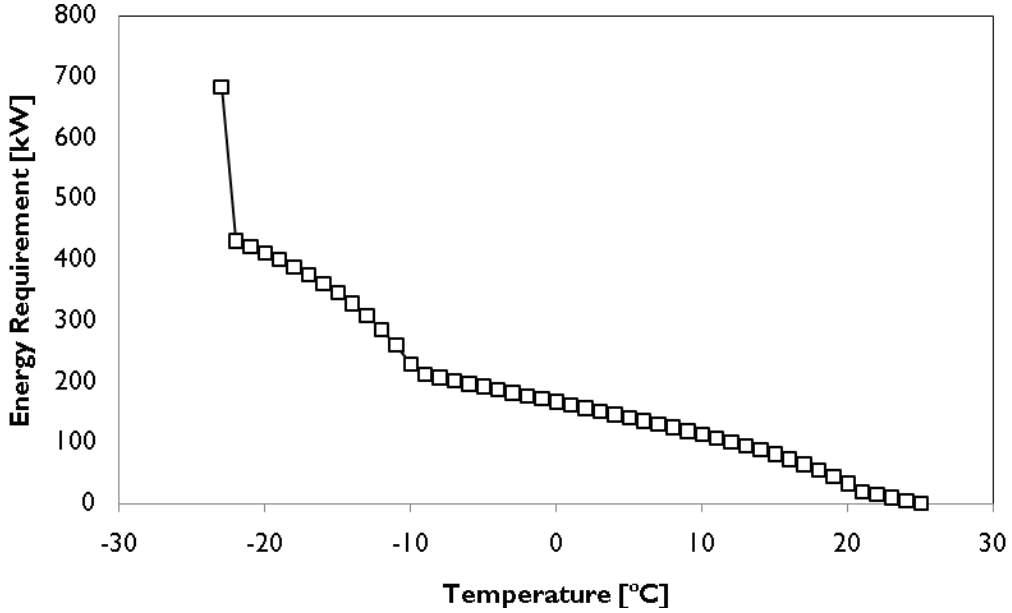

Figure 40: Cumulative cooling requirement for cooling 100 m^3/day of Brine 2 from 25°C to -23°C

The results show that the cooling requirements increase gradually between ambient temperature and -10°C. Thereafter, the cooling requirements increase more rapidly, from 229kW at -10°C to 431kW at -22°C. As the operating temperature drops below -22°C the rate of increase of the cooling requirement becomes extremely steep. These temperatures correspond to the crystallization temperatures of ice at -10°C and $NaCl.2H_2O$ at -23°C.

For a 100 m^3/day Brine 2 stream, with the first and second freeze crystallizers operating at -16°C and -23°C respectively, a summary of the respective cooling duties for the individual crystallizers and the rate of production of ice and salts are shown in Table 19.

Table 19: Summary of the respective cooling duties and the rate of production of ice and salts for 100 m^3/day of Brine 2

Crystallizer 1 (operating at -16°C)		
Cooling Duty [kW]	$Na_2SO_4.10H_2O$ produced [kg/hr]	Ice produced [kg/hr]
350	522	1398
Crystallizer 2 (operating at -23°C)		
Cooling Duty [kW]	$NaCl.2H_2O$ produced [kg/hr]	Ice produced [kg/hr]
206	897	1885

The electricity requirements and the associated costs for Crystallizers 1 and 2 for 100 m^3/day of Brine 2 based on an electricity costing of R0.46/kWh are given in Table 20.

Table 20: Compressor electricity requirements and associated costs for treating 100 m^3/day of Brine 2

Crystallizer 1 (operating at -16°C)			
Cooling Duty [kW]	Compressor Duty	Cost/day [R/day]	Cost/m^3 of brine[R/m^3]
350	166	R 1830	R 18.30
Crystallizer 2 (operating at -23°C)			
Cooling Duty [kW]	Compressor Duty	Cost/day [R/day]	Cost/m^3 of brine [R/m^3]
206	97.5	R 1080	R 10.80
Total operating cost for 100 m^3 Brine 2		R 2910/day	R 29.10/m^3

7.3 Comparing EFC to triple-effect evaporative crystallization for Brines 1 and 2

In order the establish the operating cost comparison between EFC and triple-effect evaporative crystallization, the operating costs for treating Brines 1 and 2 using triple-effect evaporative crystallisation based on the cost of the steam required for the heating duty was established. The basic flow diagram for the evaporation process is shown in Figure 41.

7.3.1 Operating cost for Brine 1 using triple-effect evaporative crystallization

The 100 m^3/day Brine 1 stream is fed to the first evaporator operating at 1bar, where the steam produced is used in the second evaporator, as is done in the third evaporator. The second and third evaporators are operated at 0.8 bar. A summary of the heating duties and the quantity of steam formed is shown in Table 21.

The main operating cost of the triple-effect evaporator i.e. the steam used to heat a 100 m^3/day of Brine 1 is based on steam at 350 kPa, costing R0.27/kg. The results of the operating cost calculation are given in Table 22.

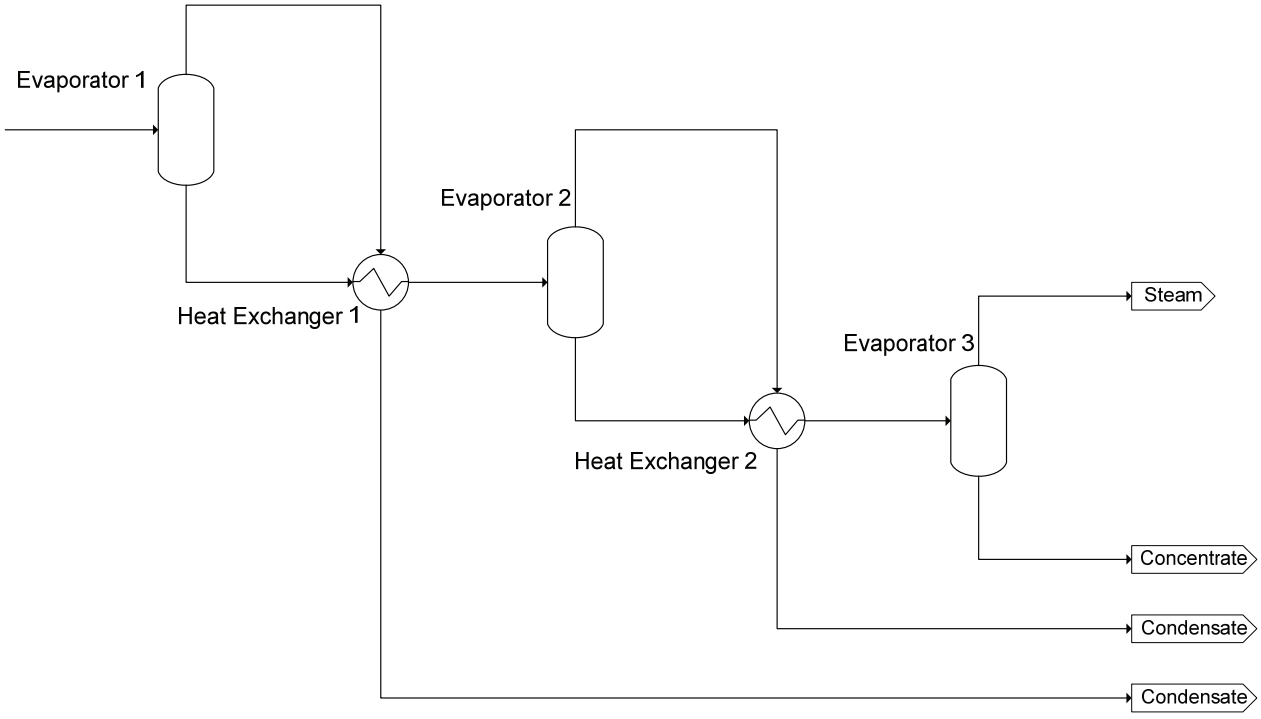

Figure 41: Basic triple effect evaporation process flow sheet for Brines 1 and 2

Table 21: Summary of the respective heating duties and the rate of production of steam for 100 m^3/day of Brine 1

Evaporative Crystallization				
	Heating Duty [kW]	Steam (water) produced [kg/hr]	Salt produced [kg/hr]	
			NaCl	$NaSO_4$
Evaporator 1	1230	1380		
Evaporator 2	871	1400		
Evaporator 3	846	1320	0.54	43.8

Table 22: Evaporative crystallizer steam requirements and associated costs for treating 100 m^3/day of Brine 1

Evaporative Crystallizer		
Heating Duty [kW]	Cost/day [R/day]	Cost/m^3 [R/m^3 of brine]
1230	R 13 200	R 132

7.3.2 Operating cost for Brine 2 using triple-effect evaporative crystallization

The 100 m^3/day Brine 2 stream is fed to the first evaporator operating at 1bar, where the steam produced is used in the second evaporator, as is done in the third evaporator. The second and third evaporators are operated at 0.8 bar. A summary of the heating duties and the quantity of steam formed is shown in Table 23.

Table 23: Summary of the respective heating duties and the rate of production of steam for 100 m^3/day of Brine 2

Evaporative Crystallization				
	Heating Duty [kW]	Steam (water) produced [kg/hr]	Salt Produced [kg/hr]	
			NaCl	$NaSO_4$
Evaporator 1	1168	1306		
Evaporator 2	826	1310		
Evaporator 3	670	1060	460	217

The triple-effect evaporator's main operating cost i.e. the steam used to heat a 100 m^3/day of Brine 2 is based on steam at 350 kPa, costing R0.27/kg. The results of the operating cost calculation are given in Table 24.

Table 24: Evaporative crystallizer steam requirements and associated costs for treating 100 m^3/day of Brine 2

Evaporative Crystallizer (operating at 112°C)		
Heating Duty [kW]	Cost/day [R/day]	Cost/m^3 [R/m^3 of brine]
1168	R 12 600	R 126

7.3.3 Comparing the estimated operating costs for EFC with triple-effect evaporative crystallization

Figure 42 below shows the daily operating cost comparison between the EFC and triple-effect evaporative crystallization (EC) for Brines 1 and 2 based on the electricity cost for the compressor in the refrigeration unit for EFC and the cost of steam for evaporative crystallization.

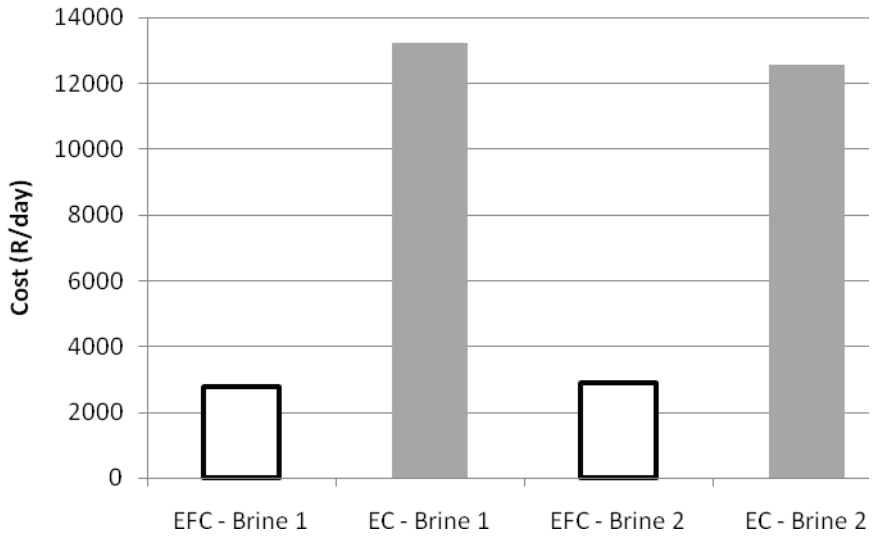

Figure 42: Comparison of daily operating costs for treating Brines 1 and 2 with EFC and multi-stage evaporation (Basis = 100 m^3/day of brine)

When comparing the approximated operating cost of EFC with EC based on the cost of energy for the compressor in EFC and the steam requirement for evaporative crystallization it is evident that EFC is significantly more cost effective than EC. The cost saving of using EFC over EC is of 79% and 77% for Brine 1 and Brine 2 respectively.

This preliminary operating cost evaluation study does not incorporate heat integration between the ice produced and the feed to the EFC crystallizer nor does it incorporate using the ice produced to cool the condenser in a two-stage refrigeration system. This would further enhance the cost effectiveness of EFC over EC.

7.4 Estimated capital costs for EFC and EC

The investment costs for treating Brines 1 and 2 using EFC were calculated in accordance with the semi-empirical method described by Vaessen (2003). The EFC investment costs for treating these brines are then compared to evaporative crystallization (EC). There are limitations to the level of accuracy with which the investment costs for a full scale plant based on a relatively new technology such as EFC can be determined. Nonetheless, the scope of this study is to generate an order of magnitude estimate that can be used to compare the costs of implementing EFC versus those for EC.

Table 25 and Table 26 below summarise the capital costs for using EFC to treat Brines 1 and 2 respectively. Similarly, Table 27 and Table 28 summarise the capital costs of using EC to treat Brines 1 and 2 respectively.

Figure 43 (page 54) shows a comparison of the capital equipment costs for EFC and EC.

As expected the capital costs for EFC, which is a relatively new technology, are 78% and 61% more than that for a triple effect EC process for Brines 1 and 2 respectively. However, it is important to note that the capital cost calculations for EC are based on a technology that is already well established, with only relatively marginal future equipment cost savings expected as a result of improvements in the existing technology. In contrast, EFC is a new technology with future improvements expected in the technology resulting in capital cost reductions in particular with regards to the EFC reactor.

Table 25: Summary of equipment costs for treating Brine 1 using EFC (2009)

Unit	Description	Calculated Cost
Scraped cooled wall crystallizer # 1 operating at -5°C	Cooling surface area per unit = 32 m^2 Cooling capacity per unit = 160 kW Number of units required = 3.15	R 2 962 969
Scraped cooled wall crystallizer # 1 operating at -23°C	Cooling surface area per unit = 32 m^2 Cooling capacity per unit = 160 kW Number of units required = 0.12	R 54 225
Wash column # 1	Diameter = 715 mm	854 950
Wash column # 2	Diameter = 152 mm	R 299 586
Belt filter # 1	Salt flow rate = 0.19 m^3/hr	R 121 435
Belt filter # 2	Salt flow rate = 0.048 m^3/hr	R 30 359
Cooling equipment crystallizer # 1	Cooling duty = 504 kW	R 1 946 796
Cooling equipment crystallizer # 2	Cooling duty = 19.3 kW	R 53 155
Ancillaries	5% of equipment cost	R 316 174
Total equipment cost		**R 6 639 648**

Table 26: Summary of equipment costs for treating Brine 2 using EFC (2009)

Unit	Description	Calculated Cost
Scraped cooled wall crystallizer # 1 operating at -5°C	Cooling surface area per unit = 32 m^2 Cooling capacity per unit = 160 kW Number of units required = 2.18	R 1 975 313
Scraped cooled wall crystallizer # 1 operating at -23°C	Cooling surface area per unit = 32 m^2 Cooling capacity per unit = 160 kW Number of units required = 1.53	R 1 162 613
Wash column # 1	Diameter = 400 mm	R 640 220
Wash column # 2	Diameter = 545 mm	R 695 064
Belt filter # 1	Salt flow rate = 2.838 m^3/hr	R 605 576
Belt filter # 2	Salt flow rate = 1.419 m^3/hr	R 302 788
Cooling equipment crystallizer # 1	Cooling duty = 345 kW	R 1 351 569
Cooling equipment crystallizer # 2	Cooling duty = 245 kW	R 838 798
Ancillaries	5% of equipment cost	R 378 597
Total equipment cost		**R 7 950 538**

Table 27: EC capital cost summary for treating Brine 1 (2009)

Unit	Description	Calculated Cost
Forced circulation crystallizer	Heating duty = 1230 kW	R 1 301 099
	Heating duty = 870 kW	R 1 021 034
	Heating duty = 845 kW	R 1 000 407
Plate evaporator	Heating duty = 1230 kW	R 360 692
	Heating duty = 870 kW	R 301 256
	Heating duty = 845 kW	R 296 723
Plate condenser	Heating duty = 615 kW	R 251 537
	Heating duty = 435 kW	R 210 088
	Heating duty = 422.5 kW	R 206 926
Ancillaries	5% of equipment cost	R 247 488
Total equipment cost		**R 5 197 251**

Table 28: EC capital cost summary for treating Brine 2 (2009)

Unit	Description	Calculated Cost
Forced circulation crystallizer	Heating duty = 1167 kW	R 1 254 084
	Heating duty = 825 kW	R 983 772
	Heating duty = 669 kW	R 849 523
Plate evaporator	Heating duty = 1167 kW	R 350 964
	Heating duty = 825 kW	R 293 050
	Heating duty = 669 kW	R 262 789
Plate condenser	Heating duty = 583.5 kW	R 244 753
	Heating duty = 412.5 kW	R 204 365
	Heating duty = 334.5 kW	R 183 262
Ancillaries	5% of equipment cost	R 231 328
Total equipment cost		**R 4 857 890**

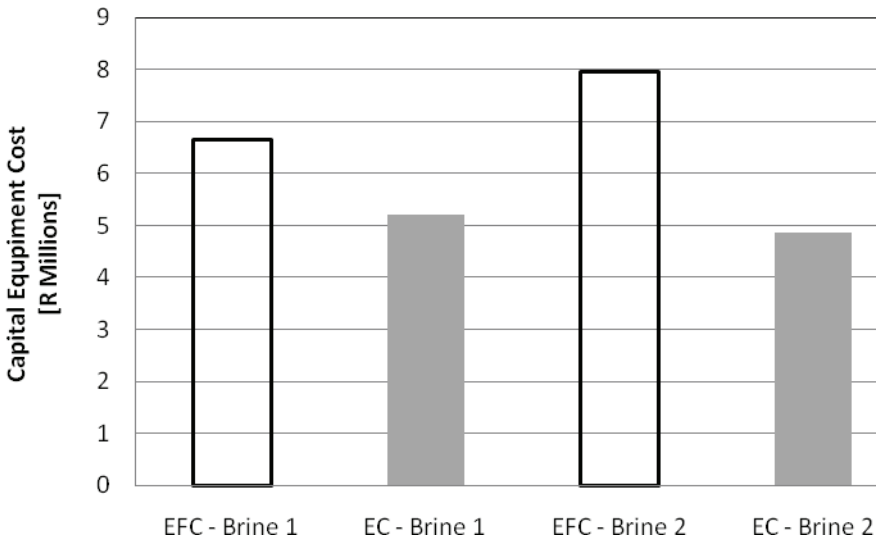

Figure 43: Comparison of the capital cost of equipment for Brines 1 and 2 for EFC and EC (Basis = 100 m^3/day of brine)

7.5 Sensitivity analysis on total costs for EFC and EC

A sensitivity analysis on the effect of increasing electricity costs on the total operating and capital costs for EFC compared to the present EC costs was carried out. The operating costs were based on Brine 2 and were assumed to increase by 10% every year for both processes. Figure 44 includes the projected electricity price increases by Eskom for the next three years, with an increase of 31% for 2009 and further increases of 25% for subsequent years.

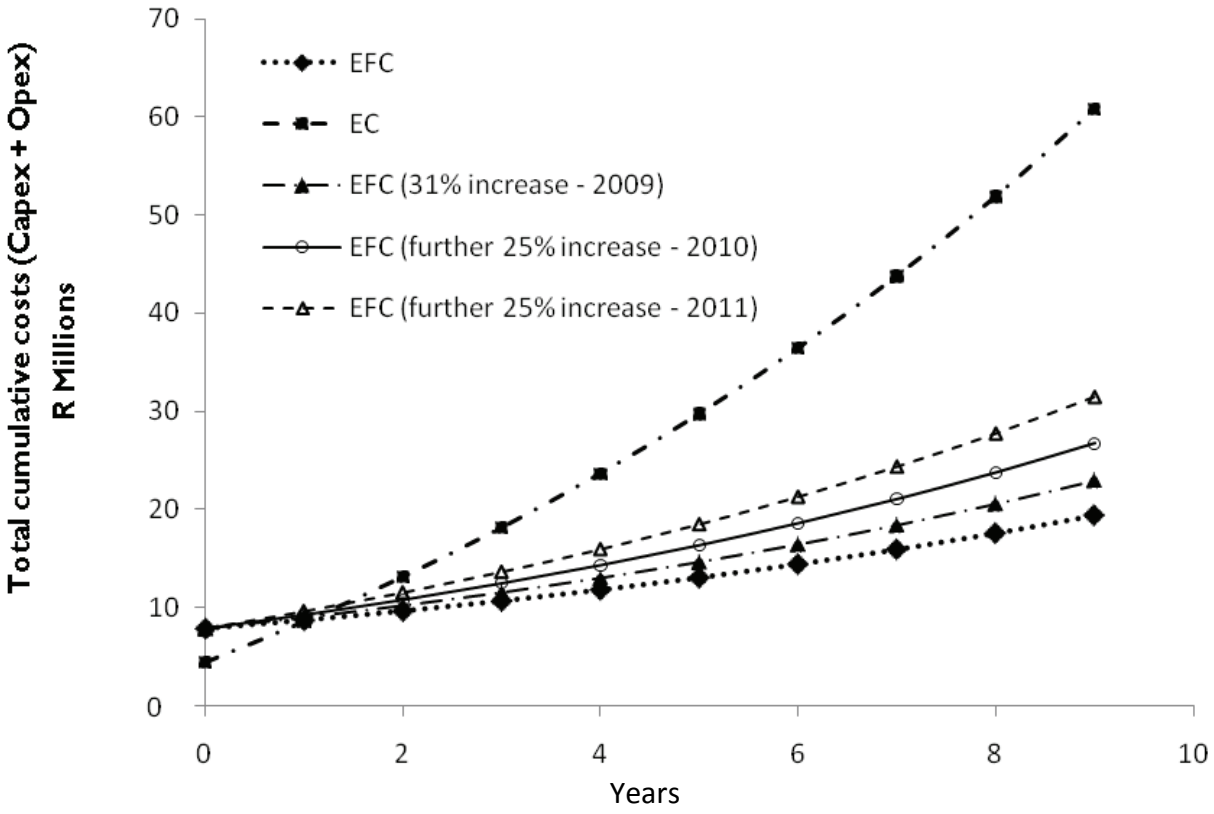

Figure 44: Total cumulative costs for EFC and EC processes

The graph above shows that despite the projected increase in electricity prices over the next three years, EFC is still found to be more economical than EC. Furthermore, it must also be noted that the projected steam price increase over the same period has not been taken into account in this study due to the unavailability of accurate projections in the future coal/steam generation prices. These are expected to increase with time and would have further enhanced the cost savings of EFC over EC.

In summary, whilst this preliminary comparative economic study between EFC and EC was based primarily on the main contributors to each process' largest operating cost (i.e. the electricity requirement for the compressor in the refrigeration unit for EFC and the cost of steam for the EC process) and that this could be further refined, the observed trends are expected to remain the same. The results of this economic study show that the operating cost savings achieved by using EFC significantly outweigh the initial higher capital cost investment required for EFC. This finding was also evident in the sensitivity analysis carried out to incorporate the current and projected increases in the electricity price tariffs as stipulated by ESKOM up to 2011. Consequently, this positions EFC as a promising innovative solution for the treatment of hypersaline brines that, when used either in isolation or in conjunction with water treatment processes such as reverse osmosis, can be effectively used towards achieving zero effluent discharge in a sustainable way that also produces pure salts that can be recycled.

8 CONCLUSIONS

Eutectic Freeze Crystallization (EFC) offers a novel, sustainable method for treating brines and concentrates that were previously regarded as difficult to treat due their complex nature and were consequently discharged to evaporation ponds. With EFC, pure water and pure individual salts can be recovered, thereby making a significant leap towards achieving zero effluent discharge.

Although EFC has been shown to be effective in separating a single salt and water, it had yet to be applied to the complex hypersaline brines that are typical of reverse osmosis retentates in South Africa. This project investigated the applicability of EFC to the hypersaline brines and inorganic effluents produced by major South African industries. Sections 81 to 8.4 present the key findings from this research project which focussed on:

1. Establishing the eutectic freeze crystallization phase diagrams for the hypersaline brines and saline effluents under investigation
2. Establishing the effect of the complex aqueous chemistry and impurities on the applicability of eutectic freeze crystallization to these aqueous systems
3. Establishing the expected costs and economic benefits of applying eutectic freeze crystallization to these aqueous systems.

8.1 Phase diagrams and modelling

- Binary phase diagrams are inadequate for the design of multicomponent EFC processes, since interactions between salts in hypersaline solutions cause multiple pseudo eutectic and eutectic temperatures.

- Ternary and quaternary phase diagrams can be generated using thermodynamic modelling and these can be used to determine the eutectic conditions

- Establishment of the metastable zone is the most critical kinetic parameter for design and operation of eutectic freeze processes.

- Thermodynamic modelling of the effects of salts on eutectic temperatures using a Reverse Osmosis retentate as the stream of interest showed that the ice always crystallizes first for low concentration streams, followed by the higher hydrated salts. No significant shifts in salt freezing points were observed due to the relatively low concentration of salts in the retentate.

- Ternary phase diagrams are essential to give information about sequential Eutectic Freeze Crystallization.

8.2 Synthetic brines

- The eutectic temperature and composition of the binary Na_2SO_4 –water system correlated well with literature values.

- For synthetic brine containing 4 wt% Na_2SO_4, the presence of low concentrations of F^-, Cl^-, K^+, Li^+, Mg^{2+}, Ca^{2+}, NO_3^- and NH_4^+ impurities depressed the eutectic temperature of $Na_2SO_4.10H_2O$ crystallization from -1.24°C to -2.22°C. Using EFC, pure ice crystals were obtained (<20 ppm impurities), ranging from 100 μm to 450 μm in size, after seven washing steps. Pure $Na_2SO_4 \cdot 10H_2O$ crystals (identified using thermal analysis), without any detectable

impurities, were also produced. The salt crystal sizes ranged from 20-100 μm one residence time after reaching eutectic conditions and 50-350 μm after three residence times.

- For a concentrated synthetic brine containing 4 wt% Na_2SO_4 and 20 wt% NaCl, the metastable point for $Na_2SO_4.10H_2O$ was reached at 6.68 wt% and 3.1°C. The freezing point for ice was depressed to -19°C. The eutectic point for the system was found to be -21.22°C. 90% recovery of $Na_2SO_4 \cdot 10H_2O$ was achieved, with crystal sizes ranging from 50-400μm. The solubility limit of NaCl was not reached for this system and NaCl was not recovered as a salt.

- The ternary Na_2SO_4-NaCl-H_2O system reached its eutectic point at approximately -21.29°C and the $Na_2SO_4 \cdot 10H_2O$ nucleated at 10.45°C. There was no significant change in the nucleation temperature as compared with Experiment E3 results. The ice reached its solubility limit at -22.5°C and greater than 90% of the $Na_2SO_4 \cdot 10H_2O$ crystals were recovered from this system. The $Na_2SO_4 \cdot 10H_2O$ crystals were pure and prismatic and monoclinic in shape. For the 4 wt% Na_2SO_4 – 23.5 wt% NaCl - brine system, the $Na_2SO_4 \cdot 10H_2O$ nucleated at 9.08°C, whereas the ice nucleated at -21.85°C. The presence of impurities did not have a significant impact on the eutectic point of the system. The system reached the eutectic point at -21.27°C. At this low temperature, the production of ice was high, leading to the crystalliser contents forming a slush mixture of ice and salt. Therefore, the purity of ice could not be determined owing to the difficulty in separation of the ice and salt from the crystalliser. Hence, it is important to establish the critical solid mass content within the reactor.

8.3 Metastable zone width determination

- The average MSZ for the ice region of the Na_2SO_4-H_2O system is 4.1°C at a cooling rate of 1.5°C/hour. The MSZ is also wider in the region of ice formation compared to the region where salt forms. The average MSW for the salt region is 2.9°C.

- A faster cooling rate increases the average MSZW for the region where ice forms. The average MSZ for the ice trendline is 4.5°C at a cooling rate if 4°C/hour, which is 0.4°C higher than the average MSZW obtained for a cooling rate of 1.5°C/hour. The average width of the MSZ for the ice line at a cooling rate of 6°C/hour is 5.5°C.

- The average MSZ at a cooling rate of 4°C/hour for the salt line is, however, 2.1°C which is 0.8°C smaller than the MSZW for a cooling rate of 1.5°C. The fastest cooling rate investigated, 6°C/hour, results in the greatest average MSZ for the salt line with a value of 3.4°C.

- The metastable eutectic composition decreases with the fastest cooling rate of 6°C/hour. The metastable eutectic composition is around 4.5 wt% for a cooling rate of 6°C/hour while for a cooling rate of 1.5°C/hour it is 4.79 wt%. However, this trend was not observed for a cooling rate of 4°C/hour.

- Seeding can be used to test the accuracy of the experimentally determined metastable boundary. Salt seeding promotes the formation of ice but only to the limit of the MSZ after which ice nucleation occurs.

8.4 Economic evaluation of EFC

The key objective of the preliminary economic evaluation was to provide an approximation of the expected operating and capital costs associated with using EFC. These were compared to triple-effect evaporative crystallization (EC). The costs of electricity to the compressor in the EFC refrigeration unit and the steam requirement for the evaporative crystallization process were identified as the major contributors to the operating costs for the two processes. Hence, these were used as the basis for calculating the operating costs.

Two brines broadly representative of typical South African industrial brines i.e. consisting of Na_2SO_4 and NaCl were investigated. The concentration factor difference between the two brines was approximately 10 with Brine 2 being more concentrated than Brine 1. A basis of 100 m^3/day of brine was used.

The operating cost calculated for using EFC to treat Brine 1, without heat integration, with a cooling requirement of 534 kW was R28/m^3. In contrast, the operating cost for a triple-effect EC process to treat Brine 1 was R132/m^3.

The operating cost calculated for using EFC to treat Brine 2, without heat integration, with a cooling requirement of 556 kW was R29/m^3. In contrast, the operating cost for a triple-effect EC process to treat Brine 2 was R126/m^3.

Hence, the operating cost savings of using EFC over EC are 79% and 76% for Brine 1 and Brine 2 respectively. The cost savings of using EFC could potentially be further enhanced by incorporating the income generated from the sale of the pure salts produced by the EFC process, as well as taking into consideration the additional mixed salt disposal costs for EC.

Three heat integration options were investigated to determine their effect on further reducing the EFC operating costs. The first option involved pre-cooling the incoming feed with the product ice stream. The second option investigated using the product ice to cool the condenser in a two-stage refrigeration system. The third option was a combination of Option 1 and 2 above. The most cost effective option was found to be Option 3. Using Option 3, the operating cost for Brine 1 was calculated to be R21/m^3 as compared to R28/m^3 without heat integration. Similarly, for Brine 2 using Option 3, the operating cost was calculated to be R21/m^3 as compared to R29/m^3 without heat integration. Thus, operating cost savings of 27% and 29% were achieved for Brines 1 and 2 respectively with heat integration according to Option 3.

The capital equipment cost for EFC for treating 100 m^3/day of Brine 1 and Brine 2 were calculated to be R6.6 million and R7.9 million respectively. In comparison, the capital costs for treating the same volume of brine using EC were R5.2 million and R4.9 million for Brine 1 and Brine 2 respectively. As expected, the EFC capital costs were significantly higher than those for EC. However, it is important to note that the capital cost calculations for EC are based on a technology that is already well established, with only relatively marginal future equipment cost savings expected as a result of improvements in the existing technology. In contrast, EFC is a new technology with future improvements expected in the technology resulting in capital cost reductions in particular with regards to the EFC reactor.

A sensitivity analysis on the effect of ESKOM's projected electricity increases over the next three years on the total operating and capital costs for EFC compared to the present EC costs revealed

that despite the projected increase in electricity prices over the next three years, EFC is still found to be more economical than EC.

In summary, the results of the experimental work aimed at investigating the effect of complex aqueous chemistry and impurities on the EFC process showed that the eutectic temperature for a pure binary system of Na_2SO_4-H_2O was -1.24°C and -21.29°C for a pure ternary system of Na_2SO_4-NaCl-H_2O. The presence of impurities, even in small concentrations, had a significant depressing impact on the eutectic temperature of the binary system. Maintaining a critical solid mass content i.e. the amount of ice and salt crystals in the reactor was found to be of significant importance as it directly affected the purity and yield of the crystalline products.

The study showed that the MSZ for ice was generally wider than that for salt, regardless of the cooling rate used. For the sodium sulphate system, a faster cooling rate resulted in a wider MSZ. The difference in the nucleation temperatures for repeat experiments was attributed to the stochastic nature of nucleation. The findings from the experimental work have emphasised the importance of identifying the appropriate EFC operating conditions (operating temperatures and the operating region within the phase diagram) in order to promote good product characteristics and maximise yields.

The results of the economic study showed that the operating cost savings achieved by using EFC over EC significantly outweighed the initial higher capital cost investment required for EFC. This continued to be the case despite the projected increases in the electricity price tariffs as stipulated by ESKOM up to 2011.

In conclusion, EFC offers an innovative solution for the treatment of hypersaline brines. It is a technology that can be used either in isolation or in conjunction with other water treatment processes such as reverse osmosis, towards achieving zero effluent discharge sustainably. Future studies in EFC will need to focus on further refining the understanding of the scientific fundamentals together with investigating key operating parameters that will enable the process to be tested at pilot scale before full-scale implementation.

9 REFERENCES AND BIBLIOGRAPHY

BARDUHN AJ and MANUDHANE A (1979) Temperatures required for eutectic freezing of natural waters, Desalination **28** 233-24.

BERTHOLD J (2001) *A guide to using the OLI Software*, OLI systems Inc, Morris Plains, New Jersey.

CONLON WM (1992), Recent improvements to the freeze crystallization method of water purification. Crystallization Powder Technology **121** 31-38.

DRUMMOND LS, VAESSEN R, HIMAWAN C, SECKLER MM, and WITKAMP, GJ (2002) A method for rapid development of eutectic freeze crystallization processes: application to potassium sulphate solution contaminated with organics. Chemical Engineering Transactions AIDIC, **1.** 921-926.

DRUMMOND LS, VAESSEN RJC, HIMAWAN C, SECKLAR MM and WITKAMP GJ (2002). A method for rapid development of eutectic freeze crystallization processes: Application to a potassium sulphate solution contaminated with organics, 15th ISIC, International Symposium on Industrial Crystallization, Sorrento, Italy 15-18 September 2002

GENCELI FE (2008) *Scaling-up of Eutectic Freeze Crystallization*, PhD dissertation, Delft University of Technology, The Netherlands.

GENCELI FE, GARTNER R, WITKAMP GJ (2005), Eutectic freeze crystallization in a 2nd generation cooled disk column crystallizer for $MgSO_4.12H_2O$ system. Journal of Crystal Growth, **275**. 1369-1372.

GERICKE G and ROUX PJ DU TOIT (2005) Eskom/Sasol Co-operative Research Initiative, *Towards the Development of Sustainable Salt Sinks: Fundamental Studies on the Co-Disposal of Brines within Inland Ash Dams*, Terms of Reference, 17 June.

GMELIN (2007) Gmelins Handbuch der Anorganischen Chemie, 8th Edition, DEUTSCHE CHEMISCHE Gesellschaft, *Weinheim: Verlag Chemie Gustafsson,* J.P. Visual Minteq Version 2.52, KTH, Department of Land and Water Resources Engineering, Stockholm, Sweden.

HARVIE CE, MOLLER N and WEAR JH (1984) The prediction of mineral solubilities in natural waters: The $Na\text{-}K\text{-}Mg\text{-}Ca\text{-}H\text{-}Cl\text{-}SO_4\text{-}OH\text{-}HCO_3\text{-}CO_3\text{-}CO_2\text{-}H_2O$ system to high ionic strengths at 25°C. Geochimica et Cosmochimica Acta **48**, 723–751.

HIMAWAN C (2005). *Characterisation and population balance modelling of eutectic freeze crystallization*, PhD Thesis, TU Delft, Netherlands.

HIMAWAN C, and WITKAMP GJ (2006) Crystallization kinetics of $MgSO_4.12H_2O$ from different scales of batch cooling scraped crystallizers. Crystal Research Technology, **41**. 865-873. http://www.phasediagram.dk/

HIMAWAN C, KRAMER HJM and WITKAMP GJ (2006) Study on the recovery of purified $MgSO_4.7H_2O$ crystals from industrial solution by eutectic freezing. Separation and Purification Technology **50** 240-248.

ITOH T, HASHIMOTO Y, SEKI H, OGAWA M, DOKI N and KUBOTA N (2002) Simulation of seeded batch cooling. 2nd International Symposium on Design, Operation and Control of Chemical Processes (PSE) Asia, Taipei. 4-6 December, pp 68

KUBOTA N (2008) A new interpretation of metastable zone widths measured for unseeded solutions. Journal of Crystal Growth, **310**. 629-634.

KUBOTA N, DOKI N, YOKOTA M, and SATO A (2001) Seeding policy in batch cooling, Powder Technology, **121 (1)** 31-38

LIDE DR (2006) CRC Handbook of Chemistry and Physics: *A ready-reference book of chemical and physical Data*, 87th Edition, CRC Press – Taylor and Francis Group, London, UK.

LOFFELMANN M, MERSMANN A (2002) How to measure supersaturation. Chemical Engineering Science, **57** 4301-4310.

LOI MI LUNG-SOMARRIBA B, MOSCOSA-SANTILLAN M, PORTE C and DELACROIX A (2004) Effect of seeded surface area on crystal size distribution on glycine batch cooling crystallization: a seeding methodology. Journal of Crystal Growth, **270**. 624-632.

MARION GM (2001) Carbonate mineral solubility at low temperatures in the Na-K-Mg-Ca-H-Cl-SO_4-OH-HCO_3-CO_3-CO_2-H_2O system, Geochimica et Cosmochimica Acta **65(12)** 1883-1896

MARION GM, and FARREN (1999) F.E Mineral solubilities in the Na-K-Mg-Ca-Cl-SO_4-H_2O system: A re-evaluation of the sulfate chemistry in the Spencer-Møller-Weare model., Geochimica et Cosmochimica Acta **63(9)** 1305-1318

MARION GM, FARREN RE and KOMROWSKI AJ (1999) Alternative pathways for seawater freezing. Cold Regions Science and Technology, **29** 259-266

MARLIACY P, SOLIMANDO R, BOUROUKBA M and SCHUFFENECKER L (2000) Thermodynamics of crystallization of sodium sulphate in H2O-NaCl-Na_2SO_4: application to Na_2SO_4.10H_2O-based latent heat storage materials, Thermochimica Acta, **344** 85-94

MULLIN JW (2001) *Crystallization*. 4th edn, Butterworth-Heinemann, London.

MYSERSON A (2002) *Handbook of Industrial Crystallization.* 2nd edn, Butterworth-Heinemann, London.

NAGY ZK, CHEW JW, FUJIWARA M and BRAATZ RD (2008) Comparative performance of concentrations and temperature controlled batch crystallizations. Journal of Process Control, **18** 399-407.

NELSON S (2002) *Crystallization in Ternary Systems*. http://www.tulane.edu/~sanelson/geol212/ternaryphdiag.htm (Accessed 21 March 2008)

NYVLT J (1971) *Industrial Crystallization from solutions*. 1st edn, Butterworth-Heinemann, London.

OLI systems Inc Stream Analyser (2004) Version 2.0.57, OLI Systems Inc, Morris Plains, New Jersey.

PITZER KS (1973) Thermodynamics of electrolytes. I. Theoretical basis and general equations. *Journal of Physical Chemistry*, **77 (2)** 268–277

PITZER KS (1975) Thermodynamics of electrolytes. V. Effects of higher order electrostatic terms *Journal of Solution Chemistry* **4** 249–265

PITZER KS and MAYORGA G (1973) Thermodynamics of electrolytes. II. Activity and osmotic coefficients with one or both ions univalent *Journal of Physical Chemistry*, **77(19)** 2300-2308

PRONK P (2006) *Fluidized bed heat exchangers to prevent fouling in ice slurry systems and industrial crystallizers*, PhD Thesis, Technical University of Delft, The Netherlands

SANDLER SI (1999) *Chemical and Engineering Thermodynamics*, John Wiley and Sons, 3rd Edition, P598-602

SERKIZ SM, ALLISON JD, PERDUE EM, ALLEN HE, and BROWN DS (1996) Correcting errors in the thermodynamic database for the equilibrium speciation model MINTEQA2 30, Water Research **69** 1930-1933

SÖHNEL O and GARSIDE J (1992) *Precipitation – Basic principles and industrial applications*, Butterworth-Heinnemann, Oxford, P75

SRINIVASEN K, MEERA K and RAMASAMY K (2000) A Novel method to enhance metastable zone width for crystal growth from solution, Crystal Research Technology, **35**, 291-297

STEPAKOFF G, SIEGELMAN D, JOHNSON R and GIBSON W (1974) Development of an eutectic freezing process for brine disposal, Desalination **14** 25-38.

STUMM W and MORGAN JJ (1996) *Aquatic Chemistry-Chemical Equilibria and Rates in Natural Waters.* 3rd Edition. John Wiley & Sons, Inc, New York, USA.

THOMSEN, K (2007) Aqueous electrolytes: Phase diagrams and process simulation / optimization. http://www.phasediagram.dk/ (Accessed 22 November 2007).

VAESSEN R (2003) *Development of scraped eutectic crystallizers*. PhD Thesis, Technical University of Delft, The Netherlands.

VAESSEN R, JANSE B, SECKLER M and WITKAMP G (2003) Evaluation of the performance of a newly developed eutectic freeze crystallizer: scraped cooled wall crystallizer. Chemical Engineering Research and Design **81** 1363-1372.

VAESSEN RJC (2003) *Development of scraped eutectic crystallizers*, PhD Thesis, Technical University of Delft, The Netherlands.

VAN DER HAM F (1999) *Eutectic Freeze Crystallization*, PhD Thesis, Technical University of Delft, The Netherlands.

VAN DER HAM F, SECKLER MM and WITKAMP GJ (2004) Eutectic freeze crystallization in a new apparatus: the cooled disk column crystallizer. Chemical Engineering and Processing **43 (2)** 161-167.

VAN DER HAM F, WITKAMP GJ, DE GRAAUW J and VAN ROSMALEN GM (1998) Eutectic freeze crystallization: Application to process streams and waste water purification, Chemical Engineering and Processing **37 (2)** 207-213.

VAN DER HAM F, WITKAMP GJ, DE GRAAUW J and VAN ROSMALEN GM (1999) Eutectic freeze crystallization simultaneous formation and separation of two solid phases, Journal Of Crystal Growth **198-199 (1)** 744-748.

ZAITSEVA NP, RASHKOVICH LN and BOGATYREVA SV (1995) Stability of KH_2PO_4 and $K(H,D)_2\ PO_4$ solutions at fast crystal growth rates. Journal for Crystal Growth **148** 276-282.

10 APPENDIX A

Phase diagrams for binary, ternary and quaternary systems are all obtained from http://www.phasediagram.dk/ or the work conducted by Kaj Thomsen at Aqueous Solutions.

10.1 Binary Systems

10.1.1 The KCl-H_2O system

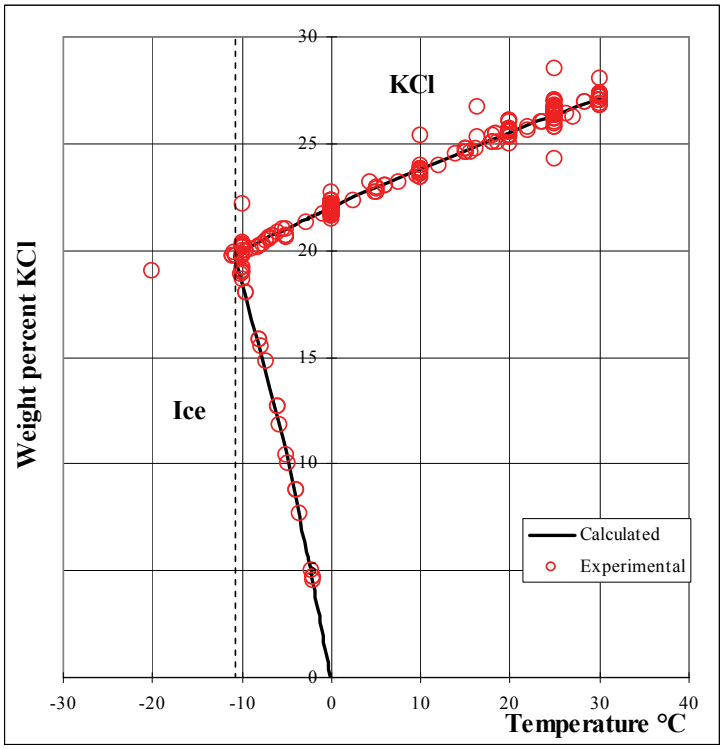

10.1.2 The $MgCl_2$-H_2O system

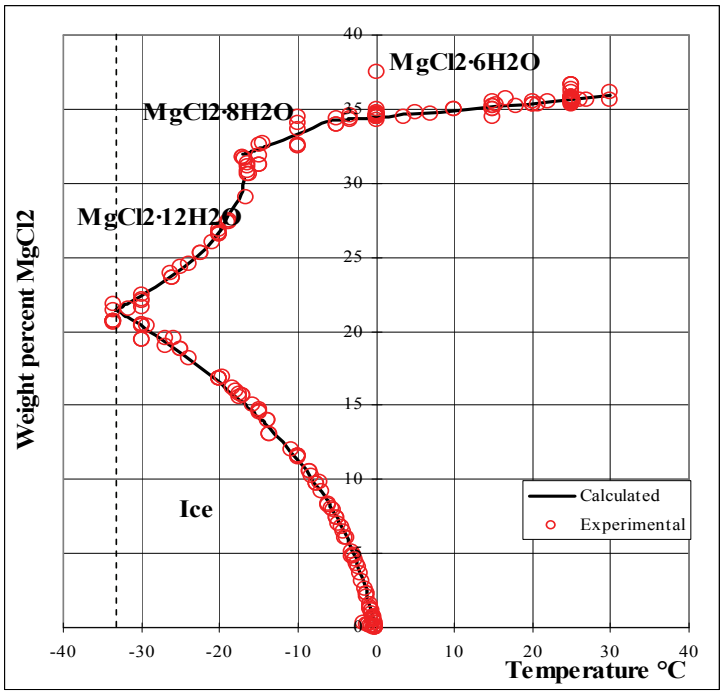

10.1.3 The $BaCl_2$-H_2O system

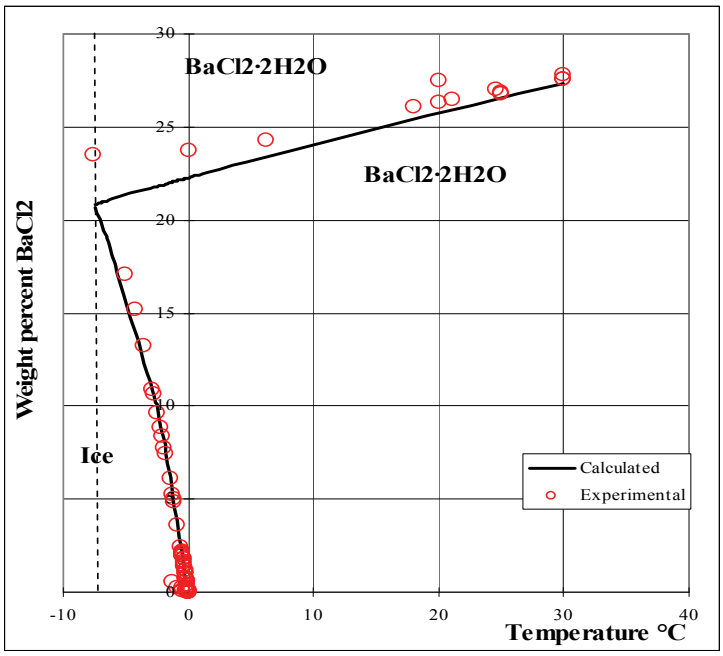

10.1.4 The $CaCl_2$-H_2O system

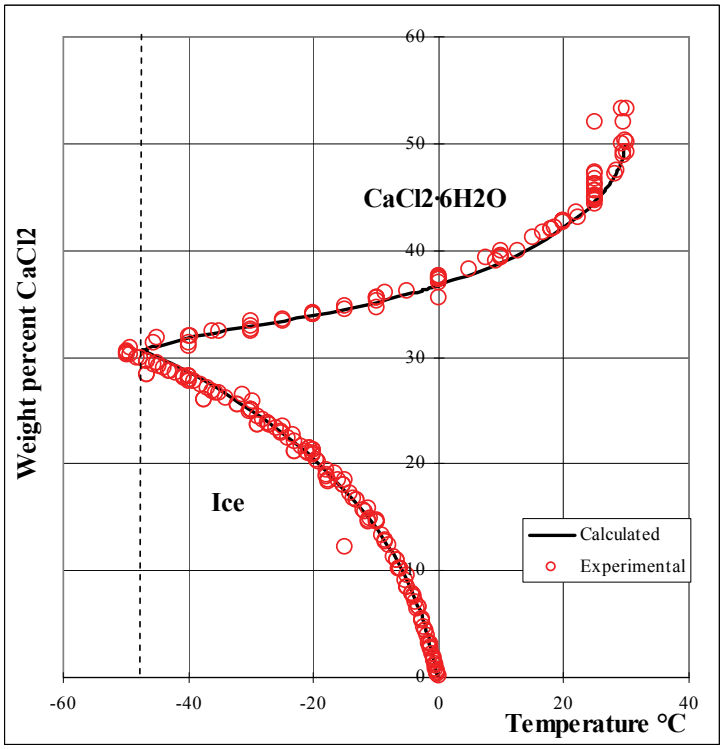

10.2 Ternary Systems

10.2.1 The $MgSO_4$-K_2SO_4-H_2O system

The solid phases encountered in this system in the temperature range from -10 to 120°C are:
H_2O (s) Ice
K_2SO_4 (potassium sulfate)
$MgSO_4 \bullet 12H_2O$ (magnesium sulfate dodecahydrate)
$MgSO_4 \bullet 7H_2O$ (epsom salt)
$MgSO_4 \bullet 6H_2O$ (hexahydrite)
$MgSO_4 \bullet H_2O$ (kieserite)
$K_2SO_4 \bullet MgSO_4 \bullet 6H_2O$ (schoenite)
$K_2SO_4 \bullet MgSO_4 \bullet 4H_2O$ (leonite)
$K_2SO_4 \bullet 2MgSO_4$ (langbeinite)

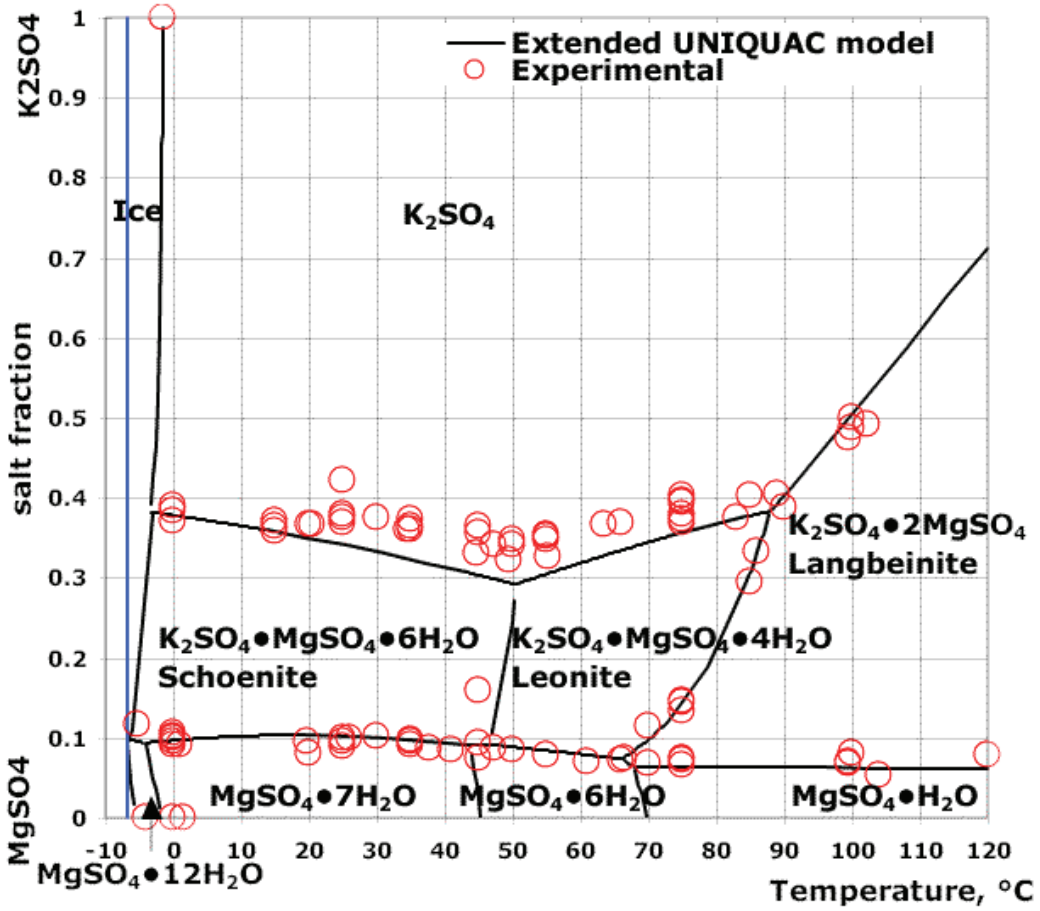

Figure 45: Phase diagram for the $MgSO_4$-K_2SO_4-H_2O system in the temperature range from -10 to 120°C

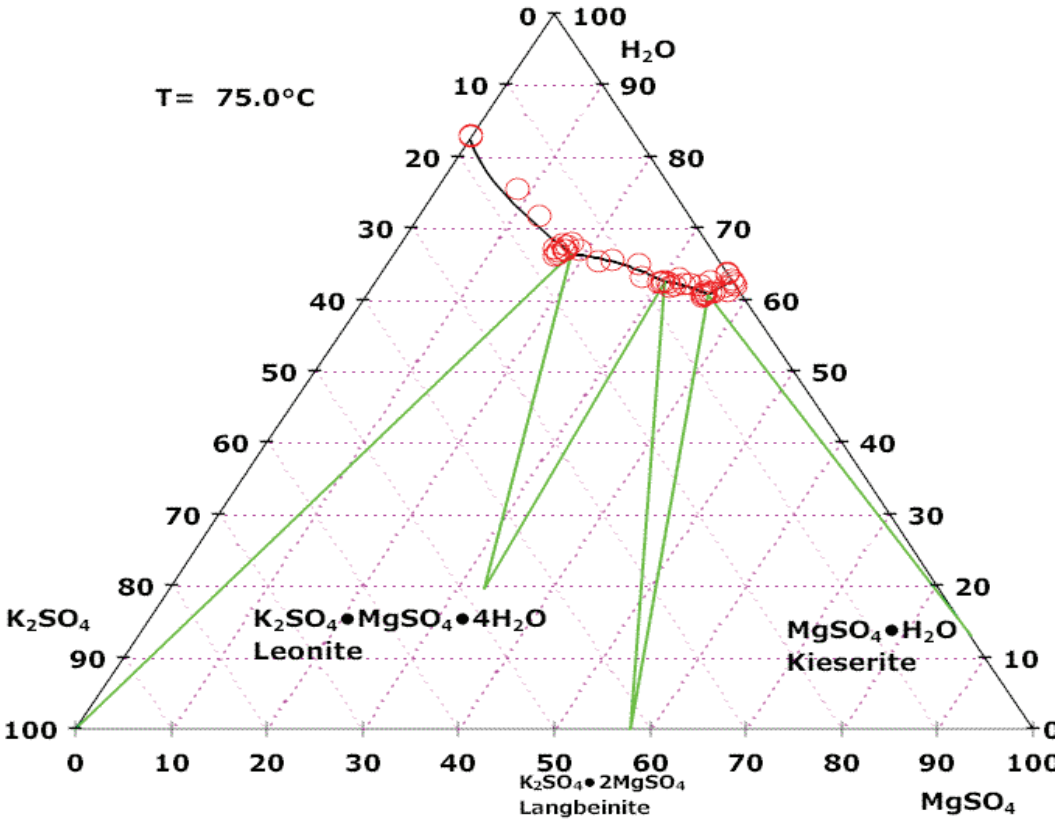

Figure 46: 75°C Isotherm for the $MgSO_4$-K_2SO_4-H_2O system

10.2.2 The NaCl-$NaNO_3$-H_2O system

The solid phases encountered in this system in the temperature range from -30 to 110°C are:
H_2O (s) Ice
$NaNO_3$ (sodium nitrate)
$NaCl•2H_2O$ (hydrohalite)
NaCl (sodium chloride, halite)

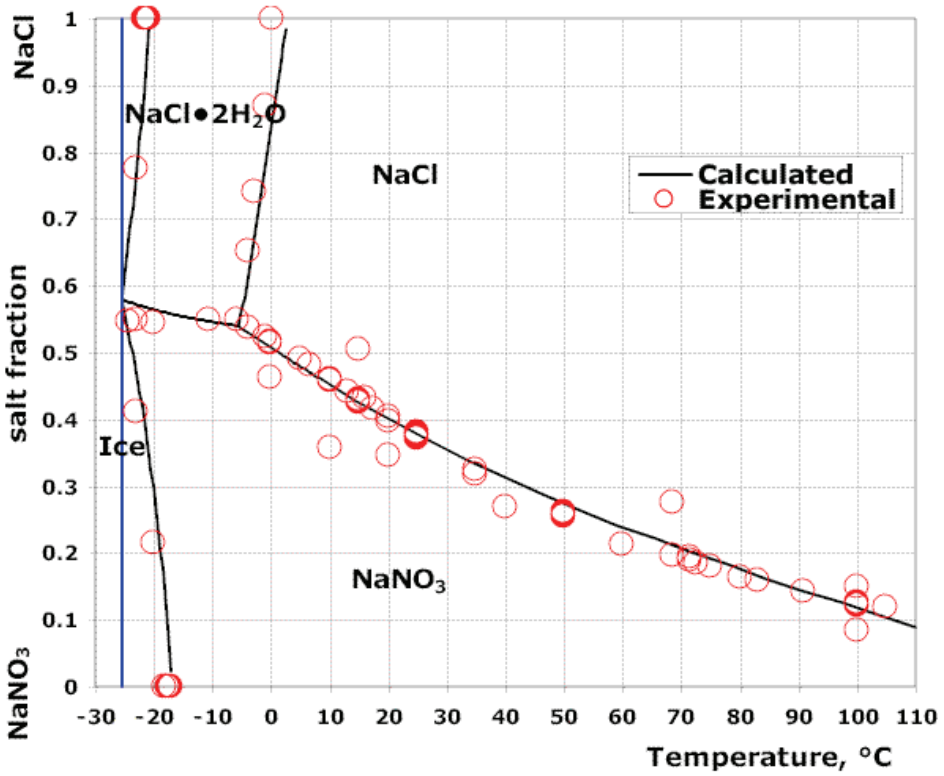

Figure 47: Phase diagram for the NaCl-$NaNO_3$-H_2O system in the temperature range from -30 to 110°C

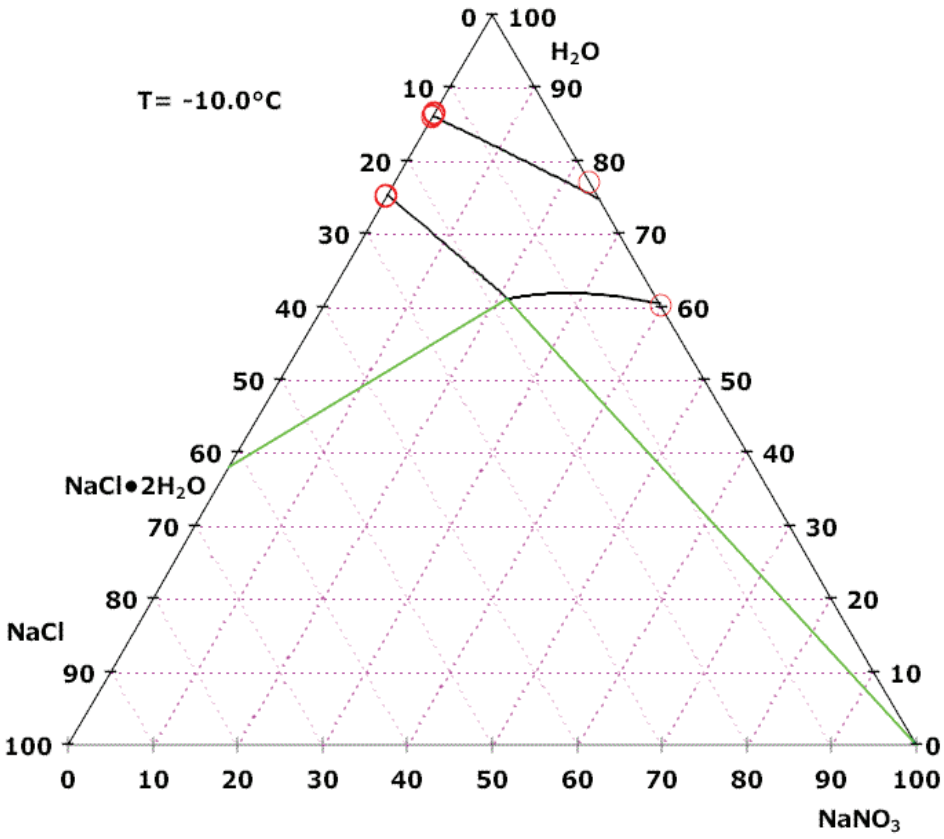

Figure 48: -10°C Isotherm for the NaCl-$NaNO_3$-H_2O system. The green lines are tie lines.

10.3 Quaternary Systems

10.3.1 The (Na^+,K^+,Ca^{2+})-Cl^--H_2O system

In the quaternary (Na^+,K^+, Ca^{2+}) - Cl^--H_2O system at 50°C, the following solid phases appear:
NaCl (halite)
KCl (sylvite)
$CaCl_2$•$2H_2O$ (sinjarite)
KCl•$CaCl_2$ (chlorocalcite, baeumlerite)

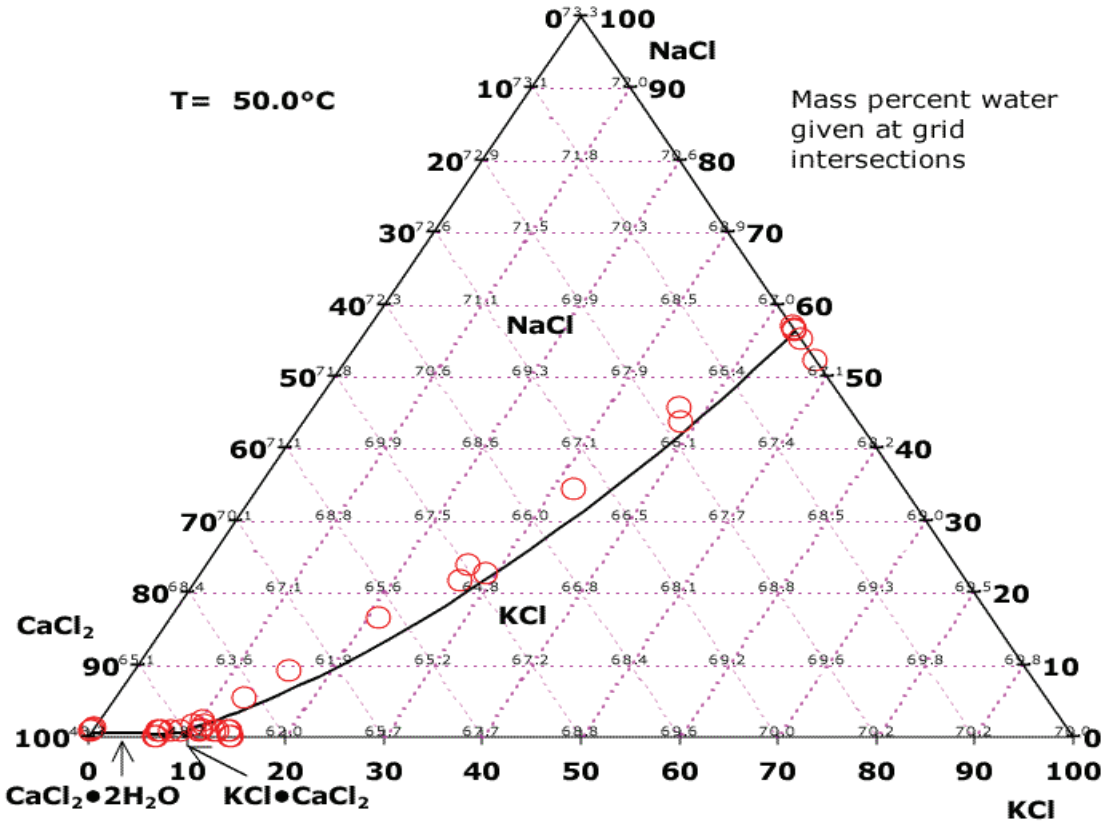

Figure 49: Jänecke projection of the phase diagram for the NaCl-KCl-$CaCl_2$-H_2O system at 50°C